Proceeding of the 4th Asian Society of Veterinary Pathologists (ASVP) Conference and Annual Meeting of The Thai Association of Veterinary Laboratory Diagnosticians (TAVLD)

"Era of Modern Diagnostic Pathology"

November 19-20, 2009 Bangkok, Thailand

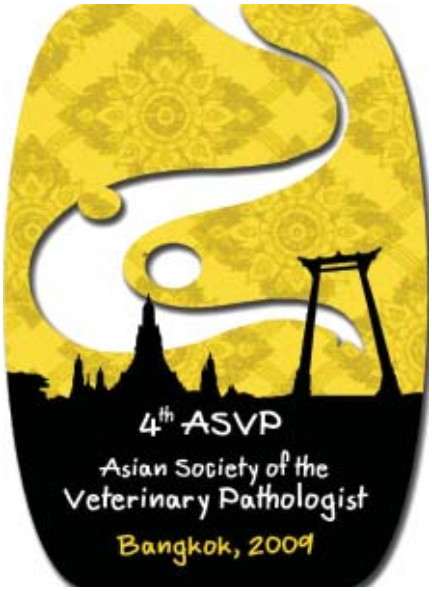

Organized by

The Asian Society of Veterinary Pathologists (ASVP)

The Veterinary Pathology Society of Thailand (VPST)

The Thai Association of Veterinary Laboratory Diagnosticians (TAVLD)

The Veterinary Oncology Center, Innovation Center for Veterinary Teaching and Services in Companion Animals

The Faculty of Veterinary Science, Chulalongkorn University, Thailand

Joint with

The Zoological Park Organization under the Royal Patronage of His Majesty the King
Chulalongkorn University Emerging and Re-emerging Infectious Diseases in Animals Center (CUEIDA)
Asian Foundation for the Advancement of Veterinary and Animal Sciences (AFAVAS)
CL Davis Foundation for the Advancement of Veterinary and Comparative Pathology
The Federation of Asian Veterinary Associations (FAVA)
Asian Society Wildlife Pathology and Parasitology (ASWPP)
The National Taiwan University

Organizing Committee

Proceeding of the 4th Asian Society of Veterinary Pathologists (ASVP) Conference and Annual Meeting of The Thai Association of Veterinary Laboratory Diagnosticians (TAVLD)

Advisor: Dean of Faculty of Veterinary Science, Chulalongkorn University, Thailand
Assoc. Dean for Administration Affair, Faculty of Veterinary Science, Chulalongkorn University, Thailand
Assoc. Dean for Academic Affair, Faculty of Veterinary Science, Chulalongkorn University, Thailand
Chair of Innovation Center for Veterinary Teaching and Services in Companion Animals
Prof. Dr. Tokuma Yanai, Japan
Prof. Dr. Pen-Heng, Chang, Taiwan
Prof. Dr. Victor Fei Pang, Taiwan
Prof. Dr. Nam Yong Park, Republic of Korea

Chair person:	Achariya	Sailasuta
Secretariat general:	Komkrich	Teankum
	Somporn	Techangamsuwan
Scientific editor:	Anudep	Rungsipipat
Committee:	Roongroje	Thanawongnuwech
	Wijit	Banlunara
	Somlak	Poungshompoo
	Nopadon	Pirarat
	Pringsri	Ingkaninan
	Theerayuth	Kaewamatawong
	Chaiyan	Kasorndorkbua
	Sirikajorn	Tangkawatana
	Tattawan	Kaewsakorn
	Taweewan	Tansathit
	Tanongsak	Mamom
	Angkana	Somanataweechai

"The 4th Asian Society of Veterinary Pathologists Conferenece"
The 4th ASVP 2009
19-20 November 2009
Chulalongkorn University, Bangkok, Thailand
Opening Ceremony
Thursday 19th November 2009
Institute Building III Auditorium, Chulalongkorn University

Opening address

By Prof. Dr. Pirom Kamonrattanakul
President of Chulalongkorn University

Honorary President of the Asian Society of the Veterinary Pathologists and the Chairman of the Organizing Committee of the 4th Asian Society of the Veterinary Pathologists Conference, Dean of the Faculty of the Veterinary Science, Chulalongkorn University, the Faculty member committee, the President of the Thai Association of the Veterinary Laboratory Diagnostician, Head of the Innovation Center for Veterinary Teaching and Services in Companion Animal, Deputy Director of the Zoological Park Organization under the Royal Patronage under His Majesty the King, President of Asian Foundation for the Advancement of Veterinary and Animal Science, CL Davis Foundation for the Advancement of the Veterinary and Comparative Pathology, President of the Federation of Asian Veterinary Associations, President of the Asian Society Wildlife Pathology and Parasitology, Representative of National Taiwan University, Guest speakers, the participants, distinguished guests ladies and gentlemen,

It is a great honor for me to give the opening address of the 4thAsian Society of the Veterinary Pathologists Conference which is held at Chulalongkorn University, Bangkok, Thailand on 19-20 November 2009. On behalf of Chulalongkorn University, I would like to welcome all the participants to the conference. Under the theme of *"Era of the Modern Diagnostic Pathology"*, emphasizes the progress of the diagnostic pathology with discovery of emerging diseases concerns human, animals and environment, I hope all of you will get benefits from the meeting by sharing experiences and learning from persons who share the same academic interests and eventually be able to implement the Pathological knowledges for prevention and control of animals and also wildlife health. Please continue our good friendship and collaboration in this field to promote an active and fruitful 4th ASVP 2009.

I would like to take this opportunity to thank all of the organizers for their supports, Faculty of Veterinary Science, Chulalongkorn University, as the host. Most of all, I wish to thank the Organizing Committee, the Thai Association of the Veterinary Laboratory Diagnostician, the Veterinary Oncology Center in the Innovation Center for Veterinary Teaching and Service on Companion Animal, the Zoological Park Organization under the Royal Patronage of His Majesty the King, all the International organizations, private sectors, and delegates who have contributed to organize and promote the 4th ASVP 2009. Let us open the conference and wish that we are going to have a successfully cooperation and friendship.

Thank you

"The 4th Asian Society of Veterinary Pathologists Conference"
The 4th ASVP 2009
19-20 November 2009
Chulalongkorn University, Bangkok, Thailand
Opening Ceremony
Thursday 19th November 2009
Institute Building III Auditorium, Chulalongkorn University

Report

by Assoc. Prof. Dr. Achariya Sailasuta
President of the Asian Society of the Veterinary Pathologists and Chairman of the Organizing Committee of the 4th ASVP 2009

The honorary President of Chulalongkorn University, Dean of the Faculty of the Veterinary Science, the Faculty member committee, President of the Thai Association of the Veterinary Laboratory Diagnostician, Head of the Innovation Center for Veterinary Teaching and Service in Companion Animal, Deputy Director General the Zoological Park Organization under the Royal Patronage of H.M. the King, the international committee, President of Asian Foundation for the Advancement of Veterinary and Animal Science, CL Davis Foundation for the Advancement of the Veterinary and Comparative Pathology, President of the Federation of Asian Veterinary Associations, President of the Asian Society Wildlife Pathology and Parasitology, Representative of National Taiwan University, Guest speakers, the participants, distinguished guests ladies and gentlemen,

The Faculty of Veterinary Science, Chulalongkorn University is honored by the Asian Society of the Veterinary Pathologists to host of the 4th Asian Society of the Veterinary Pathologists Conference under the theme *"Era of Modern Diagnostic Pathology"* with the collaboration of the Thai Association of Veterinary Laboratory Diagnostician, the Veterinary Pathology Society of Thailand, the Veterinary Oncology Center in the Innovation Center for Veterinary Teaching and Services in Companion Animal, the Zoological Park Organization under the Royal Patronage of His Majesty the King, Asian Foundation for the Advancement of Veterinary and Animal Science, CL Davis Foundation for the Advancement of the Veterinary and Comparative Pathology, The Federation of Asian Veterinary Associations, Asian Society Wildlife Pathology and Parasitology and National Taiwan University. This is the first time of the conference in Thailand. The conference is held at the Institute Building III Auditorium, Chulalongkorn University, during 19-20 November 2009. It includes the renowned 11 guest lectures, 61 poster presentations and 9 pathology slide discussion. The conference bring together approximately 180 participants from Asian and other regions of the world. All of whom will have a chance to discuss and exchange ideas or experiences with mutual interest in diagnostic pathology including oncology, zoo and wildlife pathology and emerging diseases on veterinary public health concerns. The organizing committee is very grateful to the sponsorships from private sectors.

I would like to take this opportunity to invite the President of Chulalongkorn University, Prof. Dr. Pirom Kamolrattanakul to give an opening address for the 4th Asian Society of the Veterinary Pathologists Conference

Program of the 4th Asian Society of Veterinary Pathologists (ASVP) Conference and Annual Meeting of The Thai Association of Veterinary Laboratory Diagnosticians (TAVLD)

Thursday 19 November 2009

08:00-08:45 AM	**Welcome Talk & Meeting and Registration**
08:45-8:50 AM	**The Opening Ceremony:** Prof. Dr. Pirom Kamolrattanakul *President of Chulalongkorn University*
09.00-12.00 AM	
Plenary session:	**Emerging and Re-emerging Disease in Animals: Epidemiology, Diagnosis, Control and Prevention**
09:00-09:30 AM	**A Visit from an Old Friend, Swine Influenza** Prof. Dr. Roongroje Thanawongnuwech*, *CUEIDA, Chulalongkorn University, Thailand*
09:30-10:00 AM	**Avian Influenza-Current and Perspective** Assoc. Prof. Dr. Alongkorn Amornsin, *CUEIDA, Chulalongkorn University, Thailand*
10:00-10:30 AM	**Avian Influenza in Animals** Assoc. Prof. Dr. Taweesak Songserm, *Kasetsart University, Thailand*
10.30-10.45 AM	*Morning Coffee Break*
10:45-11.30 AM	**Suppression of Rabies Virus Propagation in Mice Brain by Intracerebral Immunization of Inactivated Virus** Prof. Dr. Takashi Umemura, *President of the Japanese Society of Veterinary Pathologists*
11.30-12.10 AM	**Mammalian Models for Studies of Transmission of Highly Pathogenic Avian Influenza A (H5N1) Viruses with Meat from Infected Poultry** Dr. Yong Kuk Kwon *The National Veterinary Science and Quarantine Service (NURQS), Republic of Korea*
12:10-01:30 PM	*Lunch*
01:30-02.45 PM	**Necropsy Show and Tell** Prof. Dr. Nam Yong Park, *The CL Davis Foundation for the Advancement of Veterinary and Comparative Pathology, Republic of Korea*
02.45-03.00 PM	*Afternoon Break and Poster Session*

03.00-04:30 PM	**Descriptive Gross and Microscopic Veterinary Pathology, Necropsy, Biopsy and Surgical Pathology** Prof. Dr. Paul. C. Stromberg, *The CL Davis Foundation for the Advancement of Veterinary and Comparative Pathology, USA*
04:30-05.15 PM	**Pathology of Hepadna Virus Infection in Humans and Animals** Prof . Dr. Kenji Abe, *National Institute of Infectious Diseases, Japan*
05.15-06.00 PM	**Clinical Trials of Adipose Derived Stem Cells and Muscle Derived Stem Cells** Prof. Dr. Kyu-Shik Jeong, *Kyungpook National University, Republic of Korea*
04.30-06.00 PM	Meeting of The Asian Society of Veterinary Pathologist (ASVP) Meeting of The Veterinary Pathology Society of Thailand (VPST) Meeting of The Thai Association of Veterinary Laboratory Diagnosticians
06:30-08:30 PM	*Welcome Reception*

Friday 20 November 2009

08:30-10:00 AM	**Diagnostic Cytology in Veterinary Clinical Medicine** Prof. Dr. Hiroki Sakai, *Gifu University, Japan*
10:00-10:30 AM	*Morning coffee/Poster Session*
10:30-12:00 AM	**An Oncological Histopathological and Cytological Diagnosis** Prof. Dr. Donald Meuten, *The CL Davis Foundation for the Advancement of Veterinary and Comparative Pathology, USA* *President of American College of Veterinary Pathology (ACVP)* Prof. Dr. Mary Anna Thrall, *The CL Davis Foundation for the Advancement of Veterinary and Comparative Pathology, USA*
12:00-01:30 PM	*Lunch*
01:30-04.30 PM	**Slide Discussion** **Poster Session**
04.30-05.00 PM	**Closing Ceremony**

Program of the 4th Asian Society of Veterinary Pathologists (ASVP) Conference and Annual Meeting of The Thai Association of Veterinary Laboratory Diagnosticians (TAVLD) November 19-20, 2009 Bangkok, Thailand

Poster presentation

Canine Grade III Chondrosarcoma

Y. H. Kim, B. I. Yoon, I. C. Park, H. H. Kwak, J. H. Han*

School of Veterinary Medicine and Institute of Veterinary Science, Kangwon National University, 192-1, Hyoja-dong, Chuncheon, Gangwon 200-701, Republic of Korea

**Corresponding author: kslippy@daum.net*

Keywords: *canine, chondrosarcoma, S-100*

Introduction

Chondrosarcoma of the tumors originated in thoracic wall is the second most common primary bone tumor. However, when compared to osteosaroma, chondrosarcoma is few and far between in the dogs. Chondrosarcoma can be divided into two sub-classes, skeletal and extraskeletal chondosarcoma. In cases of masses of the thoracic wall, the most common developing location is on the seventh rib and at the costal-chondral junction, but can also occur in the sternum. The most common clinical sign is a visible growing mass on the thoracic wall. This tumor frequently affects middle-aged to older, ranging from 5.9 to 8.7 years, and medium to large dogs, especially boxers, German shepherds, golden retrievers and various mixed breeds, being rare in small breeds. Golden retrievers were at a higher risk of developing chondrosarcoma than any other breeds. Chondrosarcoma is malignant tumor in which the neoplastic cells produce variable quantities of cartilaginous or fibrillar matrix. We report this case of chondrosarcoma metastasized to lymph node and lung in a dog.

Materials and Methods

A three-year-old, male, mixed dog was presented to the hospital at the school of veterinary because of a mass on the left axillary region. The plain thoracic radiopgraph revealed a huge well-defined mass of left thoracic cavity and lysis of second rib. The oppression of mass induced an abnormal position of left first, third, forth, and fifth rib. Necropsy findings revealed a firm, white and smooth circumscribed mass in the thoracic wall (approximately 13x15x17cm in diameter) and center of the mass was filled with gelatinous and necrotic tissues. Diffused small and white nodules were also found in lung. The representative tissues were collected in 10% phosphate buffered formalin and were processed for histopathological and immunohistochemical staining, for S-100 (rabbit polyclonal anti-S-100; DAKO Inc., Carpinteria, CA, USA; 1:500) using the avidin-botin complex method according to the manufacturer's instructions

Result and Discussion

This neoplasm revealed variably disorganized lobules of chondrocytes within a chondroid matrix. The chondrocytes of various sizes and shapes were irregularly dispersed within an abundant cartilage matrix. Binucleated cells sometimes were not only present, but mitotic figures were present in tumor tissue. Frequently, the neoplasm was subdivided by bundles of collagenous tissue septae. At the center of the lobules, the neoplastic cells were individualized or congregated within lacunae surrounded by amorphous basophilic chondroid matrix, whereas peripheral cells of the lobules were similar in mesenchymal precursors of cartilage without the lacunae. Some lacunae contained more than one cell. Histological feature of this case was in accordance with Grade III in that it showed marked pleomorphic nuclei, hypercellularity and spindle cell type in the peripheral zone as well as pulmonary metastasis. Cartilage matrix in the tumor stained deeply with alcian blue-PAS staining. Neoplastic cells were also evident in the parenchyma of the lung and cortex of mandibular and pulmonary lymph node with cartilage matrix formed. The liver underwent congestion and pigmentation about the central vein due to chronic passive congestion in the lung. An immunohistochemical analysis showed that S-100 do not only distributed consistently throughout both the cytoplasm and nucleus, with cytoplasm reacting more strongly, but neoplastic cells also demonstrated cytoplasmic immunoreactivity against vimentin in the thoracic wall, lymph nodes and lung. Based on the results, this case originating in rib was confirmed as canine chondrosarcoma which be metastasized to the lung and lymph nodes through lymph vessel. In the best knowledge, this is the first report of chondrosarcoma of grade III in dog in Korea

Fig. 1 The VD radiograph (A). A huge mass of the lefr thoracic cavity. Tumor gross findings (B). Masses on both sides of thoracic wall.

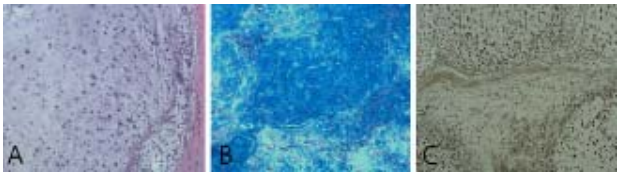

Fig. 2 Neoplastic cells, have one to four nuclei, are in lacunae surrounded by cartilage matrix Primary tumor of rib. H&E (A). Matrix and nuclei of neoplasm were positive for Alcian blue-PAS staining (B) and for S-100 (C), respectively. Magnification: x 100.

References

1. Fletcher et al., 2007. Churchill Livingstone. 3rd ed.: 1608-1613.
2. Thompson et al., 2007. Elsevier Saunders, Philadelphia. 5th ed.: 121-124.

Lack of Adaptive Response of Gamma Radiation for Protection against Neutron-induced Teratogenesis

H. Lee[1], J. Kim[1], M. Song[2], H. Seo[2], C. Moon[2], J. Kim[2], S. Jo[3], S. Kim[2*]

[1]Korea Institute of Radiological & Medical Science, Seoul, Korea 139-706 [2]College of Veterinary Medicine, Chonnam National University, Gwangju, Korea 500-757 [3]Advanced Radiation Technology Institute, KAERI, Jeongeup, Korea 580-185
[*]Corresponding author: shokim@chonnam.ac.kr

Keywords: *adaptive response, mouse, neutron, teratogenesis*

Introduction

Although there are some reports on neutron teratology, there is little information on the adaptive response of gamma radiation for protection against neutron-induced teratogenesis. This study examined whether or not a low dose of gamma radiation can induce an adaptive response in mouse fetuses exposed to a subsequent dose of neutrons *in vivo*.

Materials and Methods

Pregnant ICR mice were exposed to a priming dose of 0.3 Gy (0.9Gy/min) of gamma-rays on day 10.5 of gestation and challenged with 0.8 Gy (0.94 Gy/min) of neutrons 24 h later. The mice were sacrificed on day 18.5 of gestation. The fetuses were examined for mortality, growth retardation and other morphological abnormalities.

Table 1. Effects of Priming Dose at 0.3 Gy of Gamma-rays on Day 10.5 of Gestation Prior to a Challenging Dose at 0.8 Gy of Neutrons on Day 11.5 of Gestation on the Caesarean Section Findings in Mice

Observations	Sham exposure	Gamma-rays (0 .3 Gy)	Neutrons (0.8 Gy)	Gamma-rays (0.3 Gy) + neutrons (0.8 Gy)
No. of mother	6	6	6	6
No. of implants	12.3±1.8	13.7±1.5	13.7±2.6	11.3±4.3
No. of embryonic death	0.50±0.55	0.17±0.41	0.16±0.40	0.33±0.50
No. of fetal death	0.33±0.52	0	0.83±1.17	1.17±0.98
No. of resorption	0	0.67±0.52	1.00±0.89	0.50±0.55
Prenatal mortality (%)	6.45±7.27	5.76±4.90	15.27±10.32	21.43±14.65*
Live fetuses	11.50±1.52	12.83±0.98	11.67±1.75	9.33±4.13
Body weight (g)	1.59±0.09	1.51±0.08	0.85±0.08**	0.85±0.10**
Body length (cm)	3.45±0.63	3.48±0.42	2.53±0.12**	2.53±0.20**
Head length (cm)	1.15±0.05	1.14±0.04	0.78±0.03**	0.78±0.02**
Head width (cm)	0.84±0.02	0.80±0.03**	0.65±0.03**	0.65±0.05***
Tail length (cm)	1.25±0.03	1.10±0.05**	0.96±0.04**	0.84±0.16***
GRF No.(%)	5 (7.25)	20 (25.97)**	70 (100)**	56 (100)**
Fetuses with decreased head length (%)	2.90	25.97**	100**	100**
Fetuses with decreased head width (%)	1.45	5.19	100**	100**

The values are presented as means ± SD.
GRF: Growth retarded fetuses, calculated as the number of growth retarded fetuses/total number of live fetuses. Fetuses weighing less than two standard deviations of mean body weight of the control group were considered as growth retarded.
A head width or length of less than two standard deviations of mean the control value was defined decreased head width or length.
*Indicates a significant difference at $p<0.05$ compared with the sham exposure group.
**Indicates a significant difference at $p<0.01$ compared with the sham exposure group.
***Indicates a significant difference at $p<0.01$ compared with the sham exposure group and neutrons (0.8 Gy) group.

Results and Discussion

The tail length in the 0.3 Gy of gamma-rays + 0.8 Gy of neutrons group was significantly shorter than in the 0.8 Gy of neutrons group. Although there was no significant difference compared with the 0.8 Gy of neutrons group, the number of live fetuses in the 0.3 Gy of gamma-rays + 0.8 Gy of neutrons group was lower. There was no evidence of primed exposure-related reductions in the malformed fetuses. Although there was no significant difference compared with the unprimed group, the number of malformed offspring in the primed group was higher. Furthermore, the incidence of kinked tail and adactyly was significantly higher in the primed mice than in the unprimed mice. Overall, this study shows that exposure to 0.3 Gy of gamma-rays failed to induce an adaptive response of fetogenesis to a neutron challenge dose.

Table 2. Effects of Priming Dose at 0.3 Gy of Gamma-rays on Day 10.5 of Gestation Prior to a Challenging Dose at 0.8 Gy of Neutrons on Day 11.5 of Gestation on the Fetal Morphological Findings in Mice

Observations	Sham exposure	Gamma-rays (0 .3 Gy)	Neutrons (0.8 Gy)	Gamma-rays (0.3 Gy) + neutrons (0.8 Gy)
External malformation				
Fetuses examined	69	77	70	56
Thread-like tail	0	0 1	(1.43)	0
Short tail	0	0	3 (4.29)	5 (8.93)*
Kinked tail	0	1 (1.30)	28 (40.00)**	44 (78.57)***
Adactyly	0	0	2 (2.85)	8 (14.28)***
Ectrodactyly	0	0	33 (47.14)**	24 (42.86)**
Internal malformation				
Fetuses examined	35	39	35	30
Dilated cerebral ventricle	0	0	2 (5.71)	0
Cleft palate	0	0	10 (28.57)**	6 (20.00)*
Skeletal malformation				
Fetuses examined	34	38	35	26
Fused thoracic centrum	0	0	2 (5.71)	0
Fused lumbar centrum	0	0	1 (2.86)	2 (7.69)
Absent caudal vertebra	0	0	2 (5.71)	2 (7.69)
Misshapen caudal centrum	0	0	2 (5.71)	0
Fused caudal centrum	0	0	13 (37.14)**	19 (73.08)**
Absent rib	0	1 (2.63)	3 (8.57)	2 (7.69)
Wavy rib	0	0	3 (8.57)	2 (7.69)
Short rib	0	0	1 (2.86)	0
Bent tibia	0	0	1 (2.86)	1 (3.84)
Bent fibula	0	0	1 (2.86)	0
Absent metatarsal	0	0	5 (14.29)	2 (7.69)
Absent metacarpal	0	0	4 (11.43)	3 (11.53)
Absent phalanx	0	0	17(48.57)**	14(53.85)**
Malformed offspring	0	2 (2.60)	47 (67.14)**	50 (89.29)**

Number in the parenthesis means percentage of n for each parameter.
*Indicates a significant difference at $p<0.05$ compared with the sham exposure group.
**Indicates a significant difference at $p<0.01$ compared with the sham exposure group.
***Indicates a significant difference at $p<0.01$ compared with the sham exposure group and significant difference at $p<0.05$ compared with the neutrons (0.8 Gy) group.

Effect of HemoHIM on Ovarian Morphology and Expression of Nerve Growth Factor in Rats with Steroid-induced Polycystic Ovaries

S. Kim[1*], H. Lee[2], J. Kim[1], C. Moon[1], J. Kim[1], C. Bae[1], H. Park[3], U. Jung[3], S. Jo[3]

[1]College of Veterinary Medicine, Chonnam National University, Gwangju, South Korea 500-757 [2]Korea Institute of Radiological & Medical Science, Seoul, South Korea 139-706 [3]Advanced Radiation Technology Institute, Korea Atomic Energy Research Institute, Jeongeup, South Korea 580-185 [*]Corresponding author: shokim@chonnam.ac.kr

Key words: *HemoHIM, nerve growth factor, polycystic ovary*

Introduction

Estradiol valerate (EV)-induced polycystic ovaries (PCO) in rats cause the anovulation and cystic ovarian morphology. Presently, we investigated whether the treatment of HemoHIM influences the ovarian morphology and the expression of nerve growth factor (NGF) in an EV-induced PCO rat model.

Materials and Methods

PCO was induced by a single intramuscular injection of EV (4 mg, dissolved in sesame oil) in adult cycling rats. HemoHIM was either administered orally (100 mg/kg of bw/day) for 35 consecutive days or injected intraperitoneally (50 mg/kg of bw) every other day after EV injection.

Results and Discussion

Ovarian morphology was almost normalized and NGF was normalized in the PCO+HemoHIM group. HemoHIM lowered the high numbers of antral follicles and increased the number of corpus luteum in PCO ovaries. The results are consistent with a beneficial effect of HemoHIM in the prevention and treatment of PCO syndrome.

Table 1. Body and ovary weight measurements

Group	Body weight (g)	Ovaries weight (mg) per g body weight
Oil control	244.5±15.5	0.43±0.08
PCO	226.3±19.9	0.27±0.03
PCO + HemoHIM[1]	232.2±13.4	0.32±0.04*
PCO + HemoHIM[2]	223.5±17.6	0.31±0.07

Table 2. Number of corpus luteum in the largest cross section of the ovary

Group	Number of corpus luteum
Oil control	11.2±3.2
PCO	2.4±1.3
PCO+HemoHIM[1]	5.0±2.2*
PCO+HemoHIM[2]	4.8±1.6**

Results are expressed as mean±S.D.
The Sprague-Dawley female rats (n=7) were injected with estradiol valerate (EV) and were autopsied 35 days later.
[1]HemoHIM (100 mg/kg of bw/day, p. o.) was given for 35 days after EV injection.
[2]HemoHIM (50 mg/kg of bw) was given i.p. once every other day for 35 days after EV injection.
*p<0.05 versus the PCO group.

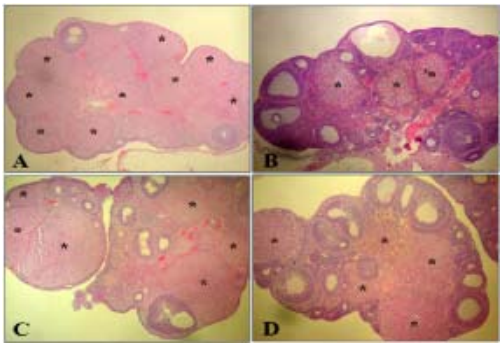

Fig. 1 Ovarian morphology. (A) Oil control group. (B) Polycystic ovary (PCO) group. (C) PCO+HemoHIM 100 mg/kg (p.o.) group. (D) PCO+HemoHIM 50 mg/kg (i.p.) group. Hematoxylin and eosin stain, x 40. *depicts corpora lutea.

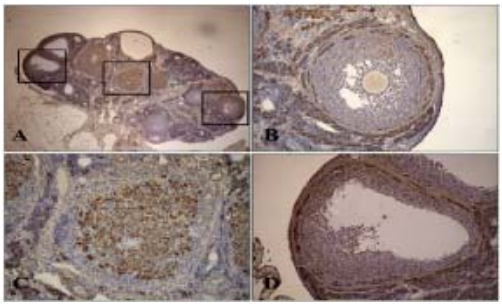

Fig. 2 Representative ovarian distribution of nerve growth factor by immunohistochemistry in the ovary tissue of an estradiol valerate-treated rat. Survey view (A) showing regressed corpus lutea, atretic follicles, and healthy growing follicles. Detailed view (B) of a healthy growing follicle (framed right area in A). Detailed view (C) of a regressed corpus luteum (framed middle area in A). Detailed view (D) of an atretic follicle (framed left area in A).

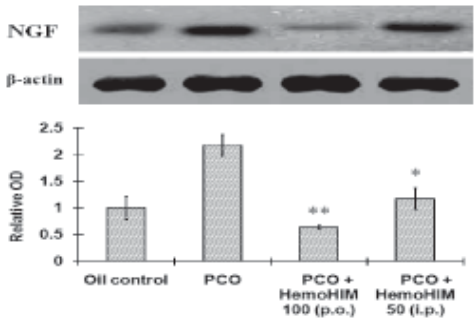

Fig. 3 Nerve growth factor (NGF) protein levels in the ovaries by western blot analysis. Ovary tissue from polycystic ovary (PCO) rats contained significantly higher levels of ovarian NGF protein than oil control ovary tissue. The level of NGF protein in ovary samples from PCO + HemoHIM rats was significantly lower than in samples from PCO rats. The relative optical densities (OD) of NGF expressions were determined by densitometry and normalized to the β-actin signals from three different samples. Values for oil controls were arbitrarily defined as 1. Values are given as mean ± S.E. *p<0.05, **p<0.01 versus the PCO group.

Differential CARM1 Expression in Prostate and Colorectal Cancers

Y.R. Kim[1], B.K. Lee[2], R.-Y. Park[1], N.T.X. Nguyen[1], D.D. Kwon[3,4], C. Jung[1,4*]

[1]Departments of Anatomy, [2]Emergency Medicine, [3]Urology, [4]Research Institute of Medical Sciences, Chonnam National University Medical School, Gwangju, Korea [*]Corresponding author: chjung@chonnam.ac.kr

Keywords: *CARM1, colorectal cancer, prostate cancer*

Introduction

Coactivator-associated arginine methyltransferase 1 (CARM1) functions as a transcriptional coactivator mainly studied in its association with nuclear hormone receptors. CARM1 showed significant role in androgen-stimulated androgen receptor (AR)-mediated transactivation. Recently, overexpression of CARM1 was shown to be involved in the development of prostate cancer (PCa), including androgen-independent PCa.

Materials and Methods

An attempt to profile an expression pattern of CARM1 in human cancers, tissue microarray was utilized to immunolocalize CARM1. To confirm the expression of CARM1, surgical specimen with full clinical data were further utilized, including colorectal cancers and androgen-refractory prostate cancers. To validate CARM1ís action mechanism in non-hormone mediated signaling pathway, reporter transcription assay was employed in various cancer cells.

Results and Discussion

Tissue microarray showed that CARM1 was particularly overexpressed in colorectal cancers while CARM1 expression was not prevalent in other tumors, including prostate and breast cancers (Table 1). Further studies using surgical specimen demonstrated that CARM1 was highly overexpressed in 75% of colorectal cancers (38 out of 54) (Fig. 1A) but not in androgen-independent PCa compared to androgen-responsive tumors (Fig. 1B). In addition, CARM1's coactivating function in AR-mediated transactivation was very minimal in androgen-independent cells. Further assays using PSA promoter showed minor coactivating function in both androgen-dependent and androgen-independent cells implying that there may be other factors that CARM1 affects (Fig. 2A-B). Correspondingly, CARM1 showed either suppressive or promoting roles in p53 and NF-kappaB target gene transcription, respectively (Fig. 2C-D). This study suggests that, in addition to its role in hormone receptors, CARM1 may function as transcriptional modulator for other growth regulators through non-AR mediated transactivation in androgen independent PCa and colorectal cancers. However, CARMís action of mechanism needs to be further clarified.

Table 1. Score of CARM1 expression in human tumors

Tumor types	Score of CARM1 expression*					
	0	1	2	3	0-1**	2-3**
Brain tumor	22	10	3	0	32	3 (8 %)
Melanoma	25	5	2	3	30	5 (14 %)
Ovarian cancer	22	7	5	1	29	6 (17 %)
Lymphoma	58	9	8	1	67	9 (12 %)
Lung cancer	61	25	8	2	86	10 (10 %)
Breast cancer	31	22	15	5	53	20 (27 %)
Colorectal cancer	16	17	39	31	33	70 (68 %)
Prostate cancer	85	17	5	2	102	7 (6 %)

*, CARM1 expressionwas scored as followed: 0, no; 1, low; 2, moderate; 3, high
**, Scores were categorized by-0 as normal expression and 23 as overexpression

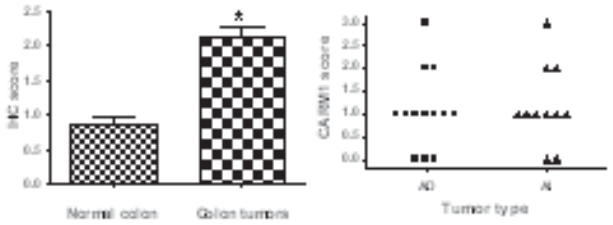

Fig. 1 Immuolocalized CARM1 was scored and demonstrated as either bar graph (A) or scattered plot (B). A. colorectal cancers, B. prostate cancers; *denoted $p<0.05$; AD, androgen dependent; AI, androgen-independent.

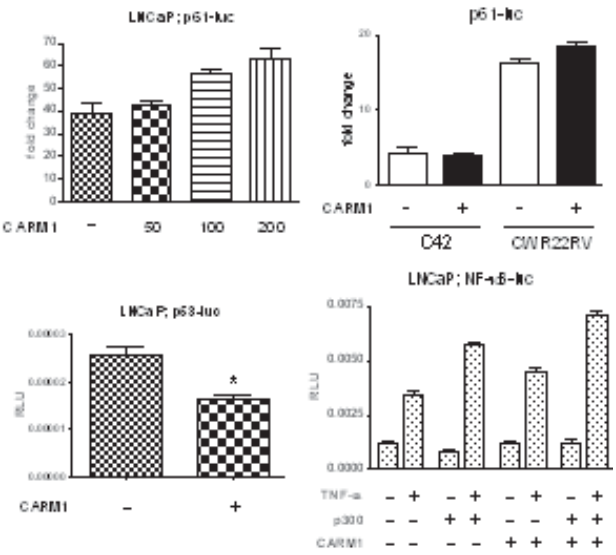

Fig. 2 CARM1 regulates p53- and NF-kappaB mediated response in addition to androgen-stimulated PSA response. Reporter transcription assay was performed in LNCaP cells with cotransfection of CARM1 and indicated luciferase DNA. Bar is shown as mean ± SD. P61-luc uses whole PSA promoter.

One Step Reverse Transcription Loop-mediated Isothermal Amplification for Influenza A Rapid Detection

H. M. Tun[1], M. Wongphatcharachai[1], T. Wisedchanwet[1], P. Kitikoon[2], A. Amonsin[1*]

[1]Department of Veterinary Public Health, [2]Department of Pathology, Faculty of Veterinary Science, Chulalongkorn University, Bangkok, Thailand 10330 [*]Corresponding author: heinmin@gmail.com

Keywords: *influenza A, loop-mediated isothermal amplification, reverse transcription*

Introduction

Influenza viruses are segmented negative-sense single strand RNA viruses that belong to the family Orthomyxoviridae. The influenza viruses can be divided into types A, B or C and type A influenza virus can further divided into different subtypes according to its surface glycoproteins, i.e. hemagglutination (HA) and neuraminidase (NA). Among these 3 types, Influenza A viruses infect humans, pigs, horses, seals and whales as well as a variety of domestic and wild birds (5). It is generally accepted that in the human influenza pandemics and numerous outbreaks in domestic and wild animals, interspecies transmission of Influenza A viruses have played a crucial role (2). Three times during the last century, influenza A viruses caused major pandemics, i.e. "Spanish flu" 1918, "Asian flu" 1957 and "Hong Kong flu" 1968, with a high mortality rate all over the world (6). And also recently the new strain of Influenza A virus caused the pandemic flu so called "Pandemic H1N1" 2009 (7). Therefore, a lot of surveillance networks had been established and were still establishing to prepare for the next influenza pandemic. For the influenza A, the viral isolation technique (VIT) is still as a gold standard diagnostic tool. But this method can be performed only by specialized laboratories, and 3 to 10 days is required for the availability of the results. Some rapid detection and easy to perform antigenic detection tests are helpful such as immunofluorescence (IFA) assays (4) and reverse transcription-PCR (8). However IFA assays have limited sensitivity compared to VIT and also need of sophisticated equipments for the application of PCR techniques. A choice of diagnostic technology can now be based on a combination of factors that includes fitness-for-purpose, technical ease, speed, sensitivity, specificity and cost (1). The loop-mediated isothermal amplification (LAMP) assay is sensitive and easy to perform when compared with reverse transcriptase-PCR. In addition, the assay is not required any expensive special equipment, such as thermal cycler. Therefore, the LAMP method would be suitable for the mobile surveillance and for unequipped laboratories in developing countries (3). In this study, we developed one step RT-LAMP technique for rapid detection of influenza A viruses.

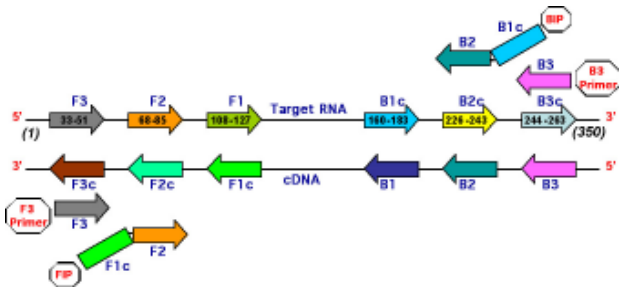

Fig. 1 Design of RT-LAMP primers

Materials and Methods

Designing the RT-LAMP primers: The LAMP primers were designed using Primer Explorer V3 software based on a conserved region of M gene identified by sequence alignment (Fig. 1).

RNA standard for detection limit (sensitivity) and specificity test: Influenza A virus (A/chicken/Thailand/CU-K2/2004 (H5N1)) was used for sensitivity test as reference virus. Total RNA was extracted from 140 µl of allantoic fluid using QIAamp Viral RNA Mini Kit (Qiagen GmbH, Hilden) according to the manufacturer's specifications. The concentration of the RNA was measured by NanoDrop1000. The RNAs were then serially diluted 10-fold. The specificity of RT-LAMP was tested against other RNA viruses caused animal diseases which are porcine reproductive and respiratory syndrome virus (PRRSV), classical swine fever virus (CSFV), Infectious bronchitis virus (IBV) and Newcastle disease virus (NDV).

RT-LAMP detection: The LAMP reaction was carried out in a volume of 25 µl containing 1x ThermoPol buffer (NEB, USA), 0.4mM dNTPs, 8mM of $MgSO_4$, 0.2 µM each of F3 and B3, 1.6 µM of FIP and BIP, 0.04 M betaine (Sigma), 5U cloned AMV reverse transcriptase (Invitrogen, USA), 8U Bst polymerase (NEB, USA) and 2 µl of RNA. To optimize the LAMP assay condition, an evaluation was

taken on the effects of reaction time (30-70 minutes) and reaction temperature (60-65°C) and then for 10 minutes at 80°C to terminate the reaction. All amplification steps were taken by using water bath.

Results and Discussion

Optimal condition for RT-LAMP assay: The effects of temperature (60, 63, 65°C) and time (30, 40, 50, 60, 70 minutes) were tested. The optimal condition for RT-LAMP assay was determined to 63°C for 1 hour then followed by 80°C for 10 minutes (Fig. 2).

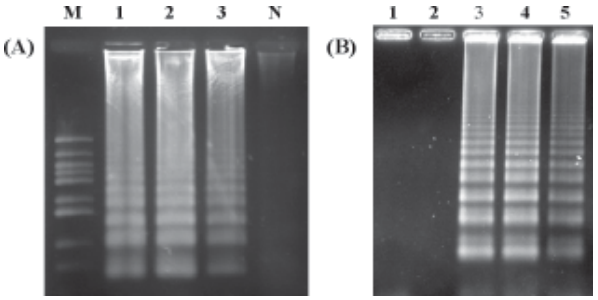

Fig. 2 Optimization of RT-LAMP reaction. (A) The effect of temperature: lane 1-3 (60, 63 and 65°C). (B) The effect of reaction time: lane 1-5 (30, 40, 50, 60 and 70 minutes).

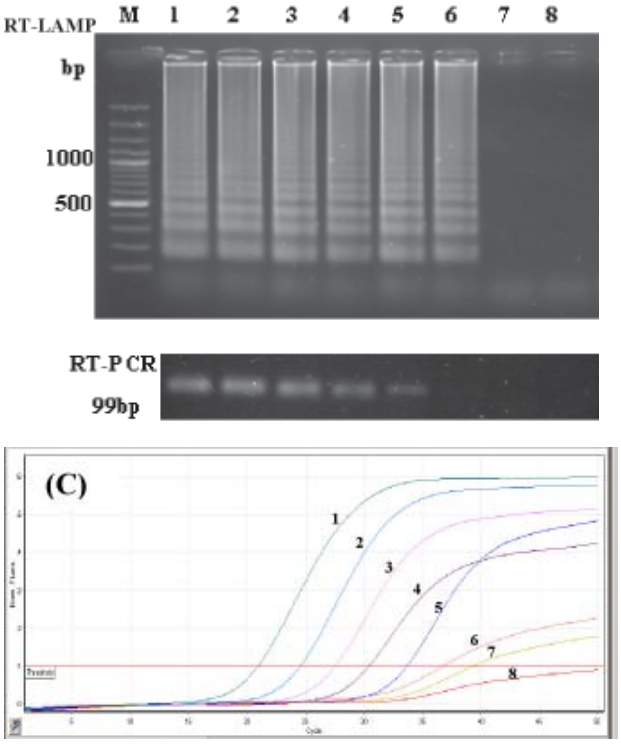

Fig. 3 (A) The sensitivity of RT-LAMP, (B) conventional one step RT-PCR and (C) real-time RT-PCR. (A, B) Lane M: DNA markers, lane 1-7: 170,000 pg, 17,000 pg, 1,700 pg, 170 pg, 17 pg, 1.7 pg and 0.17 pg of RNAs respectively and lane 8: negative control. (C) Line 1-7: 170,000 pg (Ct 21), 17,000 pg (Ct 24), 1,700 pg (Ct 27), 170 pg (Ct 30), 17 pg (Ct 33), 1.7 pg (Ct 36) and 0.17 pg (Ct 39) of RNAs and line 8: negative control.

Detection limit of RT-LAMP assay: The detection limit of RT-LAMP on M genes was 1.7 picograms of RNA which is equivalent to Ct 36 in real-time RT-PCR assay and also 10 times more sensitive when compared with conventional one step RT-PCR (17 pg).

Specificity of RT-LAMP assay: The specificity of RT-LAMP was tested against other veterinary RNA viruses and the result shown that high specificity of LAMP primers to influenza A virus.

In the present study, we developed a rapid and high sensitive influenza A detection system without the need of highly expensive equipment. This RT-LAMP assay was highly specific to influenza A and 10 times more sensitive than ordinary one step RT-PCR assay. In the future, we expected to apply this developed RT-LAMP assay to test the clinical samples and apply in the field together with easy RNA preparation where minimal laboratory facilities were provided.

Acknowledgements

We would like to thank the staffs from Veterinary Diagnostic Laboratory, Faculty of Veterinary Science, Chulalongkorn University for their assistant.

Reference

1. Charlton et al., 2009. Comp. Immunol. Microbiol. Infect. Dis. 32(4): 341-350.
2. Fouchier et al., 2003. Vaccine 21(16): 1754-1757.
3. Notomi et al., 2000. Nucleic Acids Res. 28(12): E63.
4. Waner et al., 1991. J. Clin. Microbiol. 29(3): 479-482.
5. Webster et al., 1992. Microbiol. Rev. 56(1): 152-179.
6. World Health Organization, 2005. Available from http://www.who.int/csr/disease/influenza/pandemic10things/en/
7. World Health Organization, 2009. Available from http://www.who.int/csr/disease/swineflu/en/
8. Yamada et al., 1991. Microbiol. Immunol. 35(3): 259-265.

Lectin Histochemistry Assay in Colon Tissues for Characterization of Rodents

A.S. Abdulamir[1*], F.Y. Moghaddam[2], J. R.R. Hafidh[1], F.A. Baker[1], L.I. Kadhim[3]

[1]Microbiology research, IBS, University Putra Malaysia, Malaysia [2]Department of Biology, School of Science, Ferdowsi University of Mashhad, Iran [3]Faculty of Veterinary Medicine, University Putra Malaysia, Malaysia
[*]Corresponding author: ranria77@yahoo.com

Keywords: *colon, glycoconjugate, histochemistry, lectins, rodents,*

Introduction

Lectins are ubiquitous proteins of non-immune origin which are present in animals and humans. Lectins bind specifically monosaccharides or oligosaccharide structures (1). The digestive tract of animals including rodents has taxonomic and ecologic importance due to its ability in adaptation for different environments. Whereas colon absorbs water and carbohydrates; it has a vital role ecologically and physiologically and enjoys different histological structures in different rodents with various diets (2). Nowadays, Wheat Germ Agglutinin (WGA), Peanut Agglutinin (PNA) and Concavilin (Cona) are being used widely for studying sugar compounds on the surface of cells (3). Few studies have investigated glycoconjugates in the gastroenteric mucosa by lectin histochemical methods. The aim of this current study is to investigate the characteristic distribution of certain glycoconjucates that exist in the colon of various species of rodents by means of lectin histochemistry for phylogenic characterization.

Materials and Methods

Ten different species of rodents that belong to different families were selected. The involved rodents were belonging to many families including the family of Muridae; consisting of Gerbilinae subfamily *(Jerbillus nanus, Meriones Persicus, Meriones lybicus) Microtinae (Microtus transcaspicus, Ellobius fascocapillus, Microtus sp) Dipodidae (Alactage elater, Jucullus blanfordi) and scuridae (Funambulus penantii, spermophillus folvus)*. The digestive tract of all involved rodents was removed properly and weight was measured and then the proximal colon was cut into 2-3 cm segments, fixed by Bouin solution and 4 μm thick paraffin-embedded sections were made and sections were stored at 4°C for later use. Lectin histochemistry assay was conducted.

Lectin histochemistry assay: Lectin binding was performed as previously reported by Ferri et al (4). Briefly, two horse-raddish peroxidase (HRP)-conjugated lectins were used (Sigma, USA), PNA and WGA. 200 μg of lectins were diluted in 800 μl of 0.1M Phosphate-Buffered Saline (PBS). Two sections of colon were chosen and then hydrated and rinsed for 10 min in 0.1M PBS (pH 7.4). Rehydrated sections were exposed to 3% H_2O_2 for 10 min and then incubated for 30 min at 20°C with peroxidase-labeled lectin in 0.1M PBS. The activity of the HRP was then visualized histochemically by adding 2-3 drops of 0.005% 3-3-diaminobenzidine (DAB) (Sigma, USA) All sections were counterstained with 1% solution of Alcian Blue at pH 2.5 for 5 min. The intensity of the labeling was classified as shown in (Table 1).

Table 1 The scoring system used for assessing the staining intensity of lectin binding assay (5)

Description	Grades
Negative reaction	-
Weak	+
Moderate	++
Severe	+++
Very severe	++++

Results and Discussion

Microscopic observations indicated that there were remarkable distinctions in the carbohydrates and glycoproteins content of the different layers of colon among different species of rodents. Both PNA and WGA lectin histochemistry showed high and significant discriminatory power among the studied species of

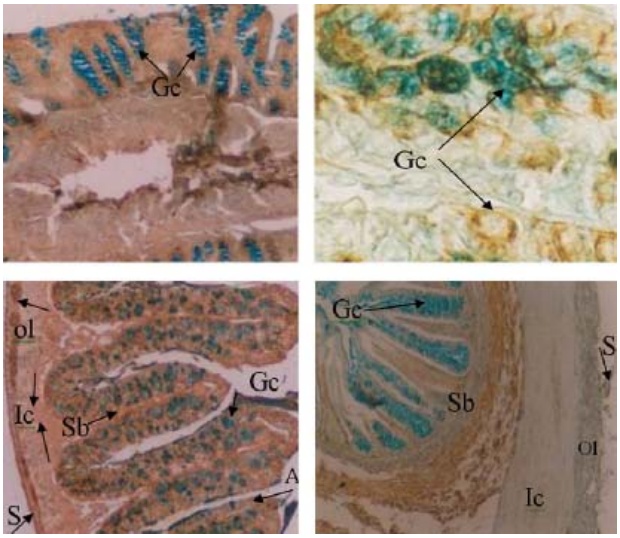

Fig. 1 (Upper left) transverse sections of proximal colon in *Funumbulus pennantii* (F.p) in reaction with PNA lectin at magnification 100X. Gc: Goblet cells showed no lectin reaction. (Upper right) transverse sections of proximal colon in *Meriones lybicus* (M.l) in reaction with WGA lectin at magnification 100X. Gc: Goblet cells, severe reaction was observed. (lower left) transverse section of proximal colon in *Ellobius fascocapillus* incubated with WGA at magnification 100X. S: Serosa layer with very severe reaction, Ol: Outer longitudinal muscle layer with severe reaction, Ic: Inner circular muscle layer with weak reaction, Sb: submucosal layer with moderate reaction, Gc: Goblet cells with no reaction, A: Absorptive cells with moderate reaction. (lower right) transverse sections of proximal colon in *Alactage elater* (A.e) with PNA lectin at magnification 100X. Sb: submucosal layer, moderate reaction. S: Serosa layer, Ol: Outer longitudinal muscle layer, and Ic: Inner circular muscle layer, Gc: Goblet cells all showed no reaction with lectin.

rodents especially lectin staining in mucosal and absorptive cells ($p<0.05$) (Fig. 1). Goblet and epithelial cells showed much lower affinity to lectins. No reaction of PNA was observed in longitudinal muscle layer, circular muscle layer, goblet cells in channel and in surface of most studied rodents. Weak to moderate reaction of PNA was observed in other layers of colon. Severe reaction was observed in serosa layer of all studied rodents except dipodidae family *Alactaga elater and Jaculus blanfordi*. Weak to strong reaction of WGA was observed in different layers of colon of rodents except in goblet cells in channel, basement and surface epithelium compartments of most rodent species. It was concluded that the use of lectin histochemistry is a valid method for the phylogenic characterization of rodents, may be other animals, depending on colon tissues. Moreover, colon tissues proved to be highly distinct and variable among rodent species. Therefore, this assay can also be used in determining the diet nature, geographical variation, diseases affection on different species of animals.

References

1. Peetermans et al., 2005. Acta. Clin. Belg. 60: 329-337.
2. Wu, 2003. J. Biomed. Sci. 10: 676-688
3. Faraidi et al., 1996. Eur. J. Histo. Chem. 40: 67-74.
4. Ferri et al., 1992. Acta. Histochem. 93: 341-349.
5. Gong et al., 1997. Exp. Eye Res. 64: 587-595.

Pathological Investigation of Reproductive Organs of Culled Boars in Thailand

K. Teankum[1*], R. Thanawongnuwech[1], P. Tummarak[2], S. Kesdangsakonwut[1], S. Lacharoch[1], J. Singlor[2], A. Kunavongkrit[2]

[1]Department of Pathology, [2]Department of Obstetrics and Gynaecology and Reproduction, Faculty of Veterinary Science, Chulalongkorn University, Bangkok, Thailand [*]Corresponding author: Komkrich.T@chula.ac.th

Keywords: *atrophy, boar, degeneration, fibrosis, testis*

Introduction

Infertility of boars is an important factor for culling and leads to an economic loss. Pathological changes of reproductive organs of boars result in poor semen quality and infertility. Various lesions of infertile/subfertile boars have been documented including testicular degeneration, hypoplasia, segmental aplasia of Wolffian ducts1 and inflammation. In Thailand, the data concerning pathology of culled boars are inadequate; therefore, this slaughter-house-based study was conducted. The objective of this study was to determine the prevalence of pathological changes of testes of culled boars.

Materials and Methods

The genital organs of boars (n = 100) from slaughter houses were pathologically examined. For histopathology, 3 sections of each testis were fixed in 10% formalin and the adjacent sections were put in Bouin's solution.

Results and Discussion

The culling causes included infertility (n = 30), old age (n = 9), leg problems (n = 13), scrotal enlargement (13%, n = 13), scrotal enlargement with leg problems (n = 2), other problems (n = 8), and the remaining had no information. The pathological findings were summarized in Table 1.

In the present study, testicular fibrosis was the most frequent lesion (n = 85), mainly occurred in mild and moderate degree. This lesion was usually accompanied with degeneration, but sometimes it could occur without degeneration. Testicular fibrosis could be the consequence of myoid cells alteration into myofibroblast[2]. The cause of the lesion is unknown but it might be associated with viral infection in cattle[3].

The second most frequent lesion found in the testes was various degrees of seminiferous tubule degeneration (n = 73). The mechanism of degeneration is related to apoptosis of germ cells, which might be the results of toxic substance or viral infection(1,4). Interestingly, small-sized testes so called testicular atrophy were often observed (n = 20) (Fig 1). The lesion was sometimes associated with various degrees of non-suppurative interstitial orchitis,

Table 1. Lesions of reproductive organs of culled boars

Lesions	Numbers / Severity			%
	+	++	+++	
Testicular fibrosis	36	28	21	85
Testicular degeneration	25	29	19	73
Testicular atrophy	5	3	12	20
Suppurative orchitis	1			1
Non-suppurative interstitial orchitis	24	12	3	39

+: mild, ++: moderate, +++: severe

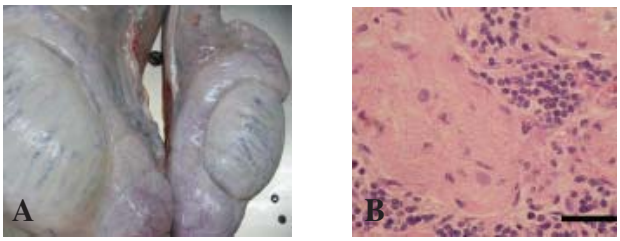

Fig. 1 Severe testicular atrophy of right testis (A), Bar = 1 cm. Histology of Fig. 1 A showing atrophic seminiferous tubules (S), with interstitial orchitis. (B), Bar = 25 μm

fibrosis and degeneration. However, the etiology of the lesion is still unclear.

In conclusion, the results suggested that testicular fibrosis and degeneration were the two most frequent lesions found in the reproductive organs of culled boars in Thailand. Though, the causes of these lesions could not be definitely determined, but clinical examinations and pathological findings could indicate the causes of infertility.

Acknowledgements

This work was financially supported by the Thailand Research Fund and Commission on Higher Education.

References

1. Kopp et al., 2008. Theriogenology 70: 1129-1135.
2. Yoshikawa et al., 2001. J. Equine Sci. 12: 9-15.
3. Barth et al., 2008. Anim. Reprod. Sci. 106: 274-288.
4. Sur et al., 1997. J. Virol. 71: 9170-9179.

Cyclophosphamide Induces Deficit for Hippocampus-dependent Learning and Memory

J.S. Kim[1], M. Yang[1], M.S. Song[1], J.C. Kim[1], C.S. Bae[1], S.S. Kang[1], S.H. Kim[1], T. Shin[2], C. Moon[1*]

[1]College of Veterinary Medicine, Chonnam National University, Gwangju 500-757, South Korea
[2]College of Veterinary Medicine, Jeju National University, Jeju 690-756, South Korea
[*]Corresponding author: toxkim@chonnam.ac.kr

Keywords: *cognitive impairment, cyclophosphamide, hippocampus, neurogenesis*

Introduction

Cyclophosphamide (CYP), a cytotoxic alkylating agent, is commonly used as an antineoplastic agent for the treatment of various cancers, as well as an immunosuppressive agent for organ transplantation, systemic lupus erythrematosus and other benign diseases.

Cognitive impairment occurs in a subset of cancer survivors and is generally subtle. Most evidence suggests an association with chemotherapy although other factors associated with the diagnosis and treatment of cancer may contribute.

In this study, we examined the behavioral change of adult mice after CYP injection by hippocampus-dependent learning paradigms. In addition, the effect of cancer chemotherapy on hippocampal neurogenesis was investigated by examining the changes in the number of DCX (immature cell marker)- and Ki-67 (proliferating cell marker)-positive cells in the dentate gyrus (DG) of hippocampus of adult mice after administration of CYP.

Materials and Methods

The behavioral dysfunction in the mice after receiving an intraperitoneal injection of CYP (40 mg/kg) was measured by open field analysis (n = 8 mice/group), passive avoidance (n = 9 mice/group), and object recognition memory test (n = 9 mice/group) at 12 h and 10 days after injection, respectively.

To elucidate the effects of CYP on neurogenesis in the adult mouse hippocampus after receiving an intraperitoneal injection of CYP (40 mg/kg), the mice were sacrificed and the hippocampi were then dissected from each group at 12, 24 h, 3 and 10 days (n = 6 mice/group) after CYP treatment.

Results and Discussion

CYP-treated mice showed normal locomotor activity. Compared to vehicle-treated controls, mice were trained 12 h after CYP treatment induced a deficit in memory of passive avoidance task and object recognition task tested 24 h after training, but mice 10 days after CYP treatment did not show any memory defect.

The Ki-67- and DCX-positive cells in the DG were decreased significantly by 6-24 h after the CYP injection (40 mg/kg), and then recovered to normal levels similar to the non-treatment controls.

In conclusion, we suggest that a cancer chemotherapeutic agent, cyclophosphamide, is sufficiently detrimental to interrupt the functioning of the hippocampus including learning and memory, possibly through the inhibition of neurogenesis.

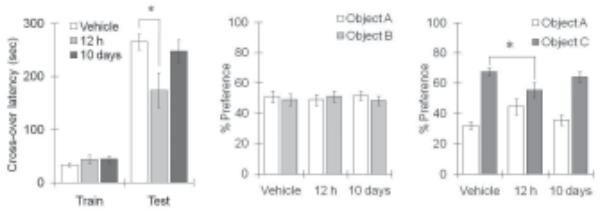

Fig. 1 CYP transiently inhibits memory retention in passive avoidance (left panel) and object recognition memory tests (middle and right panels).

Ki-67 immunoreactivity

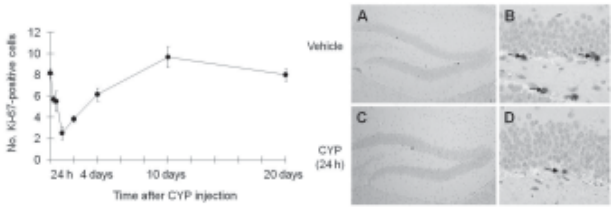

Fig. 2 CYP transiently decreases proliferating cells (Ki-67-positive cells) in the adult DG of hippocampus. (AñD) Representative images showing the Ki-67-positive cells in the DGs of adult hippocampi taken from the vehicle controls and mice 24 h after CYP injection.

DCX immunoreactivity

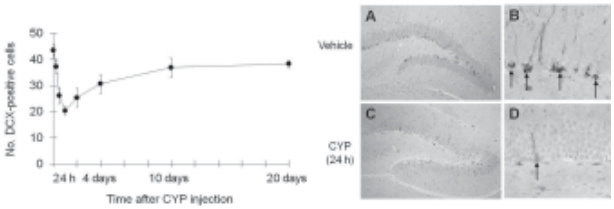

Fig. 3 CYP transiently decreases immature neuron (DCX positive cells) in the adult DG of hippocampus. (AñD) Representative images showing the DCX-positive cells in the DGs of adult hippocampi taken from the vehicle controls and mice 24 h after CYP injection.

Acknowledgment

This work was supported by National Research Foundation of Korea Grant funded by the Korean Government (2009-0068372).

Spermatotoxicity and Oxidative Stress of Epichlorohydrin in Sprague-Dawley Rats

I.S. Shin, J.H. Lim, S.H. Kim, K.H. Kim, N.H. Park, C. Moon, S.H. Kim, J.C. Kim*

College of Veterinary Medicine, Chonnam National University, Gwangju, Korea 500-757
**Corresponding author: toxkim@chonnam.ac.kr*

Keywords: *epichlorohydrin, oxidative stress, rats, reproductive dysfunction, sperm*

Introduction

Epichlorohydrin (ECH) is one of the industrial chemicals used in the manufacture of glycerol, epoxy resins, and other products. Due to its increased production and widespread use, the human exposure to ECH has steadily increased, which may result in severe health impacts.

Previous studies demonstrated that ECH is an anti-fertility agent that acts both as an epididymal toxicant and an agent capable of directly affecting sperm motility. Although it is suggested that the anti-fertility effects of ECH maybe resulted from reduced sperm motility and sperm metabolism, the mechanism underlying the ECH-induced sterility has not been fully elucidated.

In this study, we examined the spermatotoxicity and epididymal oxidative damage of ECH after repeated oral administration in male rats to better understand a possible mechanism for the spermatotoxicity of ECH.

Material and Methods

Male rats aged 6 weeks were administered ECH daily by gavage at 0, 3.3, 10, and 30 mg/kg/day for 10 weeks and sacrificed 24 h after the last administration of ECH. Spermatotoxicity was assessed by measurement of reproductive organ weights, testicular spermatid count, epididymal sperm count, motility and morphology, and histopathology. Oxidative stress was assessed by the measurement of malondialdehyde (MDA), reduced glutathione (GSH), catalase, superoxide dismutase (SOD), and glutathione-S-transferase (GST) in epididymis.

Results and Discussion

General findings: The high dose group showed treatment-related clinical signs including nasal discharge (n=4), soft feces (n=1), depression (n=2), and piloerection (n=3). The number of animals with clinical signs (n=7) was significantly increased when compared with the control group. There were no statistically significant differences in the body weight and food consumption between the groups.

Autopsy findings: Cystic pustule of the epididymidis was observed in 5 cases of the high dose group. However, the incidence of gross pathology finding observed in the group was not significantly different compared with the controls. No significant difference between the groups was seen for any reproductive organ weight measured.

Sperm findings: Testicular Spermatid count, epididymal sperm count, and sperm motility in the high dose group were significantly decreased in a dose-dependent manner compared with those of the control group. On the contrary, sperm morphological abnormalities including folded tail, short tail and no tail in the high dose group was significantly increased in comparison to the control group.

Histopathologic findings: There was a significantly higher incidence of histopathological findings in the 30 mg/kg group than the control values. Spermatic granuloma (n=6), cell debris in the ducts (n=12), epithelial cell desquamation (n=6), epithelial cell vacuolization (n=9), and oligospermia (n=3) were observed in epididymis of the 30 mg/kg group. Cell debris in the ducts (n=3) and epithelial cell vacuolization (n=6) were also found in the 10 mg/kg group.

Oxidative stress: The concentration of MDA in the 10 and 30 mg/kg groups was significantly increased in a dose-dependent manner when compared with the control group. On the contrary, the concentration of GSH was significantly decreased in all of treatment groups when compared with the control group (Fig. 3). The activities of catalase, GST, and SOD in the 10 and 30 mg/kg groups were also significantly lower than controls.

The increased incidence of cystic pustule was considered to be treatment-related effect, since this finding is uncommon in normal control rats and is consistent with the significantly increased incidence of histopathological alterations. Histopathologic changes observed in the present study included spermatic granuloma, cell debris in the ducts, desquamation of the epithelial cells, vacuolization of the epithelial cells, and oligospermia in the epididymidis.

The significant decrease of testicular spermatid count, epididymal sperm count, and sperm motility and the significant increase of sperm abnormalities observed in the high dose group were also considered to be related to the ECH administration because these changes were remarkable and showed a clear-cut dose-response relationship.

The animals treated with ECH showed decreased activities of antioxidant enzymes catalase, GST, and SOD and GSH concentration, while increased concentration of MDA in the epididymis in a dose-related manner. Increased lipid peroxidation and reduced levels of antioxidants of epididymis in rats treated with ECH may indicate an increased ROS generation and could be closely linked to its effect on the epididymal and sperm indices.

It can be concluded that administration of ECH to male rats at ≥10 mg/kg/day elicits spermatotoxicity and oxidative damage in the epididydis and that the adverse effects of ECH on spermatotoxicity may be at least partially due to the induction of oxidative stress in the epididymis.

Acknowledgment

This work was supported by the Regional Research Centers Program (Bio-housing Research Institute), granted by the Korean Ministry of Education, Science and Technology.

Postmortem Radiographic Diagnosis of Pneumothorax in Dogs

I.O. Abdulazeez, M.M. Noordin*, R. Ibrahim, M.D. Zuki

Department of Pathology and Microbiology, Faculty of Veterinary Medicine, Universiti Putra Malaysia, UPM Serdang, Selangor D.E., 43400

Corresponding author: noordin@vet.upm.edu.my

Keywords: *dog, pneumothorax, postmortem, radiography*

Introduction

Commonly used technique of incision into the thoracic cavity during necropsy is a major factor in the reduced ability to clearly diagnose pneumothorax at postmortem in dogs (3). Two-D X-radiography has been shown to be of high sensitivity and specificity in its clinical diagnosis, but have not been employed for such at necropsy (2). Advances have been made in forensic radiology in human autopsy leaving a wide gap to fill in the veterinary practice (1, 4). This study assesses the ability of diagnosing pneumothorax at postmortem examination using relatively simple and inexpensive X-radiography.

Materials and Methods

Five euthanized laterally recumbent canine carcasses were injected with 300-700 ml of air using 18G 20 ml syringe (Terumo®, Philippines) through the 7th and 8th intercostals space. Lateral (right and left) and ventrodorsal radiographic views of the carcasses were taken at 0, 60 and 120 min. Radiographs were read and interpreted blindly by UPM VTH radiologists to generate a table for sensitivity and specificity. Severity of lesion was classified as severe, moderate or mild if it spans over 2/3rd, 2/3rd or 1/3rd of the rib length, respectively.

Results and Discussion

A 100% sensitivity and specificity was recorded in the ability of radiography to diagnose pneumothorax at postmortem with (table 1) or without anamnesis (table 2). Anamnestic back up for the radiographs did not appear to have any influence on the interpretation of the radiographs for pneumothorax (Fig 1, 2). This may be due to the obvious gas opacity observable in the thoracic cavity as well as the leafing of the lungs signifying compression and collapse (Fig 3). Severity of the lesion was diagnosed based on 100% sensitivity with 63% of the radiographs being interpreted as severe, 27% moderate and 10% as mild (Table 3). These values corresponded with 300 to 400 ml of air for mild, 400 to 500 ml for moderate and 500 to 700 ml for severe. The crossover of values resulted from the method of measuring and interpreting the severity of the lesions. The mean radiolucent span of the rib length was

Table 1 Diagnosis of postmortem pneumothorax with/ without anamnesis

	Positive	Negative	Total
Pneumothorax +	45	0	45
Pneumothorax -	0	45	45

Table 2 Diagnosis of postmortem pneumothorax with/ without anamnesis

	Positive	Negative	Total
Pneumothorax +	45	0	45
Pneumothorax -	0	45	45

Table 3 Measurement of severity of pneumothorax from 45 radiographs

	Pneumothorax (%)
Severe	63
Moderate	27
Mild	10

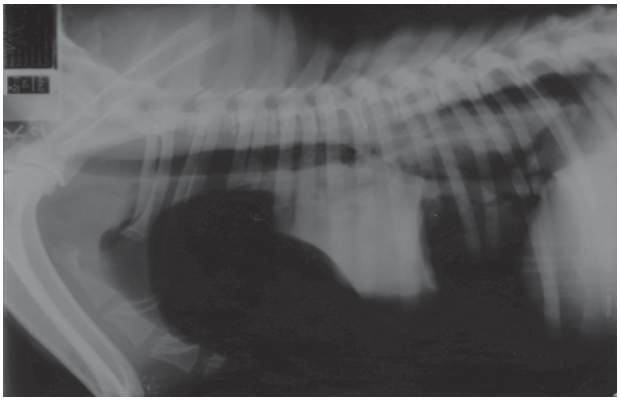

Fig. 1 Showing gas opacity on left lateral view.

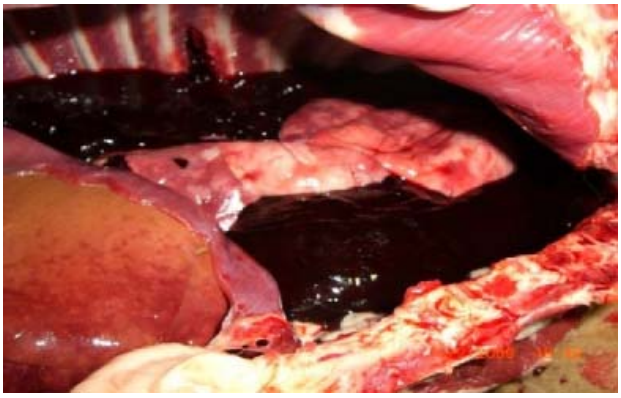

Fig. 3 showing collapsed lung at postmortem examination

taken for right and left lateral and ventrodorsal views, subjecting the values to variations effected by radiographic positioning causing fluctuations in the location of air in the thoracic cavity. Gross necropsy did not reveal a positive diagnosis of pneumothorax except for decreased negative pressure on puncture of the diaphragm.

Fig. 2 Showing gas opacity on ventrodorsal view

Postmortem radiographic diagnosis of pneumothorax is 100% specific and sensitive whereas positioning for such may affect the interpretation of severity of lesion, however the positioning technique does not require a specialist. Routine survey postmortem radiography of the thorax is valuable in the accurate diagnosis of pneumothorax in dogs.

References

1. Dirrnhofer et al., 2006. Radiographics 26: 1305-1333.
2. Hopper et al., 2004. Vet. Rad. Ultrasound 45(2): 136-138.
3. Masseau et al., 2008. Can. Vet. J. 49: 261-267.
4. Thali et al., 2007. Leg Medicine 9: 100-104.

The Effects of Gemifloxacin on Achilles Tendon in Immature Rats

D.M. Oh[1], S.E. Kim[1], Y.S. Kim[1], K.M. Shim[2], S.S. Kang[1], C.S. Bae[1*]

[1]*College of Veterinary Medicine, Chonnam National University, Gwangju 500-757, Republic of Korea*

[2]*Department of Radiology, Nambu University, Gwangju 506-706, Republic of Korea*

[*]*Corresponding author: csbae210@chonnam.ac.kr*

Keywords: *Achilles tendon, gemifloxacin, rat, tendopathy*

Introduction

Gemifloxacin is one of the recently developed fluoroquinolones. It is a potent, novel quinolone with broad-spectrum antibacterial activity against both Gram-negative and Gram-positive pathogens. The side effect profiles such as diarrhea, rash, nausea, and headache are similar to those of the older members of this class.

Tendopathy is one of the major adverse effects caused by quinolone antibacterial agents, but the incidence of tendopathy is generally low at the clinical doses of the quinolones used. This study examined the effects of gemifloxacin on the Achilles tendon in immature rats with ofloxacin and ciprofloxacin used as a comparison. A relatively high dose of quinolones, which can induce tendopathy and/or arthropathy in juvenile rats, was used in this study.

Materials and Methods

The test chemical, gemifloxacin (Factive, LG Life Sciences Ltd., Daejon, Korea) was dissolved in a saline solution and ofloxacin and ciprofloxacin were suspended in a saline solution and administered by gavage. The individual dose volume (10 ml/kg bw) was determined according to the body weight immediately before administration.

The rats were treated once daily for 5 days by oral intubation with gemifloxacin at 0 (vehicle), and 600 mg/kg body weight. The animals were treated from postnatal day 30 to day 34 before being sacrificed, and samples were collected within 24 h after the final dose. Other rats of the same age were treated with either ofloxacin or ciprofloxacin at 600 mg/kg (once daily for 5 days).

The Achilles tendon samples were prepared from the right foot of five rats from each dosage group. Tangential sections were made from the distal part of the tendon. The specimens were examined by transmission electron microscopy (TEM, Hitachi H-7600, Japan).

Results and Discussion

In comparison with the vehicle-treated controls, there were ultrastructural changes in all samples from the gemifloxacin, ofloxacin-, and ciprofloxacin-treated rats. Degenerative changes were observed in the tenocytes, and the cells that detached from the extracellular matrix were recognizable.

The degree of degenerative changes and the number of degenerated cells in the Achilles tendon were significantly higher in the treated group than in the control group. Moreover, among the quinolone-treated groups, these findings were most significant in the ofloxacin-treated group, and least significant in the gemifloxacin-treated group.

Quinolones are antibacterial agents that have the potential to cause Achilles tendon disorders such as tendinitis or even ruptures. Quinolone treatments are contraindicated in juveniles and are only used in pediatrics in rare cases. A number of toxicological studies have confirmed that quinolone-induced tendopathy is a drug-induced, dose-dependent toxic effect of these agent. Kato et al. described quinolone-induced tendopathy after the single oral administration of pefloxacin or ofloxacin. Tendon lesions were induced in immature rats (4 wks of age) but not in 12-week-old rats. Tendon lesions were inhibited by the co-administration with dexamethasone and N-nitro-*L*-arginine methyl ester. In contrast, catalase, indomethacin, pyrilamine, and cimetidine did not modify these tendon lesions. This suggests that nitric oxide and 5-lipoxygenase products partly mediate fluoroquinolone-induced tendon lesions.

Recent experiments have shown that ultrastructural alterations in tenocytes can be observed in immature and adult rats after being treated with quinolones. These effects were more pronounced when the animals were simultaneously given a magnesium-deficient diet, suggesting that the pathophysiology of tendopathy resembles that of arthropathy. When Shakibaei & Stahlmann examined the Achilles tendons from the quinolone-treated adult rats by electron microscopy 4-12 wks after treatment with single oral doses of ofloxacin, levofloxacin or fleroxacin, they could detect specific, pathological alterations already at the lowest dose (30 mg/kg), which increased in severity with increasing dose. The tenocytes detached from the extracellular matrix and showed degenerative changes such as multiple vacuoles and large vesicles in the cytoplasm, which resulted from swelling and dilatation of the cell organelles. Other findings were a general decrease in the fibril diameter and an increase in the distance between the collagenous fibrils.

The effects of gemifloxacin are of special interest because of the low chondrotoxic potential. It is unclear how ultrastructural changes in the Achilles tendons from immature rats relate to the potential risk in juvenile patients treated with gemifloxacin. However, these results underline the fact that, in principle, this new fluoroquinolone with a pyrrolidine derivative at the C-7 position has less potential to cause changes in the connective tissue structures. Further toxicological and clinical studies will be needed to characterize the conditions under which quinolone-induced tendon lesions develop.

Comparative Histological and Histochemical Inter-species Investigation of Mammalian Submandibular Salivary Glands

R.R. Hafidh*, A.S. Abdulamir, F. A. Baker

Institute of Bioscience (IBS), University Putra Malaysia (UPM), 43400 Serdang, Selangor, Malaysia

**Corresponding author: ranria77@yahoo.com*

Keywords: *histochemistery, histology, mucin, rodents, salivary, submandibular*

Introduction

Salivary glands have an important role in terrestrial animals, provide lubrication for eating and vocalization, aide digestion and supply saliva for pH buffering (1). Salivary glands of rodents are important elements regarding their adaptations to different diets, environments, and taxonomic studies (2). To reach a delicate analysis between biology and ecology of different animals, such as rodents, there is a need to study the salivary glands histology and histochemistry. Mucosal units react strongly with staining techniques, Alcian blue (AB) and PAS. Hence, this was exploited to conduct a histochemical interspecies analysis of submandibular salivary glands in rodents as a representative for mammalian animals.

Materials and Methods

The specimens of Funambulus pennati from Scuridae, *Cricetulus migratorius, Meriones libycus, Mus musculus, Nesokia indica and Apodemus sp.* from Muridae and two specimens from Dipodidae family *Allactaga elater and Jaculus blanfordi* were collected from different regions of Khorasan (Tandoureh Park, Moghan, Gonabad, Birjand and Kashmar). The whole skull was selected because it is hard to locate definitely the submandibular glands. Moreover, histological autopsy may harm the gland tissue. After washing blood off the heads with normal saline, they were placed in separate labeled buckles containing bouin's fixative. Tissue preparation histology process, microtomy and staining were done. Staining was done with hematoxylin-eosin, tetrachrome, PAS alcian blue (pH=1) and PAS alcian blue (pH=2.5). The slides of all species were studied and compared with each other.

Results and Discussion

Microscopic histological features, including existence of mucus and serous acini, presence of different kinds of tubules, and different types of ducts were shown of valuable discriminatory value. In detail, distinctive and characteristic features of the histological investigations were found regarding mucus glands, their ducts, serous gland ducts, the presence or absence of serous demilunes at mucous acini, and position of demilunes on mucous parts. Serous and mucous acini were found in the majority of submandibular glands of hamster *Nesokia indica, Cricetulus migratorius, Allactaga elater, Funambulus pennati, Meriones libycus* and *Apodemus sp.* However, Jaculus blanfordi contains only serosa acini. Based on the resulted histochemical characteristics, there were remarkable differences among the studied species. In addition, the histochemistry of acini in serosal glands showed that most of the species possess neutral mucin. And there are no mucins in ducts of the major sub mandibular glands of all species. At two different pH levels, there was weak acidic and sulfated mucin in acini of different species. In addition, laboratory hamster can be differentiated from other species because of the lack of acidic mucin in mucosal acini. There were many differences between convoluted granular tubule and acini in major submandibular glands of all studied species. Convoluted granular tubules in *Mus musculus* were abundantly present more than serous acini but in *Nesokia*

indica, laboratory hamster, *Cricetulus migratorius, Funambulus pennati, Meriones libycus, Allactaga elater, Jaculus blanfordi and Apodemus sp.,* serous acini were higher than convoluted granular tubule. There were also many differences in the types of ducts and types of dominancy of ducts among the studied species. In accessory submandibular glands, the histochemistry of serosa acini, serous demilunes, and the dominancy of mucin based on (sulfomucins sulfate mucins, sialomucins, and neutral mucins) were significantly different among the studied families and subfamilies. Moreover, the dominancy of acini and convoluted tubules and histochemistry of convoluted tubules and serosi acini based on (sulfomucins and acidic mucin and neutral mucins) were different among the studies species (Fig. 1, 2). Therefore, these comparative criteria revealed good inter-species discriminatory potential, the differences can be used very effectively in the comparative inter-species studies, and these differences might be related to factors other than environment and feeding factors. The histological and histochemical characteristics of accessory and major sub mandibular glands showed that these glands are good targets structures in mammalian comparative analysis and should not be ignored by investigators and reflect a good application in veterinary pathology for studying the relatedness of species in regards of certain diseases (3).

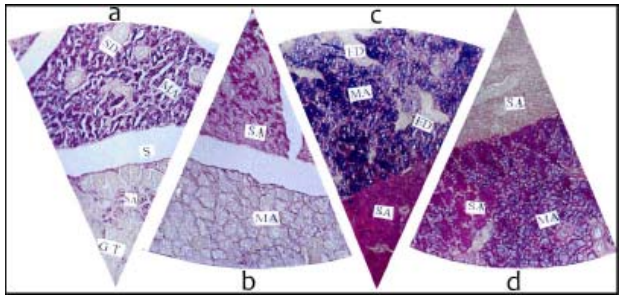

Fig. 1 PAS-Alcian blue (pH1) in major submandibular salivary glands of (a) *Mus musculus*, (b) *Laboratory hamster*, (c) *Allactaga elater* (d) *Apodemus sp*.

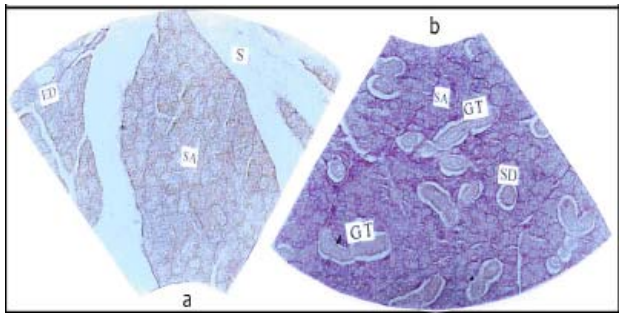

Fig. 2 PAS-Alcian blue (pH 1) in accessory submandibular salivary glands of (a) *Funambulus pennati* (b) *Cricetulus migratorius.*

References

1. Jaskoll et al., 2002. Cells Tiss. Org. 170: 83-90.
2. Stimson et al., 2007. J. Clin. Endocrinol. Metab. 92: 4480-4484.
3. Yamada et al., 2006. Biochem. Biophys. Res. Commun. 346: 386-392.

Effect of Salvianolic Acid B (Sal B) on Osteogenesis of Mouse Mesenchymal Stem Cells

K. M. Shim[1], S. E. Kim[2], C. S. Bae[2], S. S. Kang[2*]

[1]Department of Radiology, Nambu University, Gwangju, Korea 506-706 [2]College of Veterinary Medicine, Chonnam National University, Gwangju, Korea 500-757 [*]Corresponding author: vetkang@chonnam.ac.kr

Keywords: *mesenchymal stem cell, osteogenesis, salvianolic acid B,*

Introduction

The dried root of Salvia miltiorrhiza Bunge (Danshen) is a popular Traditional Chinese Medicine and has been widely used in both Asian and Western countries for the treatment of various diseases including cerebrovascular diseases, coronary artery diseases, and myocardial infarction. Salvianolic acid B (Sal B; Fig. 1) is the most abundant and bioactive component of salvianolic acid in Danshen. Extensive pharmacological studies have been carried out on this compound. The purpose of this study was to evaluate the cell-biomaterial interaction and the osteogenic capacity of Sal B.

Materials and Methods

The mouse D1 cells were cultured in the presence of osteogenic differentiation (ODM; DMEM with 10% FBS, antibiotics, 50 ug/ml sodium ascorbate, 100 nM dexamethasone, 10 mM b-glycerophosphate) for 6 days, then MSCs were treated to Sal B (3.2~50 μg/ml). Two days later the cells were used for the tests. The cell proliferation was analyzed using MTT assay. Alizarin red staining was done for mineralization. Alkaline phosphatase activity was measured using a commercial ELISA kit.

Results and Discussion

The D1 cells in the culture of ODM differentiated into osteoblasts. The stain by Alizarin red S revealed much higher intensity in ODM cultures with Sal B treatment of 3.2, 6.3, 12.5, 25, 50 μg/ml. The Alizarin red staining had increased with the ODM+Sal B culture (Fig. 2). The cell cytotoxicity of Sal B was not detected (Table 1). The activity of ALP, a marker of osteoblast differentiation, increased after Sal B treatment, as depicted in Table 2.

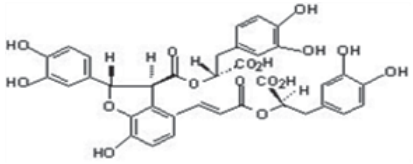

Salvianolic acid B (Sal B)

Fig. 1 Salvianolic acid B structure.

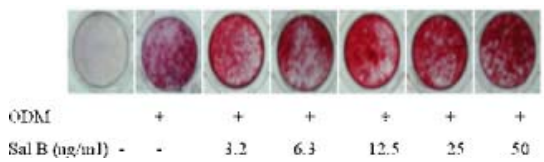

Fig. 2 Mineralization assay of mouse D1 cells treated with salvianolic acid B (3.2-50 μg/ml) was measured by using the Alizarin red staining. Accumulation of calcium was increased dose dependently.

Table 1. Effect of salvianolic acid B on mouse D1 cell viability

Group	Cell viability (%)
DMEM	100.0±3.9
ODM	98.0±4.0
Sal B 3.2 μ/ml	96.0±3.7
Sal B 6.3 μ/ml	98.0±4.9
Sal B 12.5 μ/ml	94.0±4.9
Sal B 25 μ/ml	96.0±4.5
Sal B 50 μ/ml	83.0±4.7*

*$p<0.0005$ as compared with the DMEM control group.
Values are expressed in mean±S.D. (n=3), DMEM: Dulbecco's Modified Eagle's Medium (control), ODM: osteogenic differentiation media (DMEM, 50 μ/ml sodium ascorbate, 100 nM dexamethasone, 10 mM β-glycerophosphate).

Table 2. Effect of salvianolic acid B on ALP activity of mouse D1 cell

Group	ALP activity (%)
DMEM	100.0±21.2
ODM	177.5±20.0
Sal B 3.2 μ/ml	187.0±23.5
Sal B 6.3 μ/ml	185.1±20.7
Sal B 12.5 μ/ml	194.2±53.7
Sal B 25 μ/ml	255.4±81.5
Sal B 50 μ/ml	453.0±82.2*

*$p<0.05$ as compared with the DMEM control group, Values are expressed in mean±S.D. (n=3), DMEM: Dulbecco's Modified Eagle's Medium (control), ODM: osteogenic differentiation media (DMEM, 50 μ/ml sodium ascorbate, 100 nM dexamethasone, 10 mM β-glycerophosphate)

Salvianolic acid B (Sal B) is the main hydrophilic constituent of Danshen. Previous studies have demonstrated that it has potentiality to improve angiogenesis, osteoblast activity and new bone formation. In this study, we examined the effect of Sal B on osteogenesis of mesenchymal stem cells *in vitro*. The cell proliferation was analyzed using MTT assay. Alizarin red staining was done for mineralization. Alkaline phosphatase (ALP) activity for cell metabolism was analyzed using a commercial ELISA kit. The mouse MSCs (D1 cells) were converted toward osteoblasts by ODM media culture and Sal B treatment. In the present experiment, ALP activity was significantly stimulated after Sal B treatment (Fig. 2). This phenomenon was supported by the fact that MSCs differentiated into osteoblasts by Sal B.

These data suggest that Sal B enhances the osteogenic differentiation of the mouse mesenchymal stem cells

Acknowledgement

This work was supported by the Korea Research Foundation Grant funded by the Korean Government (KRF-2007-331-E00269).

Histomoniasis in Broilers: Case Report

A. Kamlangdee[1], A. Yensuk[2], R. Jam-on[2], N. Sinwat[2], K.Witoonsatien[2], N. Upragarin[2] C. Siriwan[3], P. Siriwan[3], T. Songserm[1*]

[1]Department of Pathology, [2]Department of Farm Resources and Production Medicine, Faculty of Veterinary Medicine, Kasetsart University, Kamphaengsaen, Nakhonpathom, Thailand 73140, [3]National Institutes of Animal Health, Bangkok, Thailand 10900 [*]Corresponding author: autpon@gmail.com

Keyword: *broilers, Heterakis, Histomoniasis,*

Introduction

Histomoniasis is caused by a protozoan parasite named *Histomonas meleagridis*. Often called blackhead disease, histomoniasis primarily affects gallinaceous birds (chickens, grouse, partridge, peafowl, pheasants, quail, turkeys) and also affects to broiler chicken. The clinical signs of infected bird may include lethargy, drooping wings, eyes closed, head held close to the body, weakness, weight loss and sulfur-colored droppings. Morbidity, mortality and culling may reach 20% in chickens (1). Lesions are characterized by thickening and ulceration of the lining of the ceca and by focal necrosis in the liver. The combination of swollen, inflamed ceca with yellow, cheesy cecal cores and discrete spots of necrosis in the liver (yellow-ring necrotizing hepatitis) is considered indicative for histomoniasis. *Histomonas melagridis* usually transmitted by the cecal worm *Heterakis gallinarum* (2). However direct transmission can occur (3). The chickens during 4-6 weeks was prone to infected with *Histomonas spp*. This report describes the clinical characteristics of histomonas infection of broilers.

Materials and Method

A 2-month old, mixed-breed, broiler flock underwent depression, anorexia, palor and emaciation with approximately 10% mortality. Dead chickens was submitted for diagnosis at Faculty of Veterinary Medicine Kasetsart University, Kamphaengsaen Campus. Upon necropsy, the striking lesions were yellow-ring necrotizing hepatitis and pseudomembranous typhlitis. Organs showing lesions were fixed in 10% buffer formalin and process for routine histopathology.

Results and Discussion

The 3,500 of mixed-breed broilers were reared on semi-intensive system and fed a commercially prepared food. Water is offered *at lib*. The disease appeared gradually progress with time and most affected broilers die within a period of 1-10 days from appearance of symtoms. Postmortem examination showed ulcerative typhlitis with pseudomembrane and focal necrosis in the liver. Lung, kidney and heart were normal. Histopathologically, extensive infection of *Histomonas spp.,* presented by its schizogony in hepatic parenchyma, with severe chronic necrotic hepatitis and mononuclear cells infiltration. Typhitis with necrosis was obvious in ceca. The schizonts and inflammatory cells were present in mucosal, submucosal and muscular layers of the cecum. Although round worm, *Heterakis spp.* was not found, deworming was done. A pilot study of antiparasitic drug was performed, using dimetridazole at 250 ppm in drinking water for 7 days. The problem disappreared within 2 weeks.

The infection of histomonas in chiken have been previously reported in ducks, tukeys, broiler chickens and game fowl (1) which are reared on ground litter or exposed to range. Histomonas are spread in chicken feces, *Heterakis gallinarum* (cecal worm) eggs or earth worms. Concurrent infection with cecal coccidias have been reported to aggravate the clinical effect of histomonas infection in broiler chickens (3). In this report, we also found coinfection with cecal coccidias. In conclusion, the present case shows the clinical and histo-pathological characteristics of histomonas infection of mixed-breed broilers. The significance gross lesions including thyphlitis and yellow-ring necrotizing hepatitis were found. The schizonts of histomonas were presented in hepatic parenchyma and cecum. The diagnosis of histomoniasis was made.

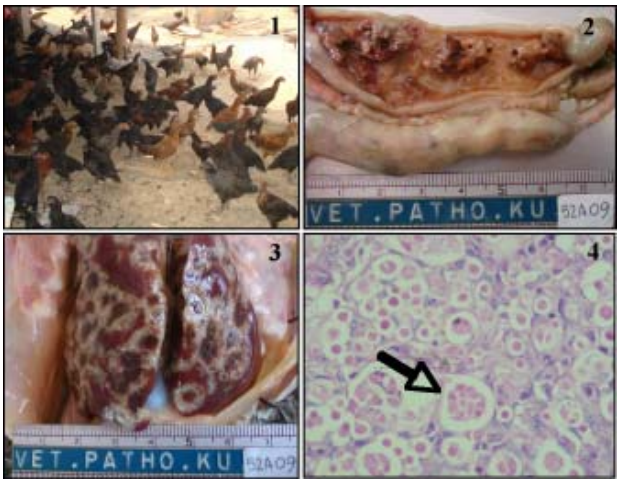

Fig. 1-4. The affected mixed-breed broilers were presented with palor, depression and emaciation. (A). Caecum was swollen and inflammed with caecal cores (B). Yellow-ring necrotizing hepatitis was found in liver (C). The schizonts of Histomonas were found in hepatic parenchyma (arrow, D).

References

1. Duffy et al., 2004. Int. J. Poul. Sci. 12: 753-757.
2. Saif, 2001. Disease of Poultry. Blackwell Pub.
3. McDougald et al., 2005. Avian Dis. 49(3): 328-331.

Metastatic Malignant Sertoli Cell Tumor with Unilateral Hydronephrosis in a Male Shih Tzu Dog: a Case Report

T. Mamom*

Department of Pathology, Faculty of Veterinary Medicine, Mahanakorn University of Technology, Bangkok, Thailand
**Corresponding author: thanonsa@mut.ac.th*

Keywords: *dog, histopathology, hydronephrosis, malignant, sertoli cell tumor*

Introduction

Sertoli cell tumor (SCT) is one of the three most common testicular tumors in dogs (1). It arises from sertoli cell located in seminiferous tubules. The tumor is commonly found in cryptorchid testicle. Breed predilection was reported in schnauzer dog with persistent Mullerian duct syndrome. About 20-30% of dog with sertoli cell tumor exhibited signs of feminization e.g. gynecomastia, male attractive, pendulous penile sheath, atrophy of contralateral testis, bilateral symmetrical alopecia and epidermal atrophy (2). Most sertoli cell tumors are benign. Metastatic rate is very low for tumor smaller than 2 cm. in size. Larger tumors are prone to metastasize especially to lymph nodes of sublumbar and pelvic regions. Two histological forms including intratubular and diffuse forms were categorized (3).

The aims of this study are to present gross and microscopic features of a dog with metastatic malignant sertoli cell tumor and to report a possible consequence of this tumor in dog.

Materials and Methods

Case History: A 7-year-old male Shih Tzu dog with signs of severe non regenerative anemia and right side inguinal cryptorchidism was clinically investigated. Clinical and ultrasonographic examination revealed a large mass within abdominal cavity. Laparoscopy found a large tumor mass with large flaccid right kidney and moderate amount of red effusion which was further classified as hemorrhagic transudate. The tentative diagnosis of sertoli cell tumor with large abscess at right kidney was made. The animal died few days later due to internal bleeding and shock. The carcass was submitted for necropsy at Mahanakorn Veterinary Diagnostic Center (MVDC). Necropsy was done and the samples were collected for histopathology using conventional method. Briefly, the tissues were processed and embedded in paraffin, sectioned on 4 micron and stained with hematoxylin and eosin (H&E). All slides were examined under light microscope. Immuno-histo-chemical staining was performed on paraffin sections using standard protocol of labeled streptavidin-biotin technique (LSAB). Antibody against vimentin (1:1000 V9, Neomarker, USA), pancytokeratin (1:200 AE1/AE3, Neomarker, USA) and Ki-67 (1:50 SP6, Neomarker, USA) were applied. The results were observed under light microscope.

Results and Discussion

Necropsy result: General appearance, the skin showed bilateral symmetrical alopecia with enlargement of all nipples and pendulous prepuce. Within abdominal cavity, a large multi-lobulated, encapsulated mass of 12x10x12 cm. was found at right lumbosarcral area adjacent to the caudal pole of right kidney and entrapped upper part of right ureter. The urine outflow from affected kidney was prohibited and severe hydronephrosis was the consequence (Fig.1). Right testis was found at inguinal area (congenital cryptorchidism) without direct connection to abdominal mass. A tumor mass of 2.5x2x 2.5 cm. with necrosis and hemorrhages were detected in right testis (Fig. 2) and epididymis (1.5x1x1.5 cm.). The contralateral testis was atrophic. Other organs including organs of alimentary system, respiratory system, nervous system, hemo-lympho-poietic system, adrenal gland and heart remained intact.

Histopathological result: The large well demarcated, encapsulated intra-abdominal mass, mass at right testis and epididymis composed the same type of neoplastic cells. Within the mass, multiple cords or sheath of neoplastic elongated cells were found with fibro-vascular stroma. The tumor cells arranged perpendicularly to the stromal scaffold (Fig. 3). Most cells had narrow cytoplasm often vacuolated. The nuclei were mostly oval with less heterochromatin and prominence one or two concentric nucleoli. Mitotic figures ranged from 0-3/HPF with few atypical mitoses (Fig. 4). Anisocytosis and anisokaryosis were observed (Fig. 5). Areas of necrosis and hemorrhages were present in especially in large tumor (Fig. 6). The contralateral testis revealed completely atrophic (Fig. 7). The skin showed severely epidermal atrophy, less number of hair follicles with hyperkeratosis of hair follicles, which mostly in telogen phase.

Immunohistochemistry result: The tumor cells stained positively for vimentin (Fig. 8) and negatively for pancytokeratin. This confirmed mesenchymal origin of tumor cell. Rare tumor cells showed immune reactivity to Ki-67, proliferation marker.

Morphological diagnosis: Malignant sertoli cell tumor at right cryptorchid testis with metastasis to epididymis and sublumbar lymph nodes and subsequence hydronephrosis in right kidney.

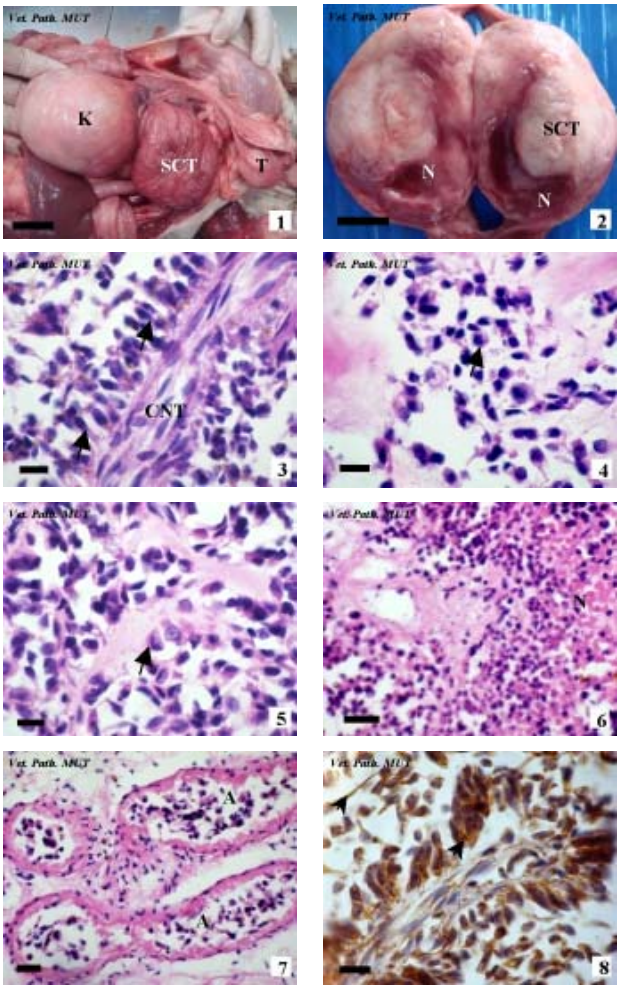

Fig. 1-8 Gross, histopathological and immunohisto-chemical findings in this dog. **Fig. 1** Metastatic sertoli cell tumor (SCT) in right sublumbar lymph node with severe hydronephrosis (K) of right kidney, Bar= 3 cm.; **Fig. 2** Sagittal sections of tumor mass (SCT) within cryptorchid testis, N: Necrosis and hemorrhage, Bar= 1 cm.; **Fig. 3** Elongated tumor cells (arrows) arranged perpendicularly to the fibrous connective tissue core (CNT), Bar = 10 μm; **Fig. 4** Mitotic figures (arrow) among polygonal tumor cells, Bar = 10 μm; **Fig. 5** Polygonal tumor cells (arrow) with anisocytosys and anisokaryosis, Bar = 10 μm; **Fig. 6** Area of necrosis (N) within tumor mass, Bar = 20 μm; **Fig. 7** No germ cells found within atrophic contralateral testis (A), Bar = 20 μm; **Fig. 8** Most tumor cells stained positively for vimentin in cytoplasm (arrow), DAB-Hematoxylin, Bar = 10 μm.

Cryptorchidism was observed about 10% of male dogs. The occurrence in right testis was two times more than the left possibly due to longer distance to descent into scrotal sac (1, 7-8). In our case, inguinal cryptorchidism was also found in right testis and sertoli cell tumor was detected without significant enlargement of the testis. Gross and histopathological findings of necrosis and hemorrhage within the tumor mass may explain why the affected testicle showed no remarkable enlargement. The larger size of metastatic tumor in sublumbar lymph nodes and severe hydronephrosis with completely loss of right renal tissue indicated the longstanding period of occurrence. The pathogenesis of hydronephrosis is clearly due to compression of enlarged sublumbar metastatic tumor nodule on right ureter adjacent to renal pelvis. In the literature, metastasis was detected in approximately 10% of SCT cases. The routes of metastasis were reported via lymphatic route to inguinal and sublumbar lymph nodes. Distance metastasis was found in liver, lung, spleen, kidney and adrenal gland (2). Hydronephrosis as a consequence of metastatic malignant sertoli cell tumor as found in this case has never been reported before. Atrophy of contralateral testis mentioned in the literature was due to inhibitory effect by excessive estrogen on anterior pituitary gland to secrete gonadotrophic hormone (3). This was also found in this animal. The dog in this case showed signs of hyperestrogenism e.g. swelling and pendulous prepuce, enlarged and elongated nipples, atrophy of epidermis and bilateral symmetrical alopecia. In the literature, feminizing syndrome was reported in one third of SCT cases in dogs (4). Additionally, the effect of prolong hyperestrogenism on bone marrow may result in bone marrow hypoplasia with subsequence non-regenerative anemia as also observed in this animal.

This report may remind veterinary surgeons or the owners about the effect and outcome of delayed castration after the first detection of the cryptorchid testicle.

Acknowledgements

The Author thanks Mahanakorn University of Technology (MUT) for financial support of this study. Special thanks were also given to Staff of Small Animal Teaching Hospital for clinical information and to Dr. Hassadin, Dr. Suwarin and Ms. Siriwan, staff of MVDC, for all technical supports.

References

1. Grieco et al., 2008. J. Comp. Path. 138: 86-89.
2. Meuten D.J., 2002. Tumor of the Testicle. In: Tumors in Domestic Animals 4th ed. 561-563.
3. Post and Kilborn, 1987. Can. Vet. J. 28(7): 427-431.
4. Pulley, 1979. Vet. Clin. North. Am. 9: 145-150.

Localization of Prostaglandin E2 Receptor Subtype 4 (EP4) in the Cervical Tissue of Bitches Developing Pyometra

K. Chatdarong[1], S. Sirivaidyapong[1], S. Srisuwatanasakul[2], P. Linharattanaruksa[1*]

[1]Department of Obstetrics, Gynecology and Reproduction, [2]Department of Anatomy, Faculty of Veterinary Science, Chulalongkorn University, Bangkok, Thailand, 10330

[*]Corresponding author: idolph@hotmail.com

Keywords: *dog, EP4, prostaglandinE2, pyometra*

Introduction

Pyometra is a reproductive disease occuring in one fourth of female dogs over 10 years of age (1). The most effective treatment is ovariohysterectomy (OVH) because this surgical technique prevents recurrence of the disease. However surgery has its limitation when bitches are risk of anesthesia and in life threatening. The alternative treatment is medical therapy such as prostaglandin F2α given to expulse exudates from the uterus but its side effect especially uterine rupture can occur in the cases of closed-cervix pyometra (2). Current literatures in other mammals indicate that PGE_2 play an important role in cervical ripening (3). PGE_2 exerts its roles by coupling to prostaglandin E2 receptors (EP) of four subtypes (EP1, EP2, EP3 and EP4) (4). In cervical tissue of pregnant rats, the expression of EP4 at term of labor is much higher than during early pregnancy and estrous stage (5). PGE_2 has been used as cervical ripening agent in human (6) and mares (7) but has not been studied in dogs. The aim of this study was to investigate the localization of EP4 and its regulation on cervical patency in pyometra bitches.

Material and Methods

Immunohistochenistry: Cervical tissues of bitches with open- (n=6) and closed-cervix pyometra (n=6) were obtained after ovariohysterectomy at the Small Animal Teaching Hospital, Chulalongkorn University. The tissues were fixed in 4% paraformaldehyde, embedded in paraffin blocks, cut into 4-μm sections and mounted on silane-coated slides. The immunohistochemical detection of EP4 was performed by using goat polyclonal anti-human EP4 (C-18: sc-16022, Santa Cruz biotechnology, CA, USA) in humidified chamber. The avidin-biotin method was used as described in ABC elite kit (Vectastatain® ABC kit, Vector Lab., CA, USA). The complex was visualized with NovaRed (Vector Lab., CA, USA). Sections were counterstained with Mayer's hematoxylin and finally mounted in glycerine gelatin.

Quantification for immunohistochemistry: The analytical processes of expression were performed semi-quantitatively in 4 different tissue layers (i.e. surface epithelium, subepithelium, glandular epithelium and myometrium. The intensity of the staining was divided into 3 grades which were weak, moderate and strong staining. The proportion of each intensity score was rated and calculated to average value. The expression index was calculated from the percentage expression multiplied by the average intensity score of staining.

Statistical analysis: Means±S.E.M. of expression index were presented. Mixed model analysis of variance (SAS version 9.0) was used to compare differences of the expression index between layers (SE-surface epithelium, Sub-subepithelium and Mus-muscular layer) of each group. Significant difference was set as $p<0.05$.

Results and Discussion

Immunohistochemical staining demonstrated that EP4 expressed in all layers of canine cervical tissue of open- and closed-cervix pyometra (Fig. 1). Although the expression was found in all layers, the highest intensity

of positively stained cells was found in the Mus and lowest in the Sub (Table 1). The mean (±S.E.M) of expression index in the SE was higher in the open-(67.1±15.9) than closed cervix pyometra (39.2±11.4) ($p<0.05$). However, the differences of the expression in SE and Mus were not observed between groups ($p<0.05$).

Table 1 Mean±S.E.M. of expression index of EP4 in cervical tissues of bitches developing pyometra.

	N	SE	Sub	Mus
Opened cervix pyometra	6	67.1±15.9[a]	84.5±13.0[a]	109.2±8.7[a]
Closed cervix pyometra	6	39.2±11.4[b]	63.9±12.6[a]	96.4±12.9[a]

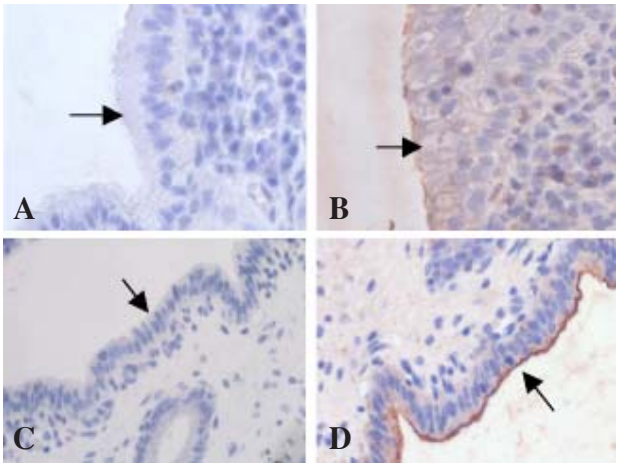

Fig. 1 EP4 expression in surface epithelium (arrow) of closed- (A), open- (B) cervix pyometra, negative control (C), and positive control (D).

EP4 expression in the surface epithelium was higher in open-cervix pyometra than closed-cervix pyometra, suggesting that PGE_2 might involve in cervical dilatation by acting through EP4. The previous study revealed that EP4 induces cervical dilatation via relaxation of the smooth muscle (8). Furthermore, the expression of EP4 was greatest in Mus, demonstrating that activation of EP4 likely to cause relaxation of smooth muscle as shown in the previous study (9). Therefore, the expression of different subtypes of prostaglandin receptors (EP1, EP2, EP3 and EP4) in the bitch cervix may be value further studied.

Acknowledgements

This research was funded by faculty of Veterinary Science, Chulalongkorn University.

References

1. Eenval et al., 2001. J. Vet. Int. Med. 15:530-538.
2. Johnston, 2001. WB Saunders ed. 206-224.
3. Huiling et al., 2008. Am. J. Obstet. Gynecol. 198: 536. e1-e7
4. Coleman et al, 1994. Pharmacol. Rev. 46: 205-229.
5. Chein et al., 2003. Am. J. Obstet. Gynecol. 189: 1501-1510.
6. Caldar, 1990. Repro. Fertil. Dev. 2: 553-556.
7. Rigby et al., 1998. Therio. 50: 897-904.
8. Lyons et al., 2003. Prosta. and other Lipid. 70: 317-329.
9. Negishi et al., 1995. Biochem. Biophys. Acta. 1259: 109-120.

Effects of Hot and Humid Climates on the Number of Mummified Fetuses in Gilts and Sows

P. Tummaruk[1*], K. Srisuwatanasagul[2]

[1]Department of Obstetrics, Gynaecology and Reproduction and [2]Department of Anatomy, Faculty of Veterinary Science, Chulalongkorm University, Bangkok, Thailand 10330 [*]Corresponding author: Padet.T@chula.ac.th

Keywords: *pig, reproductive performance, Temperature-humidity index, tropics*

Introduction

During the last decade, global warming has become a major concern for humans. Official data from the meteorological department in Thailand indicate that the environmental temperature increased during the period from 1996 to 2005 and has tended to continue to increase. The increase of the environmental temperature also has a potentially large impact on the pig industry, especially for pigs that are housed in a conventional open-housing system, which is the most common type of housing of swine commercial herds in Thailand. It is well-established that high ambient temperature and high humidity as well as a tropical climate negatively influence the reproductive performance of female pigs (1-5). A common feature of the seasonal influence on the giltís and sow's reproductive performance include prolonged weaning-to-first-service interval, decreased conception and farrowing rates, increased remating rate, and increased embryonic loss (1-5). To our knowledge, no comprehensive study on the influence of climatic factors, e.g., temperature, humidity and temperature-humidity index (THI) on the number of fetal loss in pig under tropical climate has been done. The aim of the present study was to use data from herds to demonstrate the influence of THI on the proportion of mummified fetuses per litter in gilts compared to sows parities 2, 3-5 and ≥6 in a conventional, open-housing system for swine commercial herds in the northeastern part of Thailand.

Materials and Methods

Data: Data were obtained from four swine commercial herds (A, B, C and D) in the northeastern part of Thailand. The data included sows farrowed during the period from July 2005 to June 2008. The herd data were obtained from the computer recording system of the herds from January 2005 to December 2008. The data included the sow's identities, farrowing date, parity number, number of piglets born alive per litter (BA), number of stillborn piglets per litter (stillborn), number of mummified fetuses per litter (mummy), litter's birth weight, piglet's birth weight and number of piglets at weaning. The total number of piglets born per litter (TB) was calculated by summing of BA, stillborn, and mummy totals. The proportion of mummified fetuses per litter (MF) was calculated using the number of mummified fetuses divided by TB and multiplied by 100. The data included observations on 25,835 litters from 8,100 sows.

Herd location and management: The four herds in the present study were located in the northeastern part of Thailand between latitude 14-17°N and longitude 102-103°E. The housing facilities in Herds (herd size) A, B, C and D were available for 1,200, 1,500, 1,000 and 500 sow inventories, respectively. The breeds of the sows were predominantly crossbred LY, and were mainly bred with Duroc or hybrid boars (PIC® Siam Ltd., Thailand). Conventional artificial insemination (AI) was used for all gilts and sows. In all herds, gilts and sows were housed in a conventional open-housing system with a water sprinkler and fan; the boars were kept in an environment with an evaporative cooling system. The gilts and sows were kept in individual stalls during gestation and in individual farrowing pens during lactation. In general, the gilts were mated at ≥32 weeks of age with a BW of ≥135 kg at the second or later observed oestrus. The health of the herds was monitored by the herd veterinarians. In general, the veterinarians gave the recommendation to vaccinate the gilts/sows against foot-and-mouth disease (FMD), swine fever (SF), Aujeszky's Disease (AD), porcine parvo virus (PPV) and arthrophic rhinitis (AR), at between 22-30 weeks of age in replacement gilts, and during late gestation (FMD, AR) and during lactation (PPV, SF) in sows. Mass vaccination of AD was conducted every four months. All herds were porcine reproductive and respiratory syndrome (PRRS) sero-positive herds, but no clinical outbreak was observed during the period of study. Culling due to old age was planned to be done after parity six. The gilts and sows received water up to ad libitum via water nipples. The feed was provided twice a day (about 1.5-3.5 kg/d during gestation and 5.0-7.0 kg/d during lactation). The feed was a rice-corn-soybean-fish base containing 15-18% crude protein, 2,900-3,200 kcal/kg metabolisable energy and 0.8-1.0% lysine. All of the herds were visited monthly by the first author of this study to monitor routine management and health.

Meteorological data: Outdoor temperature and humidity data were obtained from July 2005 to June 2008 from an official

meteorological station within 100 km from the herds. The average minimum-maximum daily temperatures were 21.1-33.3°C, 24.4-31.6°C and 17.9-29.9°C in the hot, rainy and cool seasons, respectively. The 24-h average humidity was 68.3%, 81.7% and 64.2% in the hot, rainy and cool seasons, respectively. THI was calculated using the following formula (6):

$$THI=DB-[0.55-(0.55xRH) \times (DB-58)$$

where DB is the average daily temperature and RH is the average daily humidity. On average, the THI was 79.2±3.5, 79.7±1.7 and 73.5±4.2 in hot, rainy and cool seasons, respectively.

Statistical analyses: The statistical analyses were carried out using SAS (SAS 2002). The influences of THI on MF were analyzed using the general linear mixed model procedure of SAS. The meteorological data were merged with the reproductive data by farrowing date (farrowing year-month-day). The means of THI during 115 days before farrowing were calculated and were used in the statistical models. The statistical models included herds (A, B, C, D), parity groups (1, 2, 3-5, 6-12), years (1,2,3), THI classes (71-72, 73-78, 79-80 and ≥81), and two ways interactions between parity and THI and between herd and THI. Since the sows included in the analyses produced 3.2±1.8 litters/sow (range 1-8 litters/sow) during the study period, the sow ID was included in the statistical model as a random effect. The classification of THI was based on information from earlier studies (7) and the frequency of the THI data. Least-square means were obtained from each class of the factors and were compared using a least-significant-difference test. A probability value of $p<0.05$ was regarded to be statistically significant.

Results and Discussion

On average, the gilts and sows in commercial herds in Thailand kept in the open-house system had 11.3±2.9 TB, 10.2±2.9 BA, 2.2% MF, 7.3% SB and 9.5±1.9 piglets at weaning. The means THI during gestation periods influenced MF ($p=0.06$). MF varied among herds from 1.6% in herd C to 2.9% in herd B ($p<0.001$). On average, MF was 3.3%, 1.8%, 1.9% and 2.6% in parity 1, 2, 3-5 and 6-12, respectively ($p<0.001$). The influence of the THI during gestation period on MF by parity groups are demonstrated in Fig. 1. As can be seen from the figure, the influence of the THI was more pronounced in the 1st parity than parity 2, 3-5 and 6-12.

It is known that a pig regulate internal temperature within a narrow range by matching the amount of heat produced through metabolism with the heat flow from animal to the surrounding environment. Under field condition, hyperthermia often occurs in pig due to the heat flow from the animal is less than internal heat production (7). In beef cow, it has been shown that increasing environmental temperature and relative humidity from 21°C, 35% relative humidity to 37°C, 38% relative humidity, during days 8th to 16th of gestation period reduced

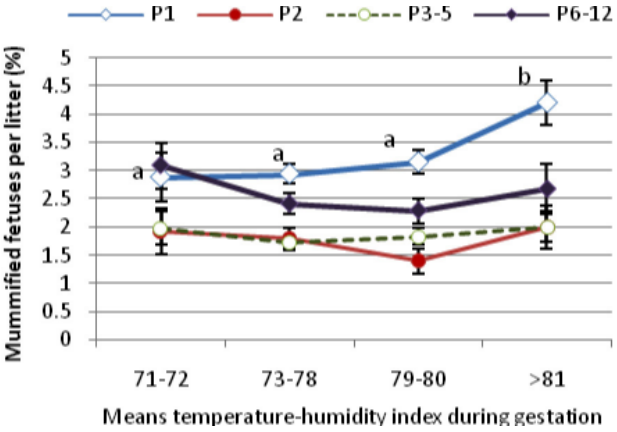

Fig. 1 Effect of means temperature-humidity index during gestation periods on the proportion of mummified

the size and weight of the conceptus (8). In Brazil, Bényei et al. (7) demonstrated that the average number of corpus luteum of superovulation cows decreased from 9.8 to 5.2 when THI increase from 70.7 during cool season to 79.7 during the El-Nino phenomenon. Earlier studies demonstrated that the high ambient temperature not only influence early embryonic and/or fetal loss, but also influence the follicular development and hence decrease the number of ovulation, the oocyte quality and/or fertilization rate (7-9).

In the present study, the average THI was 79.2±3.5, 79.7±1.7 and 73.5±4.2 in hot, rainy and cool seasons, respectively. The average THI observed during hot and rainy seasons in Thailand are almost equal to the THI that observed during the period of El-Nino phenomenon in Brazil (79.7±4.0) (7). This level of THI significantly reduced the number of ovulation and the oocytes quality in cows (7). The present study revealed that THI above 81 significantly increased MF in primiparous sows, but not in multiparous sows. Therefore, the control of environmental temperature and humidity for pregnant gilts should be emphasized.

Acknowledgements

The financial supported was provided by The National Research Council of Thailand.

References

1. Omtvedt et al., 1971. J. Anim. Sci. 32: 312-317.
2. Love et al., 1993. J. Reprod, Fertil. (Suppl) 48: 191-206.
3. Tantasuparuk et al., 2000. Theriogenology 54: 481-496.
4. Tummaruk et al., 2004. J. Vet. Med. Sci. 66: 477-482.
5. Suriyasomboon et al., 2006. Theriogenology. 65: 606-628.
6. Kelly and Bond, 1971. National Academy of Science Press, Washington D.C., USA. 77.
7. Bényei et al., 2003. Acta Veterinaria Hungarica 51: 209-218.
8. Biggers et al., 1987. J. Anim. Sci. 64: 1512-1518.
9. Roth, 2008. Reprod. Domest. Anim. 43(Suppl. 2): 238-244.

The Seroprevalence of Porcine Reproductive and Respiratory Syndrome Virus in Vaccinated and Non-vaccinated herds: a Retrospective Study

P. Tummaruk[1*], R. Tantilertcharoen[2]

[1]Department of Obstetrics, Gynaecology and Reproduction, [2]Veterinary Diagnostic Laboratory, Faculty of Veterinary Science, Chulalongkorn University, Bangkok, 10330 [*]Corresponding author: Padet.T@chula.ac.th

Keywords: *pig, PRRS, reproduction, seroprevalence*

Introduction

Porcine reproductive and respiratory syndrome (PRRS) is caused by an envelope, single-stranded positive-sense RNA virus known as PRRS virus (PRRSV) (1). The disease was observed first time in the United States of America (USA) since the late 1980s (2) and was found in Europe since 1990 (3). In Thailand, PRRSV sero-positive pig has been observed as early as 1989 (4). In 1995, the seroprevalence of PRRS was, on average, 64% with a variation among the herds from 20% to 90% (5). In general, PRRSV is classified according to their genotype as North American (US) and European (EU) strains (1, 4). In Thailand, both US and EU strains have been isolated (4). PRRSV causes many signs of reproductive failure in gilts and sow, such as infertility, abortion, death of sows and pre-weaning mortality (1, 6). Under field conditions, the infected sows develop a protective immunity and usually produce normal litters after rebreeding although the virus still circulate within the herds (7). The duration of the protective immunity is in fact unknown, but at least 604 days post infections have been proposed (7). Larger et al. (8) demonstrated that homologous PRRSV protective immunity was produced within 90 days post exposure and the virus-specific antibody was detected for at least 110 days post exposure in adult pig. Up to date, intensive acclimatization and/or vaccination in replacement gilts are commonly practiced in most breeding herds. However, high variability of the antibody titer against PRRS of the gilts is still observed both within and between herds. The objective of the present study was to retrospectively investigate the seroprevalence of PRRS antibody in pigs in 5 commercial herds in Thailand during 2004-2007. Furthermore, the seroprevalence of PRRSV between herds that vaccinated the gilts and sows with modified live virus (MLV) vaccine and those that performed intensive acclimatization in replacement gilts were compared.

Materials and Methods

Animals and data: The study was conducted in 5 commercial swine herds (A, B, C, D and E) in Thailand during January 2004 to December 2007. A total of 5,664 blood samples from 544 boars, 1,164 sows, 3,168 replacement gilts, 486 nursery pigs and 302 fattener pigs were collected and determined for PRRSV-specific antibody titer.

Herd location, management and vaccination: The herds in the present study are located in the eastern (A, E), middle (B), western (C) and northeastern (D) of Thailand between latitude 13° and 17°N and between longitude 100° and 104°E. All herds included in the present study were breeding herd and the sows on production numbering about 900-3,500 sows/herd. Two herds (A and D) produced the replacement gilts within the herds, while 3 herds (B, C, E) bought the replacement gilts from other breeders. In general, the gilts entered the gilt pools at about 22-24 wk of age at 80-100 kg body weight (BW). Water was provided to *ad lib* from water nipples. The feed were provided twice a day (about 3 kg/day). The gilts were kept in a pen with a group size of between 6-15 gilts/pen with a space allowance of 1.5-2.0 m2/gilt and pregnant gilts and sows were kept in individual stall. Lactating sows were kept in individual pens. In most cases, the herds breed the replacement at ≥32 week of age with a BW of ≥130 kg at the second or later observed oestrus. Boar contact and estrous detection was applied to the gilts between 24-35 wk of age. The health of the herds was controlled by the herd veterinarian. In all herds, removal sows were taken to acclimatize the gilts for about 4 weeks period with a ratio of 1 sow per 6-10 gilts. The acclimatized sows were rotated weekly. Before breeding, the gilts were vaccinated against Foot-and-mouth disease (FMD), Swine fever (SF), Aujeszky's disease (AD) and Porcine Parvo virus (PPV) vaccine during 22-30 week of age. In herd B, the gilts, sows and nursery pigs were also vaccinated against US-strain of MLV vaccine (Ingelvac® PRRS™ MLV, Boehringer-Ingelheim Vetmedica Inc., Missouri, USA), and in herd C and E, the EU-strain of MLV vaccine (AMERVAC®, Lab. Hipra, Spain) were used.

Serological test: Antibody of PRRS virus was tested by using HerdCheck PRRS virus antibody test kit 2XR® (IDEXX Lab., Inc., USA) (herd A, B, C and D). Briefly, the positive and negative control was also carried in the same plate as the sample. 100 µl of serum samples was added to the testing plated that coated with PRRS antigen and to the normal host cell (NHC) and incubated at room temperature for 30 min. Anti-Porcine: HRPO conjugate was added into the plate 100 µl for each sample and incubated. 100 µl of TMB substrate was added and incubated and then 100 µl of stop solution was added. OD was measured using ELISA reader at 650 nm. The serum sample/positive control (S/P) was calculated. The S/P ratio below 0.4 indicated that the sample had no antibody of PRRSV (negative), while S/P ratio ≥ 0.4 indicated that the sample had antibody of PRRSV (positive).

Statistical analyses: The statistical analyzed was performed using SAS (SAS version 9.0, Cary NC, USA.). Frequency analysis was conducted using PROC FREQ of SAS. The proportional data were analyzed using Chi-squared test. $p<0.05$ were regarded to be statistical significance.

Results and Discussion

Of all 5,664 tested samples, 4,492 pigs (79.3%) had antibody titer against PRRSV. The proportion of PRRS positive pigs were 79.4%, 82.0%, 82.6%, 84.1% and 48.4% in boars, sows, gilts, fattener and nursery pigs, respectively (Figure 1). The proportion of PRRS positive pigs were 81.7%, 67.9%, 60.6%, 80.9% and 79.3% in herds A, B, C, D and E, respectively (p<0.001). The S/P ratios were 1.5±1.1 (range 0-4.5), 1.3±1.2 (range 0-4.9), 1.0±0.9 (range 0-3.7), 1.4±0.9 (range 0-4.3) in herds A, B, C and D, respectively. Across the herds, the proportion of PRRS negative pigs varied among years from 36.6% in 2004 to 25.6%, 15.7% and 11.3% in 2005, 2006 and 2007, respectively (p<0.001). The proportion of PRRS positive boars varied among years from 69.2% in 2004 to 80.0%, 74.1% and 83.3% in 2005, 2006 and 2007, respectively (p=0.03). In the fattener, the proportion of PRRS positive pigs varied from 82.3% to 89.1% among years (p=0.7). The proportion of PRRS positive gilts were 62.1%, 78.6%, 91.5% and 94.4% in 2004, 2005, 2006 and 2007, respectively (p<0.001). The proportion of PRRS positive nursery pigs were 58.2%, 40.8%, 46.5% and 55.0% in 2004, 2005, 2006 and 2007, respectively (p=0.03). Proportion of PRRS positive pigs from 2004 to 2007 in the MLV PRRSV-vaccinated and non-vaccinated herds are demonstrated in Figure 2. Comparing between the PRRSV vaccinated and non-vaccinated herds, the proportion of PRRS positive pig was demonstrated in Figure 2. A higher proportion of PRRS-specific antibodies fattener pig was observed in the PRRSV-non-vaccinated herds than the PRRSV-vaccinated herds (p<0.05) (Fig. 3).

The present study provided descriptive data on the prevalence of PRRSV infection in 5 swine commercial herds in Thailand. The data indicated that the proportion of pigs infected with PRRS differed among herds, years and groups of pigs. The infection was found to be highest in the fattener (84.1%) and lowest in the nursery pigs (48.3%). High proportion of PRRS positive pigs were also observed in replacement gilts (82.6%) and sows (82.0%). Surprisingly, a relatively high prevalence of PRRS was found in the boars (79.4%). These indicate that the PRRSV circulation and re-infection remain relatively high either in vaccinated or in non-vaccinated herds. Boars, sows and replacement gilts seem to be the important reservoir of the virus. Interestingly, the exposure of PRRSV in the fattener pigs tended to be lower the vaccinated than the non-vaccinated herds.

Acknowledgement

The financial supported was provided by The National Research Council of Thailand.

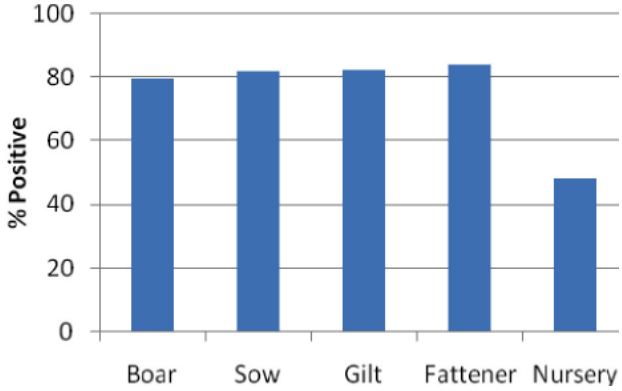

Fig. 1 Percentage of PRRS positive pigs by groups

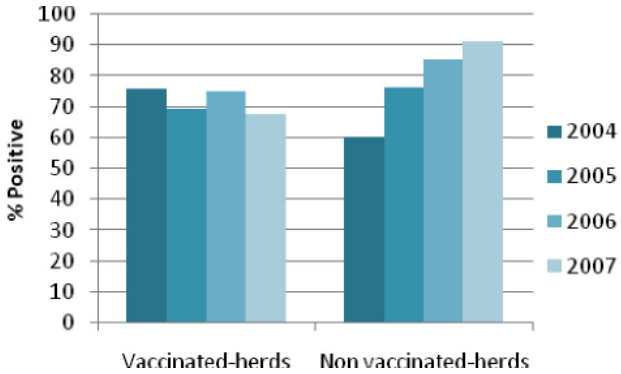

Fig. 2 Proportion of PRRS positive pigs in PRRSV vaccinated and non vaccinated herds

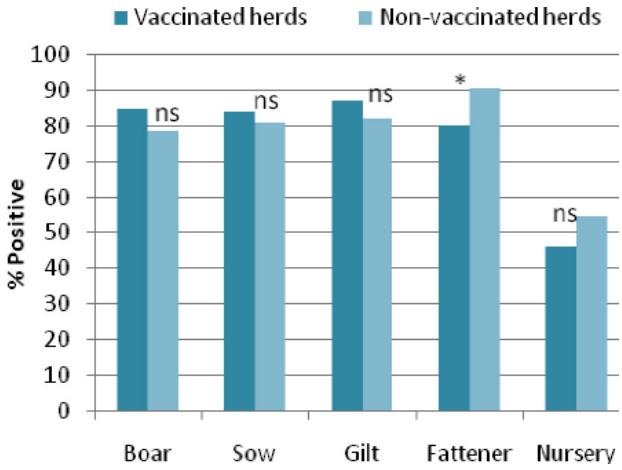

Fig. 3 Proportion of PRRS positive pigs in PRRSV vaccinated and non-vaccinated herds by groups; $^{*}p$<0.05

References

1. Cho and Dee, 2006. Theriogenology. 66: 655-662.
2. Keffaber, 1989. Am. Assoc. Swine Pract. 1: 1-10.
3. Wensvoort et al., 1991. Vet. Q. 13: 121-130.
4. Thanawongnuwech et al., 2004. Vet. Microbiol. 101: 9-21.
5. Ornveerakul, 1995. Thai J. Vet. Med. 25: 233-240.
6. Goldberg et al., 2000. Prev. Vet. Med. 43: 293-302.
7. Lager et al., 1997. Vet. Microbiol. 58: 127-133.
8. Lager et al., 1997. Vet. Microbiol. 58: 113-125.

Porcine Reproductive and Respiratory Syndrome Virus Antigen Detection in the Uterine Tissue of Gilts Correlated to the Antibody Titer

E. Olanratmanee[1*], S. Wangnaitham[2], R. Thanawongnuwech[2], A. Kunavongkrit[1], P. Tummaruk[1]

[1]Department of Obstetrics, Gynaecology and Reproduction [2]Department of Pathology, Faculty of Veterinary Science, Chulalongkorn University, Bangkok, Thailand 10330 [*]Corresponding author

Keywords: *immunohistochemistry, pig, PRRS, reproduction, uterus*

Introduction

Porcine reproductive and respiratory syndrome (PRRS) is caused by PRRS virus (PRRSV), a member of Arterivirus, family Arteriviridae (1). In general, the infection of PRRS in gilts and sows is characterized by late term abortion, mummified fetuses, stillborn piglets and low viability piglets at birth (2-4). The antibody titers against PRRSV infection are detected by 7-14 days after the animals are infected and remain for several months before declining (5). Under farm condition, intensive acclimatization and/or vaccination in replacement gilts are commonly practiced in most breeding herds. However, high variability of the antibody titer against PRRSV of the gilts is observed both within and between herds. This problem causes difficulties for the farmer to make decision to mate the gilts. Additional knowledge concerning the antibody titer of PRRS in the replacement gilts in different herds is needed to be investigated. It has been suggested that replacement management of gilts is a major source of introducing new strains of PRRSV into the herd. Our previous study has found that 73% (122/166) of the replacement gilts culled due to reproductive disturbance had been infected with PRRSV. In addition, a higher proportion of seropositive gilts was particularly found in those that were culled due to abortion (81%) and repeat breeding (81%) (6). It is well established that alveolar macrophages as well as macrophages from other tissues are the primary cell type sustaining the in vivo replication of the viruses (7). Using Immunohistochemistry (IHC) for evaluating formalin-fixed tissues, it was found that 66% and 100% of the lung tissue of piglets infected with US and EU stains of PRRS have been observed, respectively (7). An earlier study has demonstrated that 75.0%, 50.0%, 37.5%, 37.5%, 37.5% and 25.0% of IHC positive cells was observed in liver, spleen, tonsil, turbinate bone, pulmonary lymph node and ileum of the infected piglets, respectively (7). To our knowledge, the expression of PRRSV in the uterine tissue of gilts has not been dem onstrated. The objective of the present study was to determine the incidence of PRRSV in the uterine tissue of gilts in relation to the level of antibody titers.

Materials and Methods

Uterine tissues from 50 replacement gilts were collected from three commercial swine herds (A, B and C) in Thailand. All of the gilts were culled due to reproductive disturbance. The culling reasons included anestrus (n=29), vaginal discharge (n=10), repeat breeding (n=5), abortion (n=5) and not being pregnant (n=1). Historical data for all gilts was collected. All herds included in the present study were breeding herds and the sows on production were between 900-3,500 sows/herd. Herd A produced replacement gilts within the herd using their own grand parent (GP) stock, while herds B and C bought the replacement gilts from other breeders. The gilts in all herds were housed in a conventional open housing system facilitated with a water sprinkler and fan. The health of the herds was monitored by the herd veterinarian. In general, the veterinarian gave the recommendation to vaccinate the gilts against foot-and-mouth disease, classical swine fever, Aujeszkyís disease and porcine parvovirus (PPV) at between 22-30 weeks of age. In addition, herd B vaccinated the replacement gilts using US-strain modified-live virus (MLV) vaccine (Ingelvac® PRRS™ MLV, Boehringer-Ingelheim Vetmedica Inc., St. Josept, Missouri, USA), while herd A and C vaccinated the gilts using EU-strain MLV vaccine (AMERVAC®, Lab. Hipra, Girona, Spain). Blood samples were collected from jugular vein of the gilts prior to culling. Serum were obtained and kept at -20°C for analyzing antibody titer of PRRSV. After slaughter, the ovary and uterus were collected, placed on ice and transported to the laboratory within 24 h of culling. Tissue samples were collected from the uterus of the gilts, fixed in 10% neutral buffered formalin for at least 24 h and embedded in paraffin blocks. Immunohistochemistry (IHC) was performed on the uterine tissues of the gilts using the protocol of the lung tissue with some modification (7). A polymer-based non-avidin-biotin technique was applied in the present study. Primary monoclonal antibody SDOW17 (Rural Tech., Inc., USA) diluted 1:1000 was used. Negative control procedures included omission of primary antibody. Known PRRSV-positive lung and lymph node tissues served as positive controls. The sections were interpreted as positive if contained at least 1 positive cell (brown intracytoplasmic staining, Fig. 1). PRRSV antibody was

determined using a commercial enzyme-linked immunosorbent assay test kit (ELISA, HerdChek® PRRS virus antibody test kit 2XR, IDEXX Lab., Inc., USA). The protocol followed the kit's instructions. The serum sample/positive control (S/P) was calculated. The S/P ratio below 0.4 indicated that the sample had no PRRSV antibody (negative), while S/P ratio ≥ 0.4 indicated that the sample had PRRSV antibody (positive). Statistical analyses were performed using SAS (SAS, 2002). The percentage of positive tissue was compared with the detection of antibody titers against PRRSV by using ELISA (positive and negative) using Fisherís exact test. $p<0.05$ was considered as statistically significant.

Results and Discussion

PRRSV antigens were detected in the cytoplasm of macrophage-like cells in the sub-epithelial connective tissue layers of the endometrium in 28% (14/50) of the gilts. The PRRSV positive cells were observed in the cytoplasm of the macrophages in the endometrium (Figure 1). Of all the gilts, 77.6% (38/49 gilts) were positive to the ELISA test (Table 1). Of the seropositive gilts, 28.9% (11/38) had PRRSV antigen in the uterine tissues, while 18.2% (2/11) of the seronegative gilts had PRRSV antigen in the uterine tissues (p=0.70). Compared to the seronegative gilts, seropositive gilts had a 1.83 (95% confidence interval=0.34-9.89) higher odds for detecting PRRSV antigen in the uterine tissue. Among the seropositive gilts, high level of antibody titer (S/P ratio ≥1.2) was found in 47.4% of the gilts. The incidence of IHC-PRRSV positive staining cells was found in 33.3% of the high antibody titer gilts and in 25.0% of low antibody titer gilts (p=0.72).

The present study demonstrated the present of PRRSV in the uterine tissue of gilts. The site of positive cells was at the subepithelial layer of endometrium. PRRSV infection is a multisystemic disease which is characterized by viremia and subsequent virus distribution and replication in multiple organs (8). In the present study, it was found that gilts that had PRRSV antigen in the uterine tissue were culled at 287 days of age. Most of these gilts have been sent into the breeding herd and might shed the virus to the susceptible pigs in the herd. In the present study, the percentage of gilts culled due to reproductive disturbance that were detected the antibody against PRRSV was in agreement with the earlier study (6). It was not surprise to see both seropositive and seronegative gilts had PRRSV antigen presented in the uterine tissue of the culled gilts since PRRSV antibody titer cannot determine the persistent infection. Although the proportion of IHC-PRRS positive gilts tended to be higher in the gilts that had a high level of S/P ratio, a certain amount of the IHC-PRRSV positive uterine tissue were also observed in the gilts with low S/P ratio and even in the PRRSV seronegative gilts. This imply that the use of antibody titer as a criteria to introduce replacement gilts into the breeding house may not be good enough and remain a risk

Table 1 the number of gilts that were positive to IHC test in relation to the results of ELISA test

	IHC +	IHC -	Total
ELISA +	11	27	38
ELISA -	2	9	11
Total	13	36	49

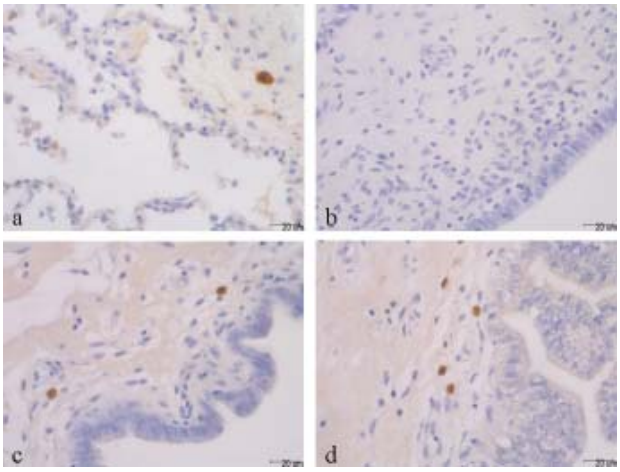

Fig. 1 Demonstration of PRRSV antigen in (a) the positive control (lung tissue), (b) the negative control and (c-d) the uterine tissue of gilts

of introducing IHC-PRRS positive gilts into the herds. It has been demonstrated that the duration of protective immunity against homologous strain of PRRSV may persist for at least 604 days post experimental exposure to the field PRRSV, while the duration of detectable PRRSV-specific antibodies that develop in sows following natural infection is thought to be as short as 4-8 months (9). These findings suggested that replacement gilts must be allowed to expose homologous strain of PRRSV before entering the breeding herds.

Acknowledgements

The financial support for the present study was provided by The National Research Council of Thailand. E. Olanratmanee is a grantee of the Royal Golden Jubilee (RGJ) Ph.D. Program, the Thailand Research Fund.

References

1. Meulenberg et al., 1993. Virology 192: 62-72.
2. Done et al., 1996. Br. Vet. J. 152: 153-174.
3. Mengeling et al., 1996. Am. J. Vet. Res. 57(6): 834-839.
4. Chung et al., 1997. Can. J. Vet. Res. 61: 292-298.
5. Murtaugh et al., 2002. Viral Immunol. 15(4): 533-547.
6. Tummaruk and Tantilertcharoen. 2008. Proc. 15th FAVA: 179-180.
7. Laohasittikul et al., 2004. Thai J. Vet. Med. 34(1): 39-48.
8. Thanawongnuwech et al., 1997. J. Vet. Diagn. Invest. 9: 334-337.
9. Lager et al., 1997. Vet. Microbiol. 58: 127-133.

Malignant Paraganglioma Case in a Siberian Tiger

S.K. Shin, B.M. Park, K.J. Na, B. Ahn*

College of Veterinary Medicine, Chungbuk National University, Cheongju 361-763, Korea
**Corresponding author: shinskm@hanmail.net*

Keywords: *chromogranin A, paraganglioma, siberian tiger, synaptophysin*

Introduction

Paraganglioma is rare tumors originating in cells of neural crest origin in the extra-adrenal paraganglia of the autonomic nervous system (1, 2). It occurred mainly in the abdominal cavity, head and neck (3). In this report, we present histopathologic and immunohistochemical evidence of malignant paraganglioma originated from retroperitoneum of a Siberian tiger, with subsequent systemic metastasis.

Material and Methods

A 14-year-old female Siberian tiger with anorexia and depression was dead. From pathologic examinations, paraganglioma was tentatively diagnosed. For more definitive diagnosis, we performed immunohistochemistry against synaptophysin (1: 20, abcam), S100 (1: 50, Dako), cytokeratin (1: 10, 34/E12, Dako), pan cytokeratin (1: 5, AE1/AE3, abcam), Glia fibrillary acidic protein (GFAP) (1: 250, Dako) chromogranin A (CgA) (1: 1600, Enzo) and vimentin (1: 200, Dako).

Results and Discussion

Grossly, several masses were observed throughout the body including 6x3x3 cm sized oval mass in the retroperitoneal cavity, a 10x5 cm mass attached ventrally to lumbar vertebrae and a 4x4x3 cm spherical mass attached to parietal pleura ventral to the heart. The peritoneal masses were firm and encapsulated with fibrous tissues with well developed blood vessels. Histologically, the tumor cells were arranged in lobular structure surrounded by delicate fibrovascular stroma. The cells had distinct borders, granular eosinophilic plump cytoplasms and binucleate or karyomegalic nuclei. Furthermore, metastasis occurred in the uterus, kidney, adrenal gland, lung and thymus. In immunohistochemistry, the tumor cells are negative for anti-S100, cytokeratin, pan-cytokeratin, vimentin, GFAP. Synaptophysin was intensely stained in the cytoplasm of the tumor cells. Malignant paraganglioma was made as a final diagnosis.

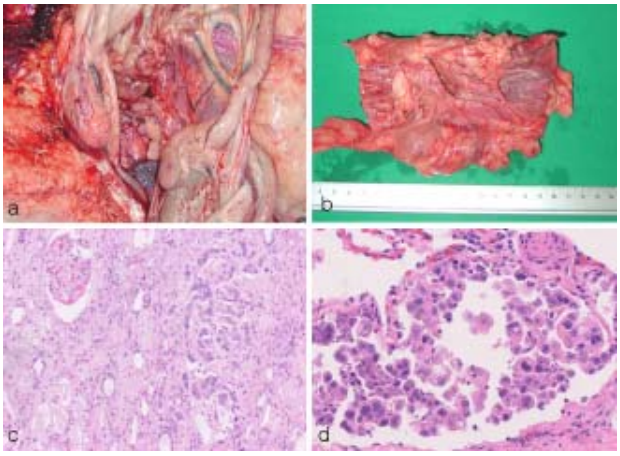

Fig. 1 (a, b) An oval mass in the retroperitoneal cavity was noted. (c) The tumor cells are arranged in various sized lobules and surrounded by a delicate, fibrovascular stroma. (d) Tumor cells were plum with distinct borders and granular eosinophilic cytoplasm. HE

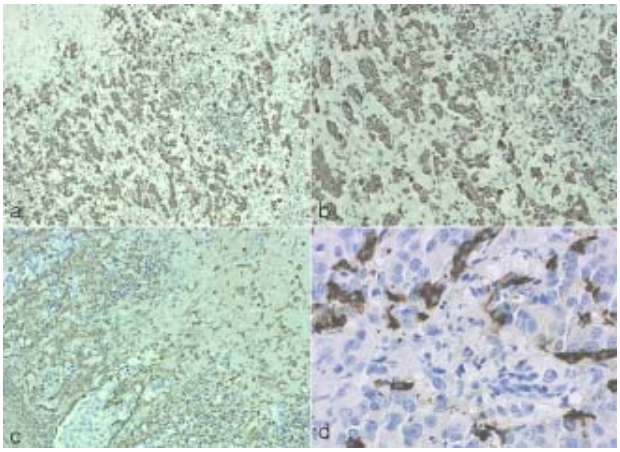

Fig. 2 Immunohistochmistry. (a, b) Synaptophysin was strongly expressed in the cytoplasm of tumor cells. (c) Vimentin was positive only in stromal cells. (d) Chromogranin A was partially positive in tumor cells. Avidin-biotin peroxidase method, Mayer's hematoxylin counterstain

Paragangliomas are rare neuroendocrine neoplasms. It is highly vascular and usually characterized by slow expan-sion and rarely metastasis. Immunohistochemical and histopathological features are used in the diagnosis of this tumor.

In this case, negative staining of the tumor cells for cytokeratins and vimentin indicates that this tumor is not originated from epithelia and/or mesenchymes. The diffuse staining for synaptophysin and partial staining for CgA mean that the origin of this tumor is neural neuroendocrine cells (4). We thought that negative staining for S100 and GFAP is due to nonspecificity of the antibodies. This case would have a great value to report as a rare paraganglioma case being occurred in the tiger.

References

1. Amar et al., 2005. J. Clin. Oncol. 23: 8812-8818.
2. Astuti et al., 2001. Am. J. Hum. Genet. 69: 49-54.
3. Caruso et al., 2006. J. Exp. Clin. Cancer Res. 25:269-275.
4. Martinez-Madrigal et al., 1991. Pathol. Res. Pract. 187: 814-823.

Peroxidative Injury of Rats Intratracheally Instilled with Benzo(a)Pyrene and Benzo(e)Pyrene

A. J. Karim[1], I. K. Latif[1], M. Mazlina[1], A.B. Zuki[2], M. Zamri-Saad[1], M. M. Noordin[1*]

[1]Dept. of Pathology, Faculty of Veterinary Medicine, [2]Dept. of Pre-clinical sciences, Faculty of Veterinary Medicine, Universiti Putra Malaysia, 43400 Serdang, Selangor, Malaysia

[*]Corresponding author: noordin@vet.upm.edu.my

Keywords: *intratracheally, MDA, oxidative stress, PAHs,*

Introduction

An increasing amount of research has focused on the role of oxidant/antioxidant imbalance occurs in lung pathologies due to exposure to polycyclic aromatic hydrocarbons (PAHs), the main constituent of air pollutants (1). The inert PAHs, (benzo(a)pyrene (BaP) and benzo(e)pyrene(BeP)), are metabolized locally in the lung epithelia (2) leading to the generation of harmful intermediates and reactive oxygen species (ROS) released by the inflammatory leukocytes, both neutrophils and macrophages (3). These ROS degrade polyunsaturated lipid, particularly of the cell membrane, forming malondialdehyde (MDA) (4). The traditional role for MDA is reacting with deoxyadenosine and deoxyguanosine in DNA, forming DNA adducts, which is mutagenic (5). The guanidine group of arginine residue condenses with MDA to give 2-aminopyrimidines, causing peroxidative injury through increased oxidative burden (6). The production of this aldehyde is used as a biomarker to measure the level of oxidative stress in an organism (7). The aim of this pulmonary study is spatial assessments of MDA production and to determine the sustainability of any observed effect in PAH exposure.

Material and Methods

All animal experiments and animal care were performed according to the Guides for the Care and Use of Laboratory Animals as approved by the Animal Care And Use Committee of the Universiti Putra Malaysia-Faculty of Veterinary Medicine (AUP No: 08R28/July 2008). Ninety, 6-8 weeks old, 150-180 gm, male Sprague Dawley rats, purchased from Northern RK company, were used for the present study. They were housed in separate cages comprising 2-3 rats each and kept in an air-conditioned room (23±1°C, 50-60% humidity) and 12 h light per day. The rats were fed with standard rat pellet and drinking water was made available *ad libitum*. A single dose (0.1 ml/kg bw) of long acting 20% oxytetracycline HCl was given intramuscularly as prophylaxis.

Animals were divided into 3 equal groups after a 1-week of adaptation period. Rats receiving only tricaprylin acted as controls. Cumulative individual doses of 13.8 ng and 13.0 ng of BaP and BeP, respectively calculated on its occurrence in Malaysia haze 1997 (8), were i.t. administered (9) at 8 frequencies for a month to the BaP and BeP groups.

Blood (2 ml) was collected by cardiac puncture into hepanirised tubes before treatment (day 0), hours (12 and 32), days (3, 7, 21, 60 and 180) p.i for estimation of MDA. Five rats from each group were necropsied at 12 hours, 3, 7, 21, 60 and 180 days p.i, after an i.m injection of ketamine:xylazine. Lung and liver samples procured at post mortem were snap frozen in liquid nitrogen and kept at (-80°C) until further use. Homogenates of lung and liver were prepared by mixing it with cold 1.15% KCl (1:10, w/v). The homogenates was centrifuged at 10,000g for 20 min and the supernatant was used for MDA assay (10).

The data were analyzed with SPSS 16.0 for Windows (SPSS Inc., Chicago, IL) by using one-way analyses of variance (ANOVA). Differences between means were determined using Tukeyís multiple range test in which the significance level was defined as $p< 0.05$.

Results and Discussion

The plasma, lung and liver MDA concentration of control rats (at all instances) and of all rats prior to the commencement of the experiment were almost identical (Tables 1-2). Following i.t instillation of BaP and BeP, the

Table 1. The plasma MDA concentrations (nmol/ml) of rats during the experimental period (Mean ± SE)

	ZERO	12h	32h	3d	7d	21d	60d	180d
Cont	1.66±0.07^{aA}	1.71±0.06^{aA}	1.64±0.03^{aA}	1.70±0.08^{aA}	1.74±0.06^{aA}	1.71±0.05^{aA}	1.69±0.05^{aA}	1.68±0.08^{aA}
Bap	1.68±0.05^{aA}	2.65±0.08^{bB}	2.73±0.05^{bB}	2.74±0.05^{bB}	2.77±0.04^{bB}	2.79±0.10^{bB}	2.83±0.04^{bB}	3.16±0.08^{cB}
Bep	1.76±0.06^{aA}	1.97±0.15^{bC}	2.32±0.19^{bC}	2.59±0.18^{bB}	2.54±0.21^{bB}	2.01±0.20^{aC}	1.77±0.07^{aA}	1.71±0.04^{aA}

^{a,b,c}Values bearing similar superscripts in same row do not differ at $p<0.05$

^{A,B,C}Values bearing similar superscripts in same column do not differ at $p<0.05$

Table 2. The pulmonary and hepatic MDA concentrations (nmol/mg.protein) of rats at post mortem (Mean ± SE)

	Groups	12h	3d	7d	21d	60d	180d
Lung	Cont	5.95±0.45^{aA}	5.89±0.50^{aA}	6.24±0.49^{aA}	6.14±0.58^{aA}	5.94±0.50^{aA}	6.08±0.50^{aA}
	Bap	9.86±0.95^{cB}	10.02±0.64^{cB}	10.22±0.58^{cB}	10.12±0.97^{cB}	10.11±0.90^{cB}	12.15±1.01^{cB}
	Bep	7.83±0.87^{bB}	7.53±0.55^{bC}	7.45±0.71^{bC}	7.11±0.88^{aA}	6.34±0.64^{aA}	6.21±0.84^{aA}
Liver	Cont	15.35±1.88^{aA}	14.92±2.51^{aA}	15.25±2.16^{aA}	18.29±2.61^{aA}	17.93±1.94^{aA}	19.27±2.24^{aA}
	Bap	26.52±3.79bB	29.05±3.62^{bB}	28.10±2.83^{bB}	30.15±3.57^{cB}	30.53±3.89^{cB}	38.51±5.71^{cB}
	Bep	21.06±3.28^{bB}	21.83±2.94^{bC}	20.48±3.65^{acA}	21.18±2.95^{abA}	19.14±2.29^{aA}	19.68±2.90^{aA}

^{a,b,c}Values bearing similar superscripts in same row do not differ at $p<0.05$

^{A,B,C}Values bearing similar superscripts in same column do not differ at $p<0.05$

concentration of MDA in the plasma was always higher ($p<0.05$) in the treated groups compared to the controls. Values returned to normal on day 21 onwards in the BeP group. Similar trends were also seen in the lung and liver. Our results showed that after i.t. instillation, the local and systemic increase of MDA levels (11) indicated that PAHs are absorbed rapidly from the alveolar type I epithelium (12), where it is metabolized locally by phase I enzymes into various polar and water soluble metabolites (12). This study also showed that the response of body to different PAHs varied. This was manifested by the prolonged high MDA levels in the BaP group, where it is diminished on day 21 in the BeP group, giving an explanation why some PAHs could initiate cancer and others not. Important to carcinogenesis, the unregulated or prolonged production of cellular oxidants has been linked to mutation (induced by oxidant-induced DNA damage), as well as modification of gene expression (13).

In conclusion, this study revealed that PAHs differ in their ability to induce MDA, which may lead to different responses to mutagenesis and carcinogenesis.

Acknowledgements

The authors wish to express their gratitude to Mr. Ghazali Mohd Yusof, Mr. Noraziman Sulaiman, Mr. Zainuddin Ibrahim, Mr. Mohammed Najib and Mr. S. Apparau for their excellent technical assistance.

References

1. Hayashi, 2005. Exp. Toxicol. Pathol. 57: 227-232.
2. Gerde et al., 1998. Carcinogenesis 19: 493-500.
3. Marriott et al., 2008. Am. J. Respir. Crit. Care Med. 177: 887-895.
4. Liu et al., 2002. Proc. Natl. Acad. Sci. U.S.A. 99: 2356-2361.
5. Muller et al., 2007. Free Radic. Biol. Med. 43: 477-503.
6. Stadtman, 1992. Science 257: 1220-1224.
7. Han et al., 2001. Biochem. J. 353: 411-416.
8. Zakaria et al., 1998. Proc. Natl. Symp. Impact of Haze. UPM, Malaysia. 10.1-10.5.
9. Oka et al., 2006. J. Toxicol. Pathol. 19: 107-109.
10. Okhawa et al., 1979. Anal. Biochem. 95: 351-358.
11. Kwiatkowska et al., 1999. Resp Med 93: 272-276.
12. Gerde et al., 1997. Carcinogenesis, 18: 1825-1832.
13. Klaunig and Kamendulis, 2004. Ann. Rev. Pharmacol. Toxicol. 44: 239-267.

Salivary Adenocarcinoma with Splenic Metastasis in a Dog

J.K. Park, S.G. Lee, I.H. Hong, A.R. Ji, M.R. Ki, S.Y. Han, C.W. Min, H.J. Shin, K.S. Jeong*

*Department of Pathology, College of Veterinary Medicine, Kyungpook National University, Daegu 702-701, Republic of Korea. *Corresponding author: jeongks@knu.ac.kr*

Keywords: *adenocarcinoma, dog, metastasis, salivary gland, spleen*

Introduction

Salivary gland tumors were rarely reported in dogs and cats with over all incidence of 0.07% (1). The salivary tumors generally occur in submandibular and parotid glands (2). Acinic cell carcinoma and adenocarcinoma have been known to occur most frequently in malignant salivary gland tumors. To date, 23 cases of salivary gland adenocarcinoma were reported, 11 in the parotid gland, 5 mandibular, 3 sublingual, 2 pharynx and 1 involving both parotid and mandibular glands in dogs (3). However, to authorís knowledge, there was no report of salivary gland adenocarcinoma with splenic metastasis so far. Here, we describe a case of salivary adenocarcinoma with splenic metastasis in a dog.

Material and Methods

An 8 year-old, female, Maltese dog had a subcutaneous firm mass on left cervical regions. In physical examination, the dog showed severe abdominal pain. In abdomen ultrasonography, hypoechoic lesions were observed in the spleen. Serum biochemistry revealed abnormally increased AST and ALT level. Fine needle aspiration of the cervical mass exhibited undifferentiated glandular epithelial cells showing anisokaryosis and a high nuclear-to-cytoplasmic ratio. A week later, the symptoms of the dog got more severe, which showed spasticity, more enlarged cervical mass, more severe pain and gasp. Finally, the dog was euthanized with owner's agreement. The organ tissue was sectioned in thickness of 4um and stained with hematoxylin and eosin (HE) and immunostained using antibodies of CK8/18 and CK19.

Results and Discussion

In necropsy, the dog showed enlarged and firm left submandibular salivary gland. There was also a mild enlargement of the adjacent submandibular lymph nodes whereas right submandibular salivary glands and lymph node showed no abnormal lesions. We also observed severely enlarged mesenteric lymph nodes and whitish foci in the spleen and liver. Other organs showed no abnormal lesions. On cut section of the affected organs, each organ showed homogeneous whitish component suspected as a metastasis of tumor cells. Microscopically, the left submandibular gland was replaced by the tumor cells completely. The tumor cells showed prominent, round, vesicular nuclei and scant cytoplasm. The tumor cells also had polygonal shape and arranged in narrow trabeculae, cords and solid sheets separated by fibrous stroma. Small area exhibited an occasional formation of acinar structures which revealed the tumor cells is glandular components. In submandlibular lymph node, mesenteric lymph nodes, liver and spleen, the metastasis of the tumor cells were observed. In immunohistochemistry using cytokeratins (CK8/18, CK19) for epithelial marker, the tumor cells showed strong positive reaction, which demonstrated the origin of tumor cells is epithelial component. On physical examination, salivary gland adenocarcinomas are generally firm, painless and attached to deeper structures in the neck, the base of the ear (parotid gland), the upper neck (mandibular gland),the floor of the mouth (sublingual gland) and in the area of lip and maxilla (zygomatic gland) (4). These neoplasms show generally locally invasion, therefore they can extend to the adjacent tissues and distant organs (4). Although salivary gland adenocarcinomas occupy the major part of the salivary gland tumors in animals, the histological features of metastasis of tumor cells to the spleen confirmed with immunohistochemistry was not reported to date.

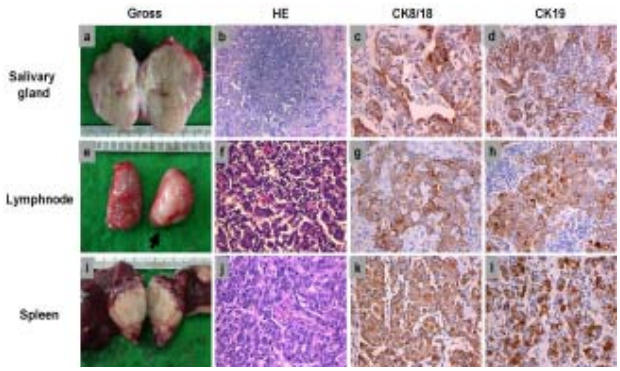

Fig. 1 (a) Cut surface of the affected salivary gland. Basophilic neoplastic tumor cells replacing the right submandibular gland (b) (x100, HE), left submandibular lymph node (f) (x200, HE) and spleen (j) (x200, HE). (e) Enlarged left submandibular lymph node (arrow). (i) Whitish metastatic lesion on cut section of the spleen. CK8/18 and CK19 positive tumor cells in salivary gland (c, x400, d, x200), lymph node (g, h, x400) and spleen (k, l, x400).

References

1. Carberry et al., 1987. Cornell. Vet. 77: 362-366.
2. Kim et al., 2008. J. Vet. Sci. 9: 331-333.
3. Meuten, 2002. Tumors in Domestic Animals, 4th ed. 410-420.
4. Militerno et al., 2005. J. Vet. Med. A. Physiol. Pathol. Clin. Med. 52: 514-516.

Ossifying Fibroma of External Auditory Canal in a Dog

J.K. Park, S.G. Lee, I.H. Hong, A.R. Ji, M.R. Ki, S.Y. Han, S.Y. Lee, C.W. Min, K.S. Jeong*

*Department of Pathology, College of Veterinary Medicine, Kyungpook National University, Daegu 702-701, Republic of Korea. *Corresponding author: jeongks@knu.ac.kr*

Keywords: *aural, dog, external auditory canal, ossifying fibroma*

Introduction

Ossifying fibroma is an uncommon benign-osseous neoplasm in humans and animals (1, 2). Histological feature of ossifying fibroma shows intermediate stage between osteoma and fibrous dysplasia (3). In veterinary literature, ossifying fibromas have been reported in dogs, cats, horses, a greater kudu, a goat, a sheep, a llama (4), a rabbit (5) and a bird (6). The mandible and maxilla were known as the most common places in which ossifying fibromas have occurred in animals (4). To date, in dogs, ossifying fibroma was reported only in the maxilla, mandible, calvarium and os penis (3). The present case describes a first report of ossifying fibroma occurred in external auditory canal in a dog. Ear canal tumor is also relatively uncommon in dogs, which was mainly associated with ceruminous gland tumors (7).

Material and Methods

A 3 year-old, male, Pomeranian dog was presented a local veterinary hospital because of a hemorrhagic externa otitis of right ear. In physical examination, the dog appeared to have no abnormal symptom. Serum biochemistry and complete blood count test results showed normal range. Upon otoscopy, the right external auditory canal was revealed to be almost obstructive by a proliferative and well-circumscribed mass adjacent to the ear drum. In cytological examination, the spindle-shaped stromal cells with oval nuclei and scant cytoplasm were observed. Surgically, the ear canal mass was excised and the mass was referred. The resected mass was sectioned in thickness of 4um and stained with hematoxylin and eosin (HE) and Massonís trichrome stain.

Results and Discussion

Grossly, the ear canal mass was well-demarcated and firm to cut. On cut section, the mass exhibited central portion of homogeneous whitish osseous components surrounded by brown-pinkish soft tissue. Histopathologically, the resected external auditory canal mass was composed of fibroblastic spindle cells which showed differentiation to metaplastic osteoblasts-like cells. The metaplastic osteoblasts formed and surrounded osteoid bony spicules. The bony spicules were separated by abundant collagens and neoplastic fibroblastic cells. The fibrous stroma of the mass was moderately vascularized and exhibited mild infiltration of neutrophils. Neoplastic spindle cells were characterized by elongated ovoid nuclei, scant cytoplasm and indistinct cell borders. Mitotic figures were not observed. Some parts of the mass adjacent to bony spicules exhibited the presence of osteoclasts. In Massonís trichrome stain, the bony spicules were differentiated clearly.

Osteoma, ossifying fibroma and fibrous dysplasia belong to a miscellaneous group of benign lesions found primarily in intramembranous bone (1). Ossifying fibromas generally show a greater density of fibroblastic spindle cells and fibers in tissue spaces between bony trabeculae than that of the marrow space of osteomas, which distinguishes ossifying fibroma from osteoma (1). To the best of author's knowledge, ossifying fibroma of external auditory canal was not reported in not only animals including dogs but also human beings.

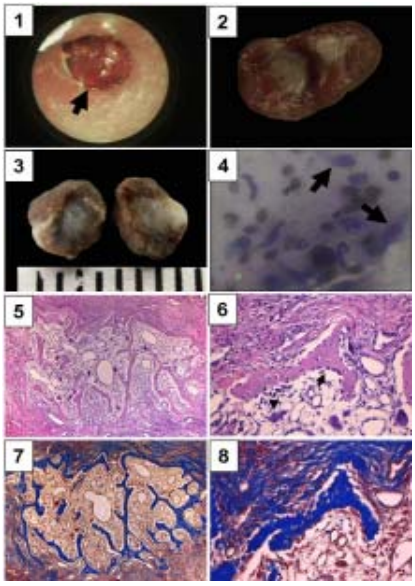

Fig. 1 osteoscopy showing a mass obstructing external auditory canal.
Fig. 2 well-demarcated mass.
Fig. 3 cut-surface of the mass showing homogeneous whitish component in the central part.
Fig. 4 Identification of spindle shaped cells in cytological examination.
Fig. 5 Ossifying component in the central part of the mass (x100, HE).
Fig. 6 well-differentiated bony trabecula lined by osteoblast (arrow). Osteoclasts were also observed (arrow head). (x400, HE).
Fig. 7, 8 Masson's trichrome stain to identify collagen fibers and bone matrix. (x100, x400).

References

1. Meuten, 2002. Tumors in Domestic Animals, 4th ed, 248-255.
2. Kaufmann et al., 1999. Head. Neck. 21: 578-581.
3. Miller et al., 2008. Vet. Pathol. 45: 203-206.
4. McCauley et al., 2000. J. Vet. Diagn. Invest. 12: 473-476.
5. Whitten et al., 2006. Vet. Pathol. 43(1): 62-64.
6. Razmyar et al., 2008. J .Avian. Med. Surg. 22: 320-322.
7. Fan et al., 2004. Vet. Clin. North. Am. Small. Anim. Pract. 34: 489-509.

Subcutaneous Leimyosarcoma in a Smad3 Hetero Mouse

A.R. Ji, I.H. Hong, J.K. Park, M.R. Ki, S.Y. Han, J.T. Kim, H.R. Cho, K.S. Jeong*

*Department of Pathology, Colleges of Veterinary Medicine, Kyungpook National University, Daegu 702-701, Republic of Korea *corresponding author: jeongks@knu.ac.kr*

Key words: alpha-smooth muscle actin, leimyosarcoma, mouse, smad3

Introduction

Superficial leiomyosarcoma, which can be divided into two groups; subcutaneous and cutaneous leimyosarcoma, is a rare malignant tumor in both humans and animals and thoughts to originate from the smooth muscle cells in blood vessels and the arrectores pilorum (1-4). This Study is a case of subcutaneous leiom yosarcoma in a Smad3$^{+/-}$ mouse, which presented a mass in the ear. Smad3 is a key modulator of the TGF-β1 signaling pathway and is related broadly with gene expression. For that reason, Smad3 transgenic mice have been widely used and have played a critical role in the research field (5, 6).

Material and Methods

The Smad3 mutant mice were obtained from the National Cancer Institute, MD, USA, and kept in a room at 22±2% with 50±10% of relative humidity on a 12 h light-dark cycle and fed standard laboratory feed and water ad libitum. After the 19-month-old ear tumor presenting male Smad3$^{+/-}$ mouse died, PCR was performed to confirm the genotype of Smad3$^{+/-}$. A tumor sample was fixed in 10% neutral buffered formalin, routinely processed, embedded in paraffin, sectioned to 4um thickness and stained with H&E. After the tumor type was determined by H&E, IHC was performed on the paraffin sections using an avidin-biotin-peroxidase complex method with 3, 3-diaminobenzidine. Anti-vimentin, anti-cytokeratin, anti-smooth muscle actin, anti-desmin, anti-myogenin and anti-S100 were used for IHC.

Results and Discussion

The auricular skin tumor was firm and the gross lesion of the cut surface showed a whitish component with reddish hemorrhaging. The histopathologic examination showed nonencapsulated partially invasive spindle to ovoid cells. Among the mixture of well-differentiated and less differentiated cells, mitoses were present (1-2 mitoses/

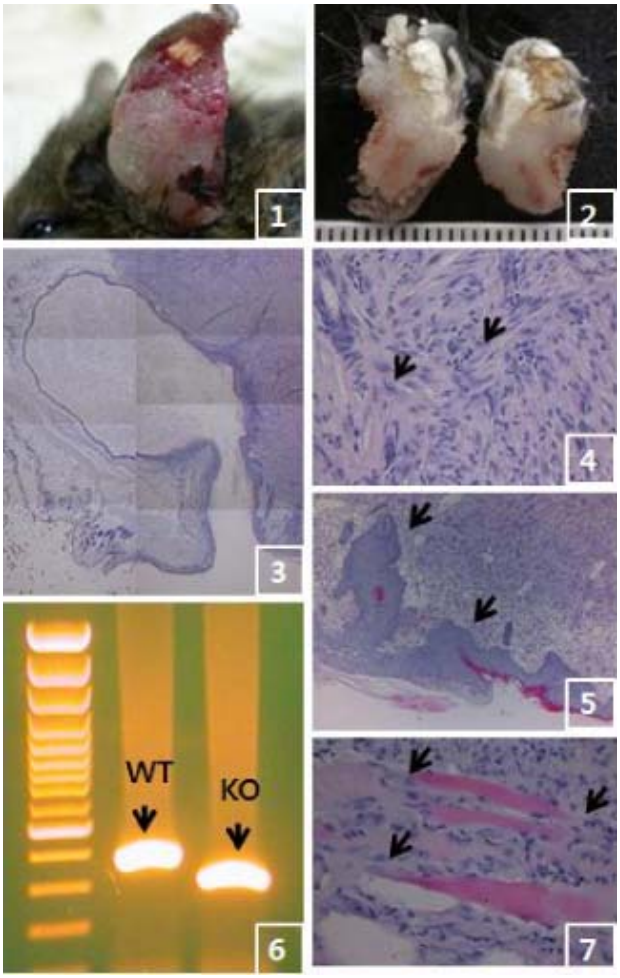

Fig. 1, 2 Gross picture of the ear tumor and cut surface
Fig. 3 Cyst formation in leiomyosarcoma (H&E)
Fig. 4 Mitotic figure of leiomyosarcoma (H&E, x400)
Fig. 5 Epidermal hyperplasia (H&E, x100)
Fig. 6 PCR result of Smad3 hetero type (wild type: 431bp, knockout type: 284bp)
Fig. 7 Tumor invasion to the skeletal muscle layer (H&E, x400)

400x field), evidence of invasion to the adjacent skeletal muscle, loss of skin adnexa, and necrosis were shown. The tumor was apt to form a cyst and epithelial cells showed inward hyperplasia. The IHC analysis of the mass shows a strong diffuse positive reaction for desmine and a-SMA, and a weak but partially strong posive vimentin in the cytoplasma of the neoplastic cells. However, Reaction for CK, S100, and myogenin were all negative. Consequently, the present case was diagnosed as a subcutaneous leiomyosarcoma via the results taken from the gross lesion, histopathologic examination and immuno-histochemistry.

The genotyping result from the mouse with subcutaneous leiomyosarcoma revealed 431bp, 284bp PCR products, which confirmed it was a $Smad3^{+/-}$ mouse.

Some of important roles of Smad3 are the G1 arrest of cell cycle, apoptosis, and recruiting inflammatory cells during the wound healing and suppression of Smad3 pathway can induce carcinogenesis (7, 8). The present case also shows some features which is related with Smad3 mutant such as epidermal hyperplasia, which usually arise form cutaneous tumor, and suppression of inflammation in an injured lesion (9).

Leiomyosarcoma of the skin and subcutis in animals reported extremely rarely and this is the first report of subcutaneous leiomyosarcoma in a Smad3 transgenic mouse to the author's knowledge.

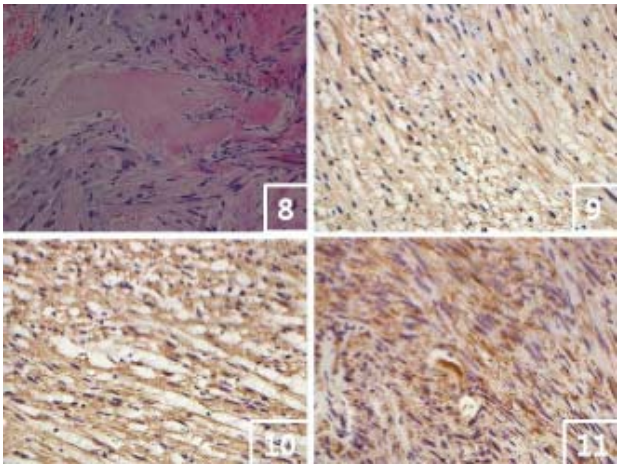

Fig. 8 Necrosis lesions in leiomyosarcoma (H&E, x400)
Fig. 9 Immunohistochemistry for vimentin (x400)
Fig. 10 Immunohistochemistry for desmin (x400)
Fig. 11 Immunohistochemistry for α-SMA (x400)

References

1. Snowden et al., 2001. Ear Nose Throat J. 80: 449-453.
2. Rouhani et al., 2008. Cancer. 113: 616-627
3. Ozturk et al., 2004. Auris Nasus Larynx 31: 323-328.
4. John et al., 2006. Urology 67: 424. e13-15.
5. Brown et al., 2007. J. Cell Biochem. 101(1): 9-33A
6. Arany et al., 2006. Proc. Natl. Acad. Sci. 103(24): 9250-9255
7. Vijayachandra et al., 2009. Mol. Carcinog. 48: 181-186.
8. Li et al., 2006. Mol. Carcinog. 45: 389-396
9. Fauth et al., 2009. J. Cut. Pathol. E-pub ahead

Porcine Multicentric B-cell Lymphosarcoma in Korea

J.H. Kwak, I.H. Hong, J.K. Park, M.R. Ki, S.Y. Han, K.S. Jeong*

*Department of Pathology, College of Veterinary Medicine, Kyungpook National University 1370 Sangyuck-dong, Buk-gu, Dae-gu 792-701, Republic of Korea. *Corresponding author: jeongks@knu.ac.kr*

Keywords: *B cell, Korea, lymphosarcoma, porcine*

Introduction

Lymphosarcoma is considered as a rare porcine disease but, common of all tumors (1). It primarily affects young animal before maturity but also in mature animal (2). It is known that lymphosarcomas are classified into three forms: multicentric, thymic and cutaneous form. In pig, most cases are the mutlicentric form (3). It has been reported from many countries, but in Korea, lymphosarcoma has been rarely reported (4). So we report a case of porcine multicentric B cell lymphosarcoma in Korea.

Material and Methods

A six-month boar died and autopsy was done with gross examinations. Tumor mass, the liver, lung, kidney, spleen and mesentery lymph node were taken for histological examination. Samples were fixed in 10% neutral buffered formalin, routinely processed and embedded in paraffin wax. Sections were cut out at 4 μm. The sections were stain with hematoxylin and eosin. Immunochemistry using CD3 and CD79a was done for differential diagnosis of B cell lymphoma and T cell lymphoma.

Results and Discussion

Grossly, large tumors were observed on the surface and the mesenteric lymph nodes were enlarged. The cut surface revealed homogenous whitish color. The liver showed many nodular masses. Masses were whitish and discovered in all liver parenchyma surfaces. The liver was almost destructed by mass showing sever invasions. The lung exhibited mild swelling and had multifocal whitish nodules in the right cranial lobe. On cut surface of the lung, the lung parenchyma was filled with yellowish exudates. The kidney had normal size and pale color. When cut the kidney, cortex was yellowish. There was no significant findings in the spleen.

Fig. 1 A) Large tumor masses of intestine. B) Liver showed many whitish nodules.

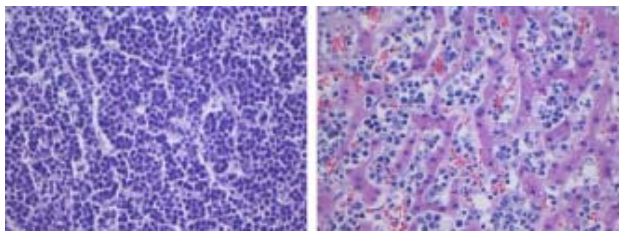

Fig. 2 A) Tumor mass showed many lymphoblastic cells, mitotic figure and apoptotic body (x400). B) Hepatocytes were degenerated by infiltrated neoplastic cells (x400).

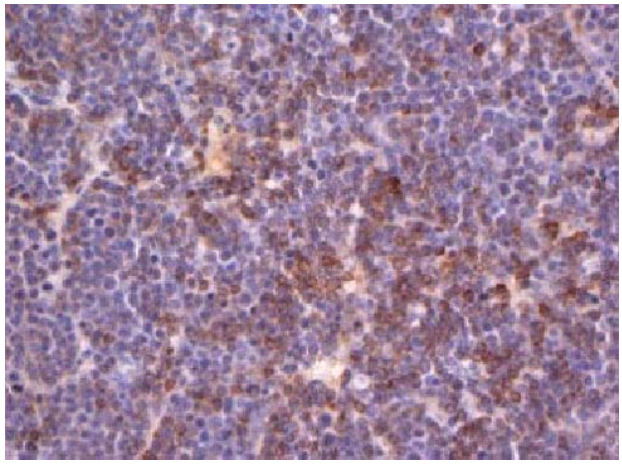

Fig. 3 The tumor cells showed a positive reaction with CD79a

Microscopically, the mesenteric lymph node parenchyma was infiltrated by many neoplastic cells and filled with homogenous lymphoblastic cells. There were many mitotic figures and apoptotic bodies. In the liver,

many neoplastic cells also infiltrated into hepatic sinusoid and hepatocytes, and hepatic lobules were almost degenerated by the neoplastic lymphoblastic cells. The lung showed mild edema and exhibited slightly interstitial pneumonia. However, there was no tumor cell metastasis. In the kidney, there were mild atrophic glomerulus but tumor metastasis was not observed.

Immunochemistry was performed with CD3 for T cell marker and CD79a for B-cell marker. In the present case, the tumor cells showed a positive reaction with CD79a and negative reaction with CD3.

Taken all together, The diagnosis of is porcine multicentric B cell lymphosarcoma. It is known that multicenteric form lymphosarcoma involve many organs from many cases. However unlike most cases, this case showed only hepatic metastasis.

Porcine lymphosarcoma was rarely reported in Korea. In 2007, it was reported that lymphosarcoma occurred in Jeju, Korea. In the case, animal was 7-year-old boar and diagnosed as multicentric T cell lymphosarcoma. According to the author's knowledge, it is the first porcine multicentric T cell lymphosarcoma in Korea (4). Howerver, unlike that case, our animal was six-month boar and multicentric B cell lymphosarcoma.

Althought, porcine lymphosarcoma is rare in Korea, it has been reported from many countries. Therefore, it is necessary for Korean clinical pig veterinarian to have more attention to the lymphosarcoma in pig..

References

1. Vo et al., 2004. J. Vet. Med. A Physiol. Pathol. Clin. Med. 51(7-8): 348-353.
2. Bostock et al., 1973. J. Natl. Cancer Inst. 50(4): 933-939.
3. Anderson et al., 1969. Natl. Cancer Inst. Monogr. 32: 343-353
4. Yang et al., 2007. Korean J. Vet. Res. 47(2): 187-190.

Bilateral Extranodal Lymphoma of the Third Eyelid Conjunctiva in a Dog

I.H. Hong, S.H. Bae, J.K. Park, A.R. Ji, S.Y. Han, M.R. Ki, J.H. Kwak, S.H. Lee, S.G. Lee, K.S. Jeong*

*Department of Pathology, College of Veterinary Medicine, Kyungpook National University, Daegu 702-701, Republic of Korea. *Corresponding author: jeongks@knu.ac.kr*

Keywords: *dog, lymphoma, third eyelid*

Introduction

The third eyelid is modified conjunctival fold in the medial canthus of some animals. Although the third eyelid is small ocular adnexa, various diseases including the tumors have been reported. Tumors of the third eyelid are rare in dogs, however, primary neoplasms, metastatic tumors, tumors extending from adjacent structures, and systemic neoplasm can affect the third eyelid. Squamous cell carcinoma, melanoma, papilloma, fibroma, hemangioma, lipomas, mast cell tumors, adenoma and adenocarcinoma have been reported in the third eyelid as primary neoplasms (1). Secondary involvement is most commonly a consequence of multicentric lymphoma. However, extranodal lymphoma of ocular conjunctiva is rare, moreover the third eyelid involvement has not been reported yet to the author's knowledge. In the present paper describes the clinical and histopathologic findings of bilateral extranodal lymphoma of the third eyelid in a dog.

Material and Methods

A 4-year-old, neutered female Cocker spaniel was presented with protrusion of third eyelid of left eye. The owner reported that protrusion was observed 1 month prior to examination. The mass was excised under general anesthesia and then referred to histological examination. The mass was fixed in 10% neutral buffered formalin, routinely processed and embedded in paraffin. Sections were cut at 4 μm and stained with hematoxylin and eosin (H&E). Immunohistochemistry for CD3 (T lymphocyte marker) and CD79a (B lymphocyte marker) were executed to define immunophenotype of the cells.

Results and Discussion

On ocular examination, the third eyelid was protruding, thickened and hyperemic (Fig. 1A). When the third eyelids from both eyes were reversed, an increase of volume of its internal surface could be verified. The third eyelid of left eye displayed a lobulated mass (0.5x0.3 cm) (Fig. 1B). The right third eyelid had a smaller one (0.2x0.2 cm) not easy to detect by owner. There were no significant findings except for both third eyelid lesions and no regional or generalized lymphdenopathy. In histological examination, the mass was consists of multiple lymphoid follicle proliferation, and lymphoid cells infiltrated into subconjunctival connective tissue. The lymphoid follicles were consisted of small and large lymphocytes with a lighter center and narrow darker mantle zone (Fig. 2A). There were observed a few apoptotic bodies with karyopyknotic and karyorrhexic nuclei in germinal center. Mitotic figures were rare. In immmunohistochemistry, almost cells in lymphoid follicles and infiltrated cells into the connective tissue in the mass were expressed for CD79a not CD3 (Fig. 2B). The tumor and the third eyelid of left eye were removed for biopsy and right one was remained. Topical therapy was prescribed with neomycin and dexamethasone ointment (Forus, Samil Pharm, Korea). At 1 year follow-up, the tumor of right third eyelid was still remained as similar size. However, the dog still showed no significant findings except those tumor with no evidence of systemic involvement.

Diffuse lymphoid follicles are normally located under the bulbar conjunctival surface of the third eyelid, and they have immunological activity. Lymphoid hyperplasia (follicular conjunctivitis) is very common disease of the third eyelid. It is due to chronic irritation and immunological stimulating proliferation of the normally present follicles on the bulbar aspect of the third eyelid. Therefore, lymphoid hyperplasia should be differential diagnosis to lymphoma in third eyelid. In the third eyelid of normal healthy dogs, B lymphocytes located in germinal centers of the lymphoid follicles and T lymphocytes are surrounding the B cell dominant germinal centers. Moreover, our present case showed tumorous features including appearance of a few apoptotic cells and mitotic figures. Therefore, a diagnosis of lymphoma on third eyelid (follicular mixed cell type, low grade) was established based on the histological and immunophenotypical features. To the author's knowledge, this is the first report of extranodal lymphoma of the third eyelid in a dog.

Fig. 1 Left eye of a dog (A) and formalin-fixed tumor (B)

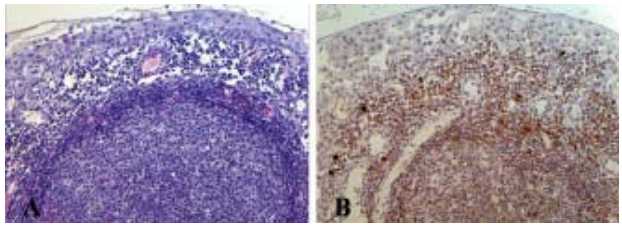

Fig. 2 H&E stain, x200 (A) immunohistochemistry of CD79a, x200 (B).

References

1. Willis, 2001 Clin. Tech. Small Anim. Pract. 16: 77-85.

A First Case Report of Histoplasmosis in a Cat in Japan

R. Kobayashi[1], F. Tanaka[2], A. Asai[2], Y. Kagawa[3], T. Ikeda[4], K. Shirota[1,5*]

[1]Research Institute of Biosciences, Azabu University, [2]Asai Animal Clinic, [3]North Lab,
[4]Laboratory of Veterinary Immunology and [5]Laboratory of Veterinary Pathology, Azabu University, Japan
[*]Corresponding author: dv0803@azabu-u.ac.jp

Keywords: *cat, histoplasmosis, intestine*

Introduction

Histoplasmosis is caused by *Histoplasma capsulatum (H. capsulatum)*, which is a dimorphic soil-borne fungus. In disseminated histoplasmosis, in which necrotizing and granulomatous inflammation develop observed in various systemic organs. There have been no reports of feline histoplasmosis in Japan. In this report, we describe cytological, histopathological, and immunohistochemical findings of intestinal histoplasmosis in a cat. This is the first report of feline histoplasmosis in Japan.

Material and Methods

A presumed 10-year-old, spayed female, domestic Japanese cat was referred to a veterinary hospital with vomiting. Physical examination revealed a palpable mass in the upper abdominal cavity. In cytologic examination of the fine needle aspiration from the mass, many yeast-like organisms were detected in macrophages (Fig 1). These organisms were observed as basophilic dots with a clear halo and measured 2 to 3 μm in diameter. The animal died on the following day. At necropsy, the upper part of the colon was markedly dilated with a thickened wall (Fig 2). The pancreatic lymph node was markedly enlarged and colored dark red. In the lungs, no significant changes were observed. The tracheobronchial lymph node was enlarged and firm. Tissue samples were collected from systemic organ for histopathological examination. For the immunohistochemistry, rabbit anti-histoplasmal yeast antibody (Meridian Diagnostics, Inc., Cincinnati, OH, U.S.A.; 1:1,000) were used as primary antibodies.

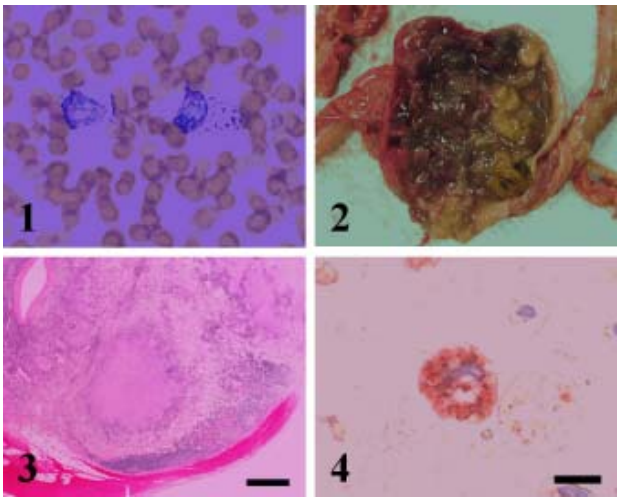

Fig. 1-4 Fig. 3 Bar = 1mm. Fig. 4 Bar = 10 μm

Results and Discussion

Microscopically, severe necrotizing and granulomatous inflammation was observed in the wall of the dilated colon (Fig 3), in the pancreatic lymph node, and in the tracheobronchial lymph node. In the dilated wall of the colon, there were many macrophages containing yeast-like bodies as irregularly shaped eosinophilic round structures throughout the necrotic lesions. Immunohistochemically, these organisms were positive for rabbit anti-histoplasmal yeast antibody (Fig 4). The lesions accompanying the yeast-like organisms were not seen in any other organs. The cytological, histopathological and immunohistochemical findings suggest that the cause of the intestinal lesion might be *H. capsulatum*.

Acknowledgements

We are indebted to Prof. Hiroyuki Taniyama (School of Veterinary Medicine, Rakuno Gakuen University) for his kind gift of the anti-histoplasmal yeast antibody.

Effect of Serum Cortisol and Progesterone on the Infiltration of Leukocyte Subpopulations in the Gilt Endometrium

A. Roongsitthichai[1*], J. Suwimonteerabutr[1], S. Koonjaenak[2], P. Tummaruk[1]

[1]Department of Obstetrics, Gynaecology and Reproduction, Faculty of Veterinary Science, Chulalongkorn University, Thailand 10330; [2]Department of Anatomy, Faculty of Veterinary Medicine, Kasetsart University, Thailand 10900

[*]Corresponding author: Padet.T@chula.ac.th

Keywords: *cortisol, endometrium, gilt, progesterone, reproduction*

Introduction

The reproductive function of the female pigs is difficult to examine under field condition. Post-mortem examination of the reproductive organs is a useful tool to obtain a potential source of information on infertility problems (1-4). Factors causing reproductive failure alter physiological status of the sow's endometrium in different pathways (5). However, the infiltration of immune cells in cyclic gilts and sows is also influenced by the estrous cycle and hormones (6-7). Progesterone (P4) increases tissue proliferation, gland development and protein secretion in the porcine endometrium (6). In addition, P4 increases the susceptibility of the endometrium to bacterial infection and may subsequently cause endometritis (8). The infiltration and distribution of leukocytes in the porcine endometrium during the estrous cycle have been comprehensively evaluated (6-7). Lymphocytes are the predominant population in the endometrium of the cyclic gilts, while the striking observation of numerous neutrophils was found in the endometrium of pre-pubertal gilts (6-7). The influence of stress on the reproductive function is well established (9). In pig, cortisol is an important hormone linked between stress and reproductive functions (9). However, information on the influence of cortisol on the distribution of immune cells in the uterine tissue of gilts and sows is limited. The present study was performed to evaluate the influence of cortisol and P4 on the distribution of leukocyte subpopulations in the giltís endometrium.

Material and Methods

Tissue collection: Genital organs from 39 Landrace x Yorkshire crossbred gilts culled due to vaginal discharge from two commercial swine herds in Thailand were collected. The organs including ovary, oviduct, uterus, cervix, vagina, vestibule, vulva and urinary bladder were collected, placed on ice, and transported to the laboratory within 24 h of culling. These organs were examined to assess the stages of the estrous cycle and gross-pathology (4). Ovarian appearance and component structures, i.e. corpora lutea (CL), corpora albicantia (CA) and follicles, on the ovaries were carefully examined. The uterine horns were opened longitudinally and the endometrium was investigated. Tissue samples were randomly collected from the uterus of the gilts including two parts of each uterine horn. The samples were fixed in 10% neutral buffered formalin for at least 24 h, embedded in paraffin, and processed by use of an automatic tissue processor. Each sample was embedded in paraffin block using embedding instrument. The paraffin embedding was cut with 5 μm thickness by microtome. The slides were left overnight at 37°C. The tissues were deparaffinized using xyline, passed different concentration of alcohol and were stained using haematoxylin for 5 min and eosin for 30 sec (H&E).

Histological examination: The sections were divided into three layers for histological examination, i.e. epithelial, subepithelial connective tissue and glandular layers. Immune cells, i.e. lymphocytes, neutrophils, eosinophils, macrophages and plasma cells in each layer were quantified under light microscope (400x). For each section and each layer, 20 microscopic fields were arbitrarily selected for investigation. Ocular micrometer with 25 squares corresponded to 15,625 μm^2 (400x) of real tissue area and 125 μm of real tissue length was used for counting the number of immune cells in each area by movement of the ocular micrometer across the entire area in a non-overlapping manner (6). The number of immune cell counts was expressed as the total number of cells per uterine section (20 microscopic fields). The degree of endometritis was categorized into mild, moderate, and severe condition on the criterion of neutrophil number infiltrated into the giltís endometrium. In the follicular phase, endometrium having neutrophils <80, 120, and >120 cells/ 20 microscopic fields, <9, 15, and >15 cells/ 20 microscopic fields in the luteal phase, and <2, 3, and >3 cells/ 20 microscopic fields in the inactive phase, were considered mild, moderate, and severe endometritis respectively (12).

Hormonal analyses: Blood samples were collected from the jugular vein prior to slaughter. They were centrifuged at 1,160x g for 10 min. The sera were collected and stored at -20°C until assay. Serum P_4 was analyzed by enzyme immunoassay (EIA) using a P_4 monoclonal antibody (CL425) (10). Briefly, plates (NUNC, Maxisorb), except for nonspecific binding wells, were coated with 50 μl of antibody (1:7,500) and incubated overnight (12 h) at 4°C. Plates were washed 5 times and 50 μl of P4 standard (0.78-200 pg/well), control and serum samples were added, followed immediately by 50 μl of P4-horseradish peroxidase (1:65,000). Plates were incubated at room temperature for 2 h followed by addition of 100 μl of ABTS substrate (40 μl, 0.5 M H_2O_2, 125 μl 40 mM ABTS in 12.5 ml

0.96% citric acid solution). Plates were read at 405 nm (ELISA reader, TECAN SUNRISE, Austria). Optical density (OD) for 0 wells was >0.7 to <1 OD. Assay sensitivity at 90% binding was 0.016 ng/ well. The intra assay CV for low and high controls was 6.15% and 9.05%, respectively. The serum cortisol level was determined by enzyme immunoassay (EIA) (Active® Cortisol EIA kit, Diagnostic Systems Laboratories, Inc., Texas, USA). The assayed was performed according to the manufacturer's instructions. The principal of the procedure follows the basic principal of EIA, which there is competition between an unlabeled antigen and an enzyme labeled antigen for a fixed number of antibody binding sites. A known amount of cortisol was added to the assay in order to calculate the intra-assay coefficients of variation, which were 0.84% and 0.33% for low and high cortisol concentration, respectively.

Statistical analyses: Data were analyzed using SAS (SAS v. 9.0, Cary, NC, USA). Numbers of cells were presented as the mean number of cells per 20 ocular fields (312,500 μm^2) in four tissue sections. The data were analyzed using general linear model procedure (PROC GLM). Normal distribution of the data was tested using the UNIVARIATE procedure. A natural logarithmic transformation was applied to the number of immune cells. Least-squares means were obtained and were compared using least significant different test. Spearman's correlation was used to analyze the association between cortisol, P4, and the number of leukocytes subpopulation. $p \leq 0.05$ was regarded to have statistical significance.

Results and Discussion

From the appraisal of genital organs, the number of gilts in follicular, luteal, and inactive phases was 10, 25, and 4 respectively. On average, cortisol concentration in the slaughtered gilts was 430.6±68.3 nmol/l (range 46.6-1,656.0). P_4 varied according to the ovarian appearance. On average, P_4 concentration was 88.3±7.7 nmol/l during luteal phase, 20.6±6.2 nmol/l during follicular phase, and 18.5±14.7 nmol/l during inactive phase. The most obvious leukocyte subpopulation in normal gilts, mild, and moderate endometritis was lymphocytes (in epithelium, subepithelial connective tissue, and glandular layers: 16.4, 88.8, and 50.9 cells in normal gilts, 34.3, 58.1, and 38.63 cells in mild endometritis gilts), meanwhile, neutrophils ware regarded as the most apparent subpopulation in gilts with severe endometritis (46.6, 126.5, and 23.0 cells in epithelial, subepithelial connective tissue, and glandular layers respectively). Vividly, the subepithelial connective tissue layer was the most prominent area in which the leukocytes infiltrated. The number of leukocyte subpopulations of the endometrium and the concentrations of cortisol and P4 classified by degree of endometritis in subepithelial connective tissue layers are demonstrated in Table 1. The gilts having severe endometritis tended to have a higher cortisol level than the gilts having normal endometrium (p=0.07).

In the epithelial layer, negative correlation between P_4 and neutrophils was observed (r= -0.44, p=0.006). In the subepithelial connective tissue layer, P4 was negatively correlated with neutrophils (r= -0.45, p= 0.004) and positively correlated with eosinophils (r=0.46, p=0.003). Serum cortisol was negatively correlated with lymphocytes in the subepithelial connective tissue layer (r= -0.2, p=0.08) and in the glandular layer (r= -0.2, p=0.09)

It is well-established that cortisol responses to stress and causes immunosuppression (9). In the present study, high cortisol concentration tended to decrease number of lymphocyte in subepithelial connective tissue and glandular layers of the gilts. Brandt et al. (11) demonstrated that the sows injected by ACTH had far higher level of serum cortisol (336±55 nmol/l) than the NaCl-injected (85±15 nmol/l) sows. The cortisol level in the present study (430.6±68.3 nmol/l) corresponded with the ACTH-induced sows of Brandt et al. (11). This implies that the endometritis gilts are stressful as indicated by the high level of serum cortisol. The correlation between serum cortisol and lymphocytes was apparently negative which seemed to determine the immunosuppressive condition.

Table 1 Levels of serum cortisol (nmol/l), P4 (nmol/l) and number of leukocyte subpopulations in the subeipthelial connective tissue layers of the giltís endometrium by degree of endometritis (mean±SEM)

Parameters	Normal	Endometritis		
		Mild	Moderate	Severe
No. of gilt	13	6	5	15
Cortisol	277±43	253±59	636±266	566±140
P_4	89±12	56±19	48±16	50±12
Lymphocytes	89±35	58±17	93±73	46±11
Neutrophils	4±3	23±11	48±23	126±26
Macrophages	1±0.5	4±2	4±3	1±0.7
Eosinophils	64±18	19±6	31±13	19±7
Plasma cells	55±24	19±10	82±45	41±14

Acknowledgement

The financial support for the present study was provided by The National Research Council of Thailand. A. Roongsitthichai is a grantee of the Royal Golden Jubilee (RGJ) Ph.D. Program, the Thailand Research Fund.

References

1. Dalin et al., 1997. Acta Vet. Scand. 38: 253-262.
2. Heinonen et al., 1998. Anim. Reprod. Sci. 52: 235-244.
3. Karveliene et al., 2007. Reprod. Dom. Anim. 42: 275-281.
4. Tummaruk et al., 2009. Theriogenology. 71: 369-375.
5. Dalin et al., 2004. Anim. Reprod. Sci. 82-83: 401-413.
6. Kaeoket et al., 2001. Anim. Reprod. Sci. 65: 95-114.
7. Bischof et al., 1994. J. Reprod. Immunol. 26: 111-129.
8. Wulster-Radeliffe et al., 2003. J. Anim. Sci. 81, 1242-1252.
9. Einarsson et al., 2008. Acta Vet. Scan. 50: 48.
10. Munro and Stabenfeldt, 1984. J. Endocrinol. 101: 41-49.
11. Brandt et al., 2009. Anim. Reprod. Sci. 110: 172-185.
12. de Winter et al., 1995. Anim. Reprod. Sci. 37: 325-335.

The Expression of Caspase 3 in the Chicken Bursa Cell in Tasik'98 Infectious Bursal Disease Virus Infection

H. Plumeriastuti

Department of Veterinary Pathology, Faculty of Veterinary Medicine, Airlangga University

Keywords: *apoptosis, chicken, infectious bursal disease*

Introduction

Infectious bursal disease (IBDV) is a highly contagious viral infection of chickens that is seen worldwide. The bursa of Fabricius is the primary target organ of IBDV (4). The virus replicates in immature bursa-derived lymphocytes (B-lymphocytes). The chickens which survive the disease are permanently immunosuppressed. Therefore they are more susceptible to other disease causing agents and don't respond adequately to vaccinations which are an essential part of poultry management systems (6, 7). Virulence of field strains of the virus varies considerably. Very virulent (vv) strains of the virus that cause high mortality and morbidity were detected first in Europe. These spread throughout the Old World in the last decade and in 1999 were in South America. Infection by this virus due to depletion of lymphocyte in the bursa of Fabricius because of necrosis and apoptosis (5, 8). Tasik'98 is one of vv IBDV field strain from Indonesia, which can cause an acute clinical disease characterized by devastating mortality and the sever depletion of bursa of Fabricius.

The main purpose of this study was to proof the increasing of bursa cells apoptosis by detection of Caspase 3 expression in bursa of Fabricius. The Caspase 3 is a main effecter caspase in apoptosis process. Direct or indirect activation of caspase 3 are responsible for target proteine cleavage due to a specific DNA and also in specific morphologic changes of apoptotic cells (1). When caspase 3 has activated, the cell commited to death and the apoptosis may called due to the point of no return (3, 4). The expression of activated caspase 3 in the cell occured at the early apoptosis process before appears clasical morphologic changes of cell death, so detection of the increasing of caspase 3 expression in the cell by immunohistocemestry can be used as the base for detection of apoptotic cell.

Material and Methods

Animal trial in this study were specific pathogenic free day old chick. Virus that used for infection was Tasik '98 isolate IBDV.

The study consists of two parts. Forty-four chickens on the first step of experiment are devided into 2 groups. Chickens in Group I were infected with 1000 TCID 50 of Tasik'98 isolate IBDV through intraocular, peroral, and intracloacal routes. Chickens in group II were treated with NaCl through intraocular, peroral and intracloacal routes as placebo. Randomly, each two chickens from 2 groups, were sacrificed on 12, 14, 16, 18, 20, 22, 24, 48, 72, 96, 120 day post infection. The bursa was collected and fixed in formalin buffer for histologigy and immunohistochemistry. Primary antibody was monoclonal rabbit anti caspase 3 antibody (LabVision Corp.). Caspase 3 expression was evaluated by counting the number of positive cells in percent. The time when caspase 3 expression increases for 25% will be determination of a time for sacrificing chicken in the second step of experiment.

Sixteen chickens on the second step of experiment are divided into 2 groups. Chickens in Group I were infected with 1000 $TCID_{50}$ of Tasik'98 isolate IBDV through intraocular, peroral and intracloacal routes. Chickens in group II were treated with NaCl by intraocular, peroral and intracloacal routes as placebo. On the time that was determined in first step of experiment, all of the chickens were sacrificed. The bursa were collected for histology and were evaluated on Caspase 3 expression used the method like the one that was done in

the first step of experiment above. The data were analysed by student t test.

Results and Discussion

The result of first step experiment showed that the 25% increasing of caspase 3 expression were found on 48 hours post infection. It was used for determination for sacrificing chicken in the second step of experiment.

The result of the second experiment showed that the expression of caspase 3 in bursa were significant difference ($p<0.05$) between infected chicken and non-infected chicken. Expression of caspase 3 increased from 1.25±1.05% in the non infected chickens became 29.94±2.01% in the infected chickens like showed in Fig. 1.

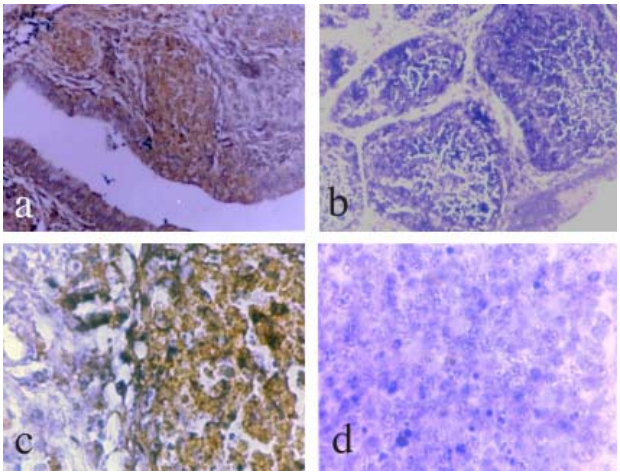

Fig 1 Caspase 3 was strongly expressed in infected chicken bursa (a, c) and there is almost negative in uninfected chicken bursa (b, d).

There are three apoptosis mechanisms that involve caspase activation. The first, granzyme/perforin mediated pathway. The second is dead receptor mediated pathway. Fas is one of the dead receptor, it was expressed in the cell membrane surface when the cell has been infected by a virus. The third, cytocrom c released from mitochondria bind Apaf-1 can induce the activation of caspase 9 (caspase inisiator). Caspase 9 will activate the effecter caspase due to apoptosis (1, 4).

The mechanism of bursal apoptosis in infectious bursal disease virus infected chicken still has not been fully understood. It was thought that the mechanism trough the Fas-Fas ligand pathway that could be explained with increasing of Fas and caspase 3 expressions, or perforin-granzyme pathway that could be explained with increasing of granzyme and caspase 3 expressions.

The result of this study showed that there was the increasing of caspase 3 expression in IBDV infected chicken bursa. It means that there was increasing of apoptosis in chicken bursa of Fabricius in Tasik'98 isolate IBDV infection. The increasing of caspase 3 expression could be described that bursa cell contained virus express Fas. Fas will bind Fas ligand of cytotoxic T lymphocyte. This binding will activate Fas associated dead domain and then run to cascade caspase activation. The other ways, activated cytotoxic T lymphocyte will releases perphorin and granzyme. Perphorin makes a pore in the virus infected cell membrane and then the granzyme enter the cell through the pore. Granzyme can activate caspase cascade.

References

1. Aschkenazi et al., 2002. Biol. Reprod. 66: 1853-1861
2. Balkundi et al., 2003. Biol. Reprod. 69: 718-724
3. Deneckert et al., 2001. Cell Mol. Life Sci. 58: 356-370.
4. Gupta, 2003. Intern. J. Oncol. 22: 15-20.
5. Jungmann et al., 2001. J. Gen. Virol. 2: 1107-1115.
6. Kim et al., 1998. Vet. Immunol. Immunopathol. 61: 331-341.
7. Nakamura et al., 1992. Avian Dis. 36: 891-896.
8. Tanimura and Sharma, 1998. J. Comp. Path. 118: 15-27.

Pathological Study on the Pulmonary Toxicity Induced by the Intratracheally Instilled Asian Sand Dust in Mice

M. Naota[1], T. Mukaiyama[1], A. Shimada[1, 2*], T. Morita[1]

[1]Department of Veterinary Pathology, [2]Arid Land Research Center, Tottori University, Tottori-shi, Tottori, 680-0001, Japan [*]Corresponding author: aki@muses.tottori-u.ac.jp

Keywords: *acute inflammation, asian sand dust, intratracheal instillation, lung*

Introduction

With global climate change, frequency and volume of asian sand dust (ASD), which originates from Gobi desert, are increasing in east Asian region since 2000 (1) resulting in one of the air pollution related threats to both human and animal health. Epidemiological studies showed that ambient ASD particles are associated with an increase in pulmonary and cardiovascular morbidity and mortality in Korea (2) and Taiwan (3).

There are, however, few reports on the pathological study of the pulmonary toxicity induced by ASD. In this study, we examined changes in the bronchoalveolar lavage fluids (BALF) and lung tissues of mice intratracheally instilled with ASD.

Material and Methods

0.05 ml of saline containing 50, 200, 800 and 3000 μg of ASDs (CJ-2 originated from Tengger desert, General Science Corp., Japan) were intratracheally instilled to ICR male mice. 0.05 ml of a saline solution was instilled to control mice. Animals were sacrificed at 24 h following exposures. Bronchoalveolar lavage fluid analysis (cell viability, differential cell counts and total protein concentration), histopathological examination and immunohistochemistry (TNF-α) of the lung tissues were assessed.

Results and Discussion

The intratracheal instillation of 800 and 3000 μg ASD significantly decreased the cell viability compared to the control group. Changes in the increased number of neutrophils and total protein concentration in BALF were dose dependent.

The histopathological examination revealed that ASD -induced severe inflammation around the dusts with neutrophils and macrophages and hemorrhage. In addition, TNF-α immunoreactivity was observed mainly in the inflammatory cells of the legion in lung tissues.

These results suggest that ASD induce acute pulmonary inflammatory changes. Mechanisms of health effect by particulate matter include direct effects of particle components and indirect effects by pro-inflammatory mediators released from particulate matter-stimulated macrophages (4). The inflammatory lung injury in this study may be caused by both ASD particle itself and the cytokines released in the lesion.

Table 1 Bronchioalveolar large fluid (BALF) analysis in mice after exposure to asian sand dust

Dose of instillation (μg/animal)	Percentage of neutrophils (%)	Concentration of total protein (μg/ml)
0	0.02±0.05	243.0±47.4
50	0.14±0.23	275.6±108.4
200	0.36±0.38	420.1±137.1
800	14.33±6.40*	1178.5±50.8
3000	44.38±2.69*	2375.0±116.4

*Significant different from the control group ($p<0.05$)

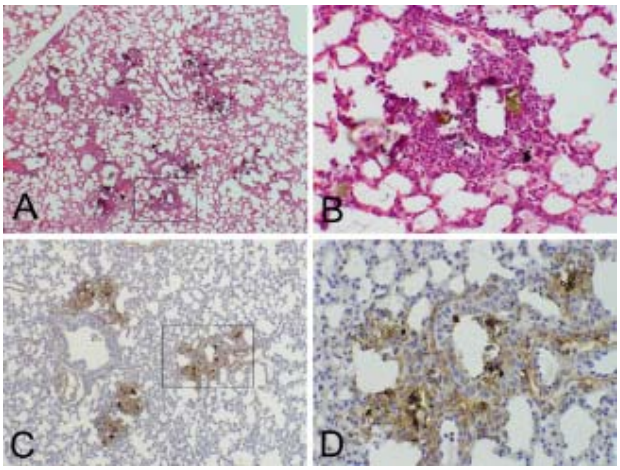

Fig. 1 Histopathology of the lungs from mice following the intratracheal instillation of 3000 μg ASDs.
(A) Hematoxylin and eosin stain, (B) high magnification of (A), (C) Expression of TNF-μ in the inflammatory region, (D) High magnification of (C).

In conclusion, this study demonstrated that mineralogical components of asian sand dust particles, free from chemical and biological pollutants in the atmosphere, induce acute inflammatory changes in the lung tissue and BALF *in vivo*.

References

1. Mori et al., 2003. Atomos. Environ. 37: 4253-4263.
2. Kwon et al., 2002. Environ. Res. 90: 1-5.
3. Chen et al., 2004. Environ. Res. 95: 151-155.
4. Gonzalez-Flecha. 2004. Mol. Aspects Med. 25: 169-182.

Pathological Study of Neurodegenerative Process of Equine Motor Neuron Disease

H. Matsuo[1], T. Morita[1*], R. Ito[1], K. Kikuchi[1], A. Shimada[1], Y. Hikasa[2], T. Amaya[3]

[1]Department of Veterinary Pathology, [2]Veterinary Internal Medicine, School of Veterinary Medicine, Faculty of Agriculture, Tottori University, Japan [3]Yamato-Kogen Animal Medical Clinic, Japan

[*]Coresponding author: aki@muses.tottori-u.ac.jp

Keywords: blood spinal cord barrier, equine motor neuron disease, leakage, lipopigment, oxidative stress

Introduction

Equine motor neuron disease (EMND) is a sporadic and progressive neurodegenerative disorder characterized by selective degeneration and loss of motor neuron, gliosis and formation of eosinophilic intracytoplasmic inclusion body in the spinal cord and certain cranial nerve nuclei (1).

Although Vitamin E deficiency is considered as a risk factor of EMND (2), the detail pathological process of neuronal loss in EMND is unknown. Because accumulation of endothelial lipopigment is observed in the small vessels of the spinal cord (3), it is suspected that motor neuron degeneration is mediated by blood spinal cord barrier (BSCB) disruption. This hypothesis is also supported by the recent studies of human motor neuron disease, amyotrophic lateral sclerosis (ALS) which closely resembles EMND (4).

Material and Methods

3 EMND cases and 3 control cases with no neurologic disorder were used. Complete postmortem examination was performed on all horses, and selected tissues were fixed in 10% neutral phosphatate buffered formalin. The tissues were routinely processed and stained with luxol fast blue (LFB) staining and Prussian blue-DAB post- DAB enhancement staining (5). Basement membrane degeneration, serum protein leakage and production of free radical were examined by immunohisto-chemical method. Primary antibodies were polyclonal rabbit anti-fibronectin antibody (ABR), anti-horse IgG antibody (ROCKLAND) and monoclonal mouse anti-metallothionein antibody (DAKO).

Results and Discussion

Grossly, the ear canal mass was well-demarcated and firm to cut. On cut section, the mass exhibited central portion of homogeneous whitish osseous components surrounded by brown-pinkish soft tissue. Histopathologically, the resected external auditory canal mass was composed of fibroblastic spindle cells which showed differentiation to metaplastic osteoblasts-like cells. The metaplastic osteoblasts formed and surrounded osteoid bony spicules. The bony spicules were separated by abundant collagens and neoplastic fibroblastic cells. The fibrous stroma of the mass was moderately vascularized and exhibited mild infiltration of neutrophils. Neoplastic spindle cells were characterized by elongated ovoid nuclei, scant cytoplasm and indistinct cell borders. Mitotic figures were not observed. Some parts of the mass adjacent to bony spicules exhibited the presence of osteoclasts. In Massonís trichrome stain, the bony spicules were differentiated clearly.

Osteoma, ossifying fibroma and fibrous dysplasia belong to a miscellaneous group of benign lesions found primarily in intramembranous bone (1). Ossifying fibromas generally show a greater density of fibroblastic spindle cells and fibers in tissue spaces between bony trabeculae than that of the marrow space of osteomas, which distinguishes ossifying fibroma from osteoma (1). To the best of author's knowledge, ossifying fibroma of external auditory canal was not reported in not only animals including dogs but also human beings.

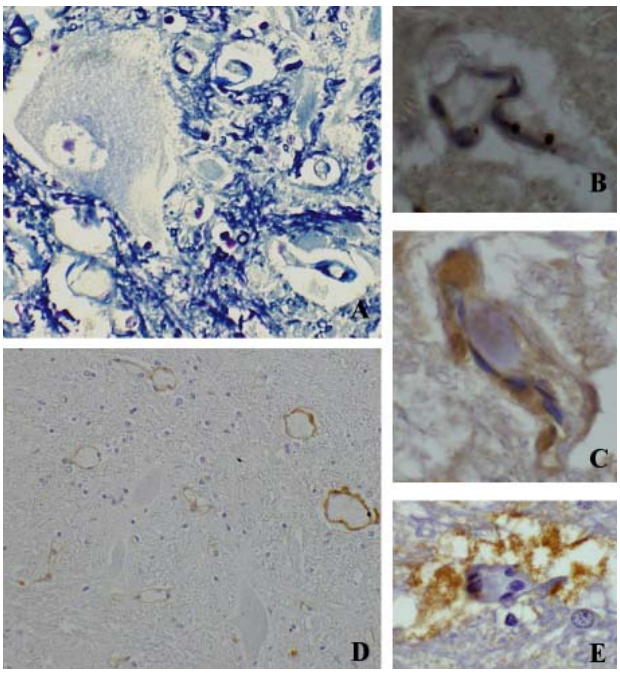

Fig. 1 Luxol fast blue staining (A), Prussian blue-DAB post-DAB enhancement staining (B), Immunostaining for IgG (C), Immunostaining for fibronectin (D), Immunostaining for metallothionein (E).

References

1. Cummings et al., 1990. Cornell Vet. 80: 357-379.
2. Divers et al., 2006. Am. J. Vet. Res. 67: 120-126.
3. Cummings et al., 1995. Acta Neuropathol. 90: 266-272.
4. Zhihui et al., 2008. Nature Neurosci. 11: 420-422.
5. Morita et al., 2005. J. Comp. Pathol. 133: 14-22.

Cerebellar Ataxia Induced by Plant Toxicosis in a Goat in Mongolia

S. Takeda[1], A. Shimada[1, 2*], T. Morita[1], G. Yandag[3], O.Gungaa[3]

[1]Department of Veterinary Pathology, [2]Arid Land Research Center, Tottori University, Tottori-shi, Tottori, 680-0001, Japan
[3]Institute of Vertinary Medicine, Zaisan 210153, Ulaanbaatar, Mongolia [*]Corresponding author: aki@muses.tottori-u.ac.jp

Keywords: *ataxia, cerebellum, goat, plant toxin, Purkinje cell*

Introduction

With global climate change (abnormal climate, warming temperature, drought) and human activity (over depasturaging, water pollution), vegetation dynamics are rapidly changing in Mongolia resulting in overgrowth of particular poisonous plants in the pasture field. In June 2009, a locomotor disorder developed in some goats that had grazed *Oxytropis glabra* in the Khovd province of Mongolia (Fig. 1). Affected goats displayed neurological signs including limb paresis, knuckling over in the fetlocks, fine head tremor, incoordination and an equilibrium disturbance characterized by frequent falling. Epidemiology indicates that the ingestion of *Oxytropis glabra*, by which plant Mongolian pasture has been replaced in the past 10 years by the significant environmental changes, is involved in the etiology of the disease. Here, we describe pathological findings of a goat with cerebellar ataxia in Mongolia.

Material and Methods

A goat with cerebellar ataxia was euthanased and necropsied. The brain and other organs (liver, spleen, kidney, heart, lung) were corrected, and tissues were fixed in formalin and embedded in paraffin. Sections were cut and stained with hematoxylin and eosin.

Results and Discussion

No gross pathological changes were seen in the goat. The microscopic examination of the cerebellum demonstrated decreased number of Purkinje cells (Fig. 2), increased number of glial cells (astrocytes and microglia) in the medulla (Fig. 3). These were no significant change in the other organs.

Purkinje cell loss and the gliosis present in the cerebellum were prominent. These pathological changes are in agreement with clinical neurological symptoms. Cerebellar ataxia due to plant poisoning was reported in sheep in Australian Merinos, goats grazing *Solanum cinereum* in Australia and *S. viarum* in the United States, and cattle grazing *S. kwebense* in South Africa, *S. dimidiatum* in the United States, *S. fastigiatum* in Brazil, and *S. bonariensis* in Uruguay(1). This is the first report of cerebellar ataxia in animals ingested *Oxytropis glabra*. Identification of the toxin and study on the mechanisms of Purkinje cell loss are required. The disease observed in the domestic animal may be one of the important indicators of the global environmental changes.

Fig. 1 *Oxytropis glabra* in the Mongolian pasture (Khovd province)

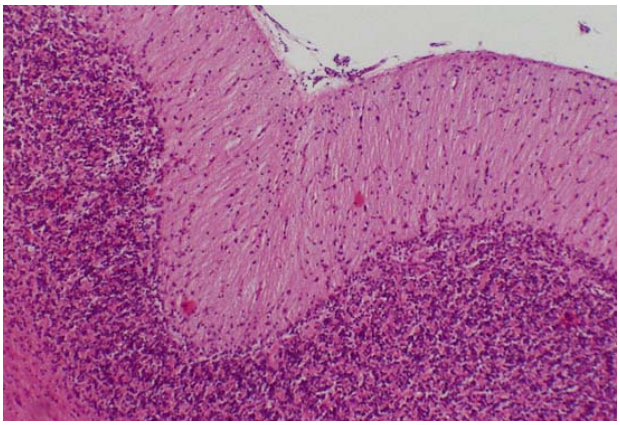

Fig. 2 Purkinje cell layer in the cerebellum of the goat affected with cerebellar ataxia, showing marked loss of Purkinje cells.

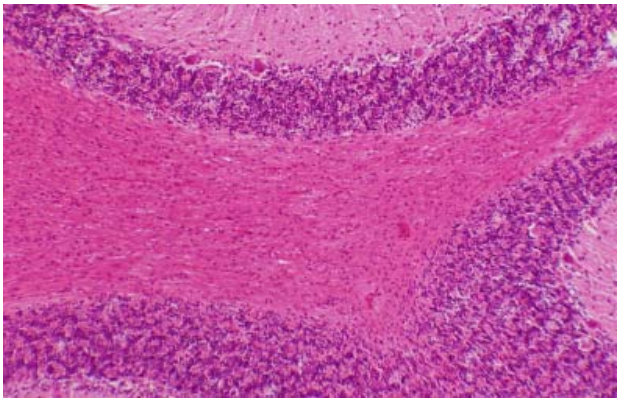

Fig. 3 Increased number of glial cells (astrocytes and microglia) in the medulla.

References

1. Bourke et al., 2008. Aust. Vet. J. 86: 354-357.

Two Cases of Feline Panleukopenia without Prominent Diarrhea

H. Imura[1], S. Shiotsu[1], A. Shimada[1*], T. Morita[1], K. Nishida[2]

[1]Department of Veterinary Pathology, Tottori University, Tottori, 680-8553, Japan
[2]Medical center Nishida, Osaka-shi, Japan [*]Corresponding author: aki@muses.tottori-u.ac.jp

Keywords: *cat, enteritis, panleukopenia, parvovirus infection*

Introduction

Feline panleukopenia is caused by *Feline panleukopenia virus* (FPV), which belongs to Parvovirinae. This disease is characterized by a panleukopenia, vomit, and diarrhea. FPV is highly contagious so this disease often takes an acute course with sudden death. Two cats with acute panleukocytopenia and no prominent diarrhea, negative for FPV immnomigration test, were pathologically examined in the study.

Material and Methods

One year old two adult male mix cats, kept together, died suddenly without prominent diarrhea. Hematological examination and immunomigration tests for detection of parvo viral antigen in fecal samples were conducted. After death of these 2 cats, necropsy and sample correction were performed. Tissue samples were taken from the digestive tract in addition to the liver, spleen, kidney, heart, lung and mesenteric lymph nodes. These samples were stained with haematoxylin and eosin.

Results and Discussion

Hematological examination revealed marked decrease of total white blood cell count, platelets, total protein and albumin (Table 1). FPV immnomigration test for detection of viral antigen was negative. At necropsy, swelling of the peritoneal lymph nodes, especially mesenteric lymph node, and erosive changes in the stomach, small and large intestines and icterus were observed. On histological examination, the lesions from duodenum to colon were characterized by extensive degeneration and loss of mucosal epithelium. Dilation of crypts (Fig. 1A), regeneration of mucosal epithelium and existence of numerous bacterial colonies were observed. Necrotizing enteritis with amphophilic intranuclear inclusion bodies was prominent in the colon (Fig. 1B). In lymph nodes, atrophy of lymph follicles with lymphocytic depletion was marked (Fig. 2). The bone marrow showed few megakaryocytes and bone marrow hypoplasia (Fig. 3).

FPV have an affinity and requirement for actively dividing cells. The main target tissues are the rapidly dividing cells of lymphoid tissue and the bone marrow, leading to panleukopenia, and the crypt epithelium of the intestinal mucosa, leading to enteritis. These 2 cats didn't show prominent diarrhea and positive response for FPV immunomigration test. However, marked necrotizing enteritis with amphophilic intranuclear inclusion bodies, which are characteristic findings of FPV enteritis, were observed in addition to the atrophic findings in lymphoid tissue and the bone marrow.

Based on these clinical and pathological findings, the two cats were diagnosed as feline panleukopenia (FPV enteritis).

Table. 1 Hematological findings (Cat No.1)

	Day 1	Day 2	Day 4	Reference range
White blood cells (x10^2/μl)	1.0	21.0	4.0	60-150
Platelets (x10^4/μl)	21.0	10.2	4.7	20-45
Total protein (g/dl)	6.4	5.0	5.1	5.6-7.8
Albumin (g/dl)	2.5	1.9	1.7	2.8-4.0

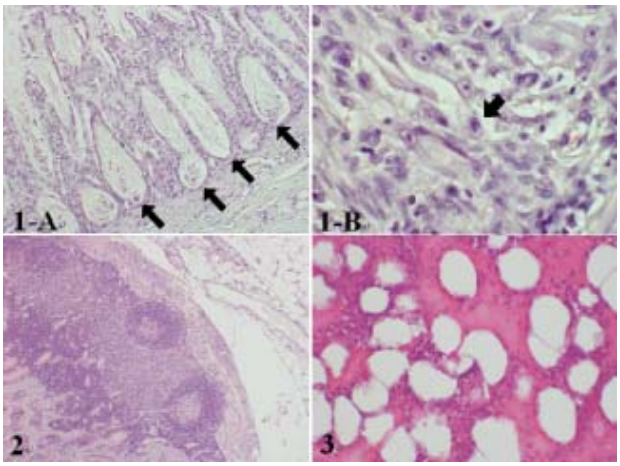

Fig. 1A Colon; cat No.1 dilation of crypts (arrow).
Fig. 1B Colon; cat No.1 amphophilic intranuclear inclusion body in mucosal epithelial cell (arrow).
Fig. 2 Mesenteric lymph node; cat No.1 atrophy of lymphoid follicles with lymphoid depletion.
Fig. 3 Bone marrow; cat No.2. Bone marrow hypoplasia.

References

1. Brown et al., 2007. Pathology of Domestic Animals Vol. 2, 5th ed. 178-180.
2. Ettinger et al., 2005. Veterinary Internal Medicine Vol. 2, 6th ed. 669.

Malignant Odontogenic Tumor in a Dog

M. Sakurai[1], T. Morita[1*], A. Shimada[1], Y. Yamaga[2], T. Uchida[3]

[1]Department of Veterinary Pathology, Tottori University, Tottori, 680-8553, Japan [2]Elm Animal Hospital, Niigata-shi, Niigata, 950-2055, Japan [3]Department of Oral Anatomy, School of Dentistry, Hiroshima University, Hiroshima, 734-8553, Japan. [*]Corresponding author: aki@muses.tottori-u.ac.jp

Keywords: *dog, malignant, odontogenic tumor*

Introduction

Tumors of odontogenic origin are rare in domestic animals. They often occur in young animals. They are classified according to whether they are of epithelial (ameloblastoma, amyloid-producing odontogenic tumor etc) mesenchymal (cementoma, cementifying fibroma etc) or of mixed epithelial and mesenchymal origin (ameloblastic fibroma, ameloblastic fibro-odontoma etc) (1,2). Odontogenic tumor is generally considered as benign in animals. There are a few reports on malignant odontogenic tumor in dogs (3). In this study, we describe a malignant odontogenic tumor which occurred in gingival of a dog.

Material and Methods

A 1-year-old female Labrador retriever dog had a mass on left lower jaw gingiva. The mass was surgically removed. But one month later, the mass recurred and rapidly grew. Radiologically, a tooth-like material was present in the mass .The mass showed osteolysis (Fig. 1) and infiltrated lower jaw bone.

For light microscopical examination, removed mass was fixed in 10% formalin. The tissues were routinely processed and stained with hematoxylin and eosin (HE). Immunohistochemical analysis was performed using antibodies specific for amelogenin, cytokeratin and vimentin by Labeled Streptavidin-Biotin (LSAB) method.

Results and Discussion

Histologically, the mass was composed of neoplastic spindle to ovoid cells. Most neoplastic cells showed diffuse growth pattern with fibrous stroma. They showed marked atypia and many mitotic figures. So we thought it was much undifferentiated. In addition, moderate to marked hemorrhage and necrosis of neoplastic cells were seen. These findings suggested malignancy of the tumor.

Occasionally, deposition of eosionophilic substance with calcification (Fig. 2) were observed. The neoplastic cells around them were arranged in cord, like odontogenic epithelium (Fig. 3). Immunohistochemically, the neoplastic cells and eosinophilic substance were amelogenin-positive (Fig. 4). Amelogenin is an enamel matrix protein produced by ameloblast (4). So we thought eosinophilic material was enamel and amelogenin-positive neoplastic cells were derived from ameloblast. Thus, we diagnosed this tumor as malignant odontogenic tumor.

To examine more details, immunohistochemical analysis for cytokeratin and vimentin was performed. Most of neoplastic cells were positive for vimentin (Fig. 5). Cytokeratin-positive cells were partly observed as small foci. This tumor was considered as mixed epithelial and mesenchymal origin. We thought it might be ameloblastic fibro-odontoma, because this tumor consisted of many vimentin-positive cells (thought to be derived form mesenchymal cells), amelogenin-positive cells (thought to be derived from ameloblast) and deposition of enamel (1, 2). However, the characteristic findings (dental-pulp-like structure, enamel-organ-like structure), which are common in ameloblastic fibro-odontoma, were not demonstrated in the tumor.

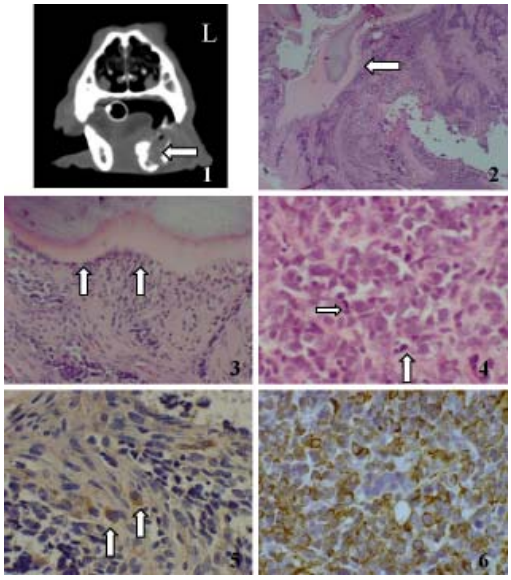

Fig. 1 Radiograph, osteolysis of left lower jaw (arrow).
Fig. 2 Low magnification of HE stain, eosinophilic materials with calcification (arrow).
Fig. 3 High magnification of HE stain. neoplastic cells are arranged in cord (arrows).
Fig. 4 High magnification of HE stain, marked atypism and many mitotic figures (arrows) of neoplastic cells.
Fig. 5 Immunohistochemically, some amelogenin- positive cells are found (arrows).
Fig. 6 Immunohistochemically, many vimentin-positive cells are seen.

References

1. Corrie et al., 2007. Pathology of Domestic Animals Vol. 2, 5th ed. 24-27.
2. Head et al., 2002. Tumors in Domestic Animals, 4th ed. 402-410.
3. Ueki et al., 2004. Vet. Pathol. 41: 183-185.
4. Uchida et al., 1998. Eur. J. Oral Sci.106: 308-314.

Pathological Findings of "Cherry Eye" in Two Dogs

K. Azuma[1], A. Shimada[1*], T. Morita[1], K. Nishida[2], S. Katano[3]

[1]Department of Veterinary Pathology, Tottori University, Tottori, 680-8553, Japan [2]Medical center Nishida, Osaka-shi, Japan [3]Katano veterinary clinic, Niigata-shi, Japan

[*]Corresponding author: aki@muses.tottori-u.ac.jp

Keywords: *cherry eye, third eyelid gland, third eyelid (nictitating membrane)*

Introduction

Cherry eye is the term used to refer to canine third eye lid gland prolapse. Commonly affected breeds include the Bulldog, Chihuahua, Cocker Spaniel, Beagle, Pekingese, Neapolitan Mastiff, and Basset Hound. The third eyelid gland, known as the nictitating membrane, prolapses and becomes visible. The exact mechanism is not known, however, cherry eye may be caused by a hereditary weakness in the connective tissue surrounding the gland. It is most common in puppies. It appears as a red mass in the inner corner of the eye. After gland prolapse, the eye becomes chronically inflamed and there is often a discharge. Because the gland is responsible for about 30% of the eye's tear production, the eye can eventually suffer from dryness. Dry eye may eventually occur in 30 to 40 percent of dogs that have the gland removed. Thus, cherry eye is defined from the stand point of gross pathological finding, but not defined from the stand point of histopathological finding. In the present paper, histological findings of "Cherry eye" are reported.

Material and Methods

Two young dogs, one male, Beagle dog about 4 months old (case 1) and one female, Bulldog about 3months old (case 2) were used. Prolapsed nictitating membranes in the right eyes of the two dogs were taken and prepared for histological examination. Four-micron-thick sections were cut, stained with hematoxylin and eosin, and examined under light microscope.

Results and Discussion

Case 1: Mild glandular hyperplasia of the third eye lid gland was observed.

Case 2: Moderate glandular hyperplasia of the third eye lid gland with interlobular fibrosis was observed. Marked infiltration of inflammatory cells (neutrophils, macrophages and lymphocytes) at the surface of the prolapsed nictitating membrane was also observed.

Both two dogs, young and belong to particular breeds known to be commonly affected, showed "Cherry eye" with hyperplastic changes of third eyelid gland. The observed hyperplastic changes in the gland may develop secondary to the inflammation (observed in case 2). Further study is required to elucidate the mechanism of prolapse of the nictitating membrane.

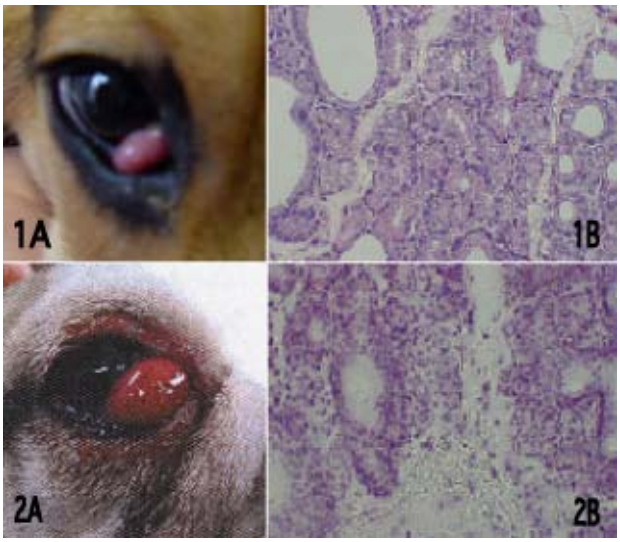

Fig. 1A "Cherry eye" in the right eye of the Beagle (case 1).
Fig. 1B Third eyelid gland, showing glandular hyperplasia (case 1).
Fig. 2A "Cherry eye" in the right eye of the Bulldog (case 2).
Fig. 2B Third eyelid gland, showing glandular hyperplasia with prominent interlobular fibrosis and mild infiltration of inflammatory cells (case 2).

References

1. Herrera, 2005. Proc. 30th WSAVA
2. Schoofs, 1999. J. Am. Anim. Hosp. Assoc. 35(3): 240-242
3. Gelatt, 1999. Veterinary Ophthalmology, 3rd ed.

Visceral Gout with Amyloidosis in a Humboldt Penguin *(Spheniscus humboldti)*

H. Tanaka[1], A. Shimada[1*], T. Morita[1], K Miura[2]

[1]Department of Veterinary Pathology, Tottori University, Tottori, 680-8553, Japan
[2]Miyajima Aquarium, Hiroshima, Japan, [*]Corresponding author: aki@muses.tottori-u.ac.jp

Keywords: *amyloidosis, Humboldt Penguin, visceral gout*

Introduction

Gout is a common finding during necropsy of poultry (1). It is the result of abnormal accumulation of urates and occurs as tow distinct syndromes.

Articular gout is characterized by tophi, deposits of urates around joints, particularly those of the feet. As it has been reproduced by feeding high-protein diets, gout are suggested to result from excess production of uric acid. Defect in tubular secretion of the uric acid may be involved in the development of the disease (1).

Visceral gout, known as visceral urate deposition, is characterized by precipitation of urates in the kidneys and on serous surface of the heart, liver, mesenteries, air sacs and peritoneum. In severe cases, involvement of parenchyma of the liver and spleen may be observed. Because much urate is lost during the tissue process for histology, the lesion of urate deposits are observed as blue or pink amorphous material under microscope. Visceral urate deposition is generally due to a failure of urinary excretion. This may be due to obstruction of ureters, renal damage or dehydration. Dehydration due to water deprivation is a common cause of visceral gout in domestic poultry. Outbreaks of visceral gout in poultry have also been attributed to vitamin A deficiency, excess dietary calcium, treatment with sodium bicarbonate, and a mycotoxin, oosporein.

There are few reports on the occurrence of visceral gout in penguin. Here, we report clinical and pathological findings of the visceral gout in a Humboldt penguin *(Spheniscus humboldti)*.

Material and Methods

A 16-year-old, female, Humboldt penguin died suddenly after prolonged treatment by antibiotics for the inflammatory foot lesions. Hematology and blood chemistry demonstrated increased number of white blood cells (12,000) and increased level of uric acid (17.1 mg%) and blood urea nitrogen (42.2 mg%). Calcium level was within a normal range (11.5 mg%). At necropsy, the animal was emaciated; 2.74 kg in body weight, showing one kg loss in the past one month before death. On gross examination, liver was swollen and had thickened capsule and tiny yellowish white nodules in the parenchyma (Fig. 1). Yellowish white tiny spots were also observed in the kidney. Three yellowish nodules, 1x1x1 mm, were observed in the canal of the ureter. Tissue samples from a variety of organs were taken and prepared for histological examination. Four-micron-thick sections were cut, stained with hematoxylin and eosin and examined under light microscopy.

Results and Discussion

Histological examination showed a large number of amyloid nodules consisting of amorphous pink material in the liver (Fig. 2). Tiny nodules (tophi) with bluish crystals were observed in the kidney (Fig 3). Based on these clinical and pathological findings, the animal was diagnosed as visceral gout with amyloidosis. Presence of some tiny nodules in the ureter of the bird suggests that failure of urinary excretion may be involved in the disease process. Precise mechanism of the disease entity in this penguin is to be elucidated.

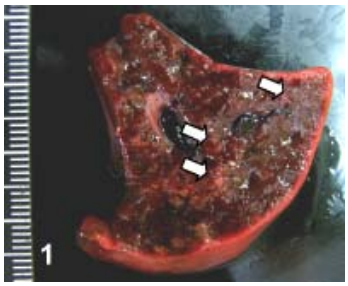

Fig. 1 Cut surface of the liver showing thickening of the capsule and yellowish white tiny nodules in parenchyma.

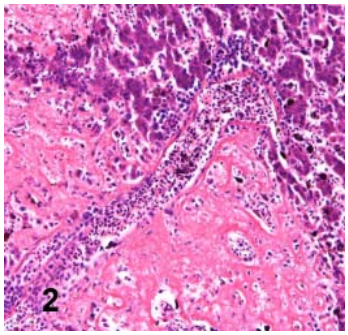

Fig. 2 The liver nodules consist of amyloid deposits.

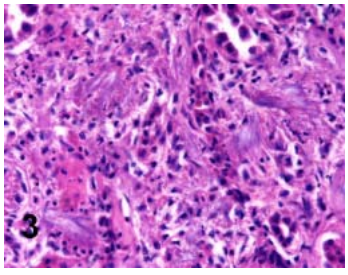

Fig. 3 Tophi with bluish crystals in the kidney.

References

1. Riddle, 1997. Diseases of Poultry, 10th ed., Mosby 936-937.

Glaucoma Induced by Lens Luxation in the Serow: A Case Report

N. Tuntivanich[1*], P. Tuntivanich[1], S. Sanannu[2], K. Kanjanapitakkul[2], R. Thanawongnuwech[3], A. Rungsipipat[3]

[1]Department of Surgery, [2]Dusit Zoo, The Zoological Park Organization, Bangkok 10300 [3]Department of Pathology, Faculty of Veterinary Science, Chulalongkorn University, Bangkok, Thailand 10330

[*]Corresponding author: Nalinee.T@chula.ac.th

Keywords: *enucleation, glaucoma, intraocular pressure, lens luxation, serow*

Introduction

Luxation of the lens is a result of rupture of the zonular fibers. The lens displaced in the anterior chamber obstructs the flow of aqueous humor, which likely leads to glaucoma (1). We report in the present study secondary glaucoma possibly induced by lens luxation in the serow *(Capricornis sumatraensis)*, a relatively short-bodied, long-legged goat-antelopes in family Bovidae that is considered reserved animal of Thailand under the Thai Wildlife Protection Act and Vulnerable Animal (VU) under IUCN Red List of Threatened Species (2).

Material and Methods

A nineteen-year old, male serow at Dusit Zoo, the Zoological Park Organization, Bangkok, Thailand had had right ocular pain for one week prior to a referral to the Ophthalmology Clinic, Animal Teaching Hospital, Faculty of Veterinary Science, Chulalongkorn University, Bangkok. Thorough ophthalmic examinations of the right eye were performed under general. Globe was slightly enlarged. The cornea was entirely edematous. Deep corneal vascularization was noticed, along with an inflammation of the conjunctiva. The mean intraocular pressure (IOP) measured with an applanation tonometer (Tono-pen XL®; Medtronic Solan, FL, USA) one week prior to the surgery was 36 mmHg on the right eye and 11 mmHg on the other. When examined with slit-lamp biomicroscope, the right lens was displaced into the ventral part of the anterior chamber.

Transpalpebral enucleation of the right eyeball was performed. An eyeball was submerged into 10% buffered formalin for routine histological process. It was embedded in paraffin wax, cut at 4 μm thickness and stained with hematoxylin & eosin.

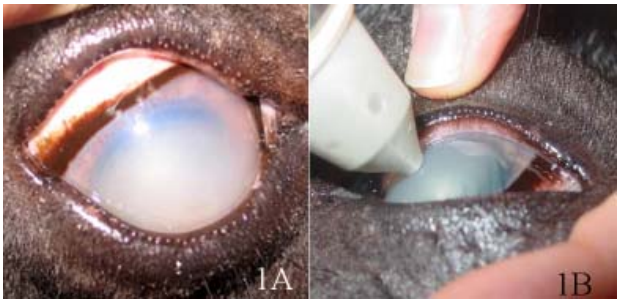

Fig. 1 Ophthalmic examination with (A) focal light revealed corneal edema, keratitis and anterior lens luxation, (B) applanation tonometer to measure the IOP.

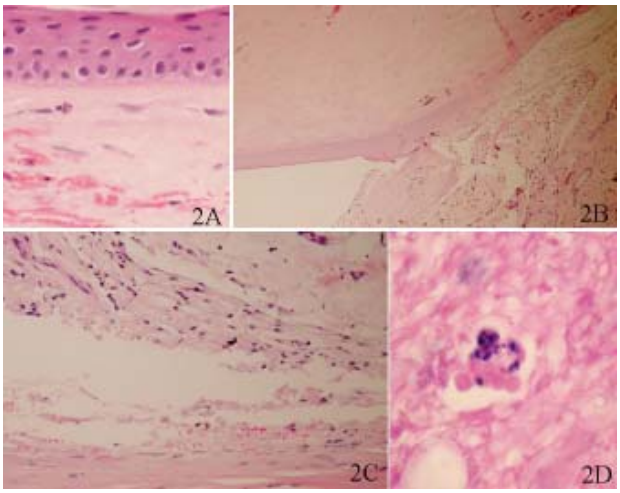

Fig. 2 Paraffin-embedded sections demonstrating (A) vacuolations in columnar cells and cells infiltration in stroma of the cornea (x40), (B) a narrowing of trabecular meshwork (x10) (C) cells infiltration in the iridocorneal angle (x40), (D) apoptotic cell in the lamina cribrosa (x40).

Results and Discussion

Vacuolation of epithelial columnar cells may be intraepithelial edema that was associated with severe corneal edema. Increase number of small capillaries apparent in the superficial corneal stroma was an indication of keratitis possibly associated with an elevation of the IOP and displaced lens (3, 4). Not only collapse of the trabecular meshwork could be recognized. There was also an accumulation of red blood cells and a few inflammatory cells close to the ciliary cleft. Retina and optic nerve had not been histopathologically affected by the secondary glaucoma in this early stage.

Removal of the eyeball via transpalpebral approach was selected for better quality of life. The animal recovered well from the surgery without complications. Glaucoma in serow could be induced by lens luxation.

References

1. Curtis R, 1990. Vet Clin North Am Small Anim Pract. 20(3): 755-773.
2. IUCN Red List, 2008. [Online]. Available: http://www.iucnredlist.org/details/3812/0(Oct 19, 2008)
3. Sawamoto and Umeoka, 2004. J. Toxicol. Pathol. 17: 275-278.
4. Peiffer et al., 1999. Veterinary Ophthalmology, 3rd ed. Febign, Philadelphia. 407-408.

Apoptosis in Normal Bitch Mammary Tissues in Relation to Ovarian Steroid Hormones

S. Manee-in[1*], S. Srisuwatanasagul[2]

[1]Department of Clinical Science and Public Health Medicine, Faculty of Veterinary Science, Mahidol University, Nakhon Prathom, Thailand, 73170 [2]Department of Anatomy, Faculty of Veterinary Science, Chulalongkorn University, Bangkok, Thailand, 10330 [*]Corresponding author: smaneein@yahoo.com

Keywords: *apoptosis, bitch, estrous cycle, mammary gland*

Introduction

Apoptosis is a key role to maintain mammary tissue homeostasis in the absence of pregnancy and lactation. Previous study on apoptosis in mice mammary tissue during estrous cycle revealed that apoptosis is regulated by estrogen and progesterone (1). However, apoptosis in bitch mammary tissues during estrous cycle have not been done before. Therefore, this study aim to investigate the apoptosis in bitch mammary tissues correlated with ovarian steroid hormones levels.

Material and Methods

Five bitches, all without mammary gland lesion were used. The estrous cycle of each bitch was determined and categorized into 6 stages (anestrus, proestrus, estrus, early diestrus, mid diestrus and late diestrus) by vaginal cytology, serum progesterone level (2). Apoptosis of bitch mammary tissues during different stages of estrous cycle were studied by using TUNEL assay.

Results and Discussion

The apoptotic bodies were found in the epithelia (both alveolar and tubular epithelium) and stromal tissue (Fig. 1). The highest percentage of apoptotic bodies in alveolar, tubular epitheliums and stromal tissue were observed at mid-diestrus when compared with the others (Table 1). This finding suggested the positive correlation between apoptotic rate of the mammary tissues and the progesterone level. This is similar to the mice mammary tissue that found high apoptotic rate during diestrus. The results of our study supported the finding that proliferative and secretory activity of mammary cells are also undergo cell death and it demonstrated that during each cycle, the mammary epithelial cells are terminally differentiated and removed by means of apoptosis.

Table 1 Apoptosis percentage of bitch mammary tissue

Stage	Alveolar epithelium	Tubular epithelium	Stroma
Anestrus	9.41±10.51	5.38±5.55	Negative
Proestrus	15.34±6.05	10.28±12.66	3.43±5.51
Estrus	10.49±6.15	6.32±5.59	Negative
Early diestrus	14.47±12.38	18.90±13.46	3.07±6.87
Mid diestrus	52.86±12.86	30.36±9.04	18.16±18.12
Late diestrus	6.75±8.28	2.21±2.05	Negative

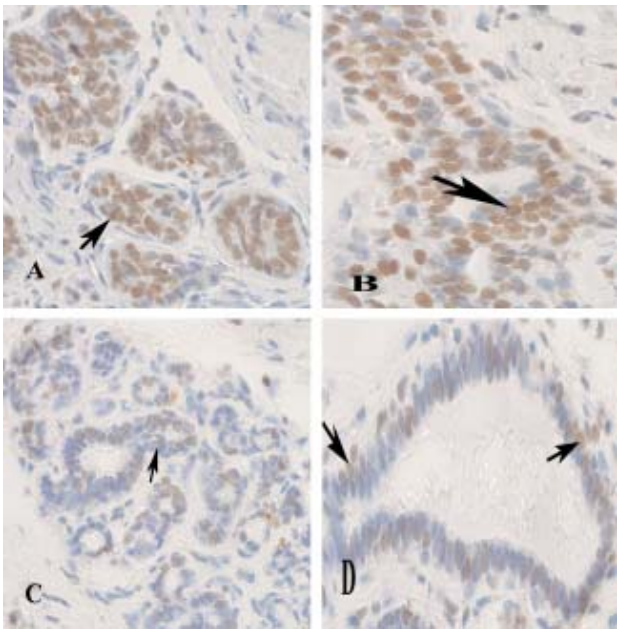

Fig. 1 Apoptotic body in alveolar epithelium (A) and tubular epithelium (B) during mid diestrus (Arrow) and alveolar epithelium (C) and tubular epithelium (D) during anestrus

Acknowledgements

This work was granted by Faculty of Veterinary Science, Mahidol University

References

1. Andres and Strange, 1999. J. Mam. Biol. Neo. 4: 221-228.
2. Feldman and Nelson, 1996. Canine and feline Endocrinology and Reproduction. 526-546.

Study of Sex Steroid Receptors in True Hermaphrodite Gilts

S. Manee-in[1*], S. Srisuwatanasagul[2], P. Tummaruk[3], S. Kesdangsakonwut[4]

[1]Department of Clinical Science and Public Health Medicine, Faculty of Veterinary Science, Mahidol University, Puttamonthon, Nakorn-pathom, 73170, Thailand [2]Department of Anatomy, [3]Department of Obstetrics, Gynaecology and Reproduction, [4]Department of Pathology, Faculty of Veterinary Science, Chulalongkorn University, Bangkok, 10330, Thailand [*]Corresponding author: smaneein@yahoo.com

Keywords: *gilt, sex steroid receptor, true hermaphrodite*

Introduction

True hermaphrodite is a condition that gonadal tissues of both sexes are present in an animal. Though, it was rarely found in domestic animals, the high frequency was reported in pig (1, 2). There are studies about the steroid levels in intersex female pigs and it reported the changes from the normal levels of sex hormones in these gilts (2, 3). However, the study of steroid receptors in these hermaphrodite gilts has not been done before. Therefore, the present study aims to investigate the expression of sex steroid receptors in different gonadal tissue of hermaphrodite gilts.

Material and Methods

Two hermaphrodite gilts were studied. Their genital organs were collected from the slaughter house and histologically processed. Immunohistochemistry was applied to study the expression of oestrogen receptor alpha (ERα) and progesterone receptor (PR) in various genital organs of hermaphrodite gilts.

Results and Discussion

In two hermaphrodite gilts used in this study, both gilts showed ovotestis in one side of the ovary. Moreover, one gilt had shown ductus deferent-like structure at the mesometrial side of the uterus. For the results of immunohistochemistry, in most genital organs examined which were ovotestis, uterus, ductus deferent-like structure, it was shown that there was almost no expression of ERα and PR in these gonadal tissues. However, in the ovarian tissue of the ovotestis, few positive ERα cells could be observed in the granulosa cells of the ovarian follicles. However, as ERα and PR may not be the major subtypes of steroid receptors in the ovary and testis, therefore the expression of these receptors may be restricted in these genital organs. When comparing immunostaining results of the uterus from hermaphrodite gilts to positive controls which was the uterus from normal gilt, strong staining was found in all compartments of the normal uterus. In the uterus of hermaphrodite gilts, no positive cells was found in the present study may suggest that the absence of these steroid receptors may involve with the pathological changes in these hermaphrodite gilts. In summary, since sex steroid hormones and their receptors interplay the role of regulating various reproductive physiology, the defects in reproductive functions in these gilts may be the results from the absence of these steroid receptors in gonadal tissues.

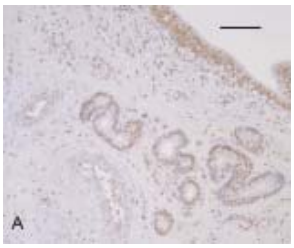

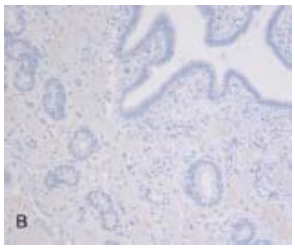

Fig. A ERα positive control, uterus from normal gilts. Bar represents 100 μm

Fig. B ERα immunostaining in the uterine tissue of hermaphrodite gilt

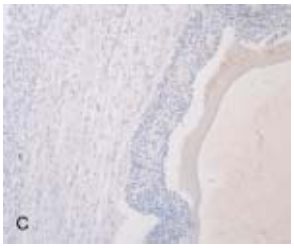

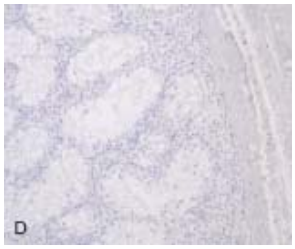

Fig. C ERα immunostaining in the ovarian tissue of ovotestis

Fig. D ERα immunostaining in the testicular tissue of ovotestis

References

1. Bansal et al., 2005. J. Vet. Sci.6: 83-85.
2. Pailhoux et al., 2001. J. Exp. Zool. 290: 700-708.
3. Hunter et al., 1982. J. Reprod. Fertil. 64: 217-222.
4. Hunter et al., 1985. J. Endocrinol. 106: 233-242.

Study of Doxorubicin Chemotherapy for Malignant Canine Mammary Gland Tumors

S. Manee-in[1*], C. Lohachit[2], S. Sirivaidyapong[2], S. Srisuwatanasagul[3]

[1]Department of Clinical Science and Public Health Medicine, Mahidol University, Nakhon Prathom, Thailand, 73170
[2]Department of Obstetric Gynaecology and Reproduction, [3]Department of Anatomy, Chulalongkorn University, Bangkok, Thailand, 10330 [*]Corresponding author: smaneein@yahoo.com

Keywords: *canine, doxorubicin, malignant, mammary gland tumor*

Introduction

Mammary gland tumor is the high incident disease which could be found secondly after skin tumor in the dogs. In general, mammary gland tumor could be found more frequently in bitch than male dog (1) and it accounts to 25-50 percent of various kinds of tumor found in the bitch (2, 3). Moreover, with in this numbers, there is a fifty percent tendency of the tumors to become malignant. Until present, the classical treatment which is most effective is the surgical removal of these tumors, but there still be high risk of surgical complication. Chemotherapy is an alternative treatment that are able to apply in bitch which prone to have surgical complication. Therefore, the aim of this present study is to investigate the effect of doxorubicin chemotherapy on canine mammary tumors.

Material and Methods

Fifteen dogs with mammary gland tumors were used in the present study. The chemotherapy with doxorubicin in a dosage of 30 mg/m^2 was administered to these dogs intravenously. In order to study the effect of doxorubicin on the mammary tumor, the diameter of tumor mass and histopathological changes were determined before and after the treatment.

Results and Discussion

The results showed that diameters before and after treatment were not statistical different. After the treatment with doxorubicin, the results demonstrated partial remission (PR) in 2 dogs (13.33 %), stable disease (SD) in 11 dogs (73.34 %) and progressive disease (PD) in 2 dogs (13.33%). Histopathological changes showed more collagen and fibroblast cells in 3 dogs. It can be concluded that doxorubicin 30 mg/m^2 may have some effects on the growth or stabilize the progress of the tumor and that doxorubicin alone is not suitable for treatment canine mammary gland tumor. Moreover, the results of this study may suggest the surgical removal of the tumor in addition with doxorubicin therapy especially in the early stage of the mammary gland tumor.

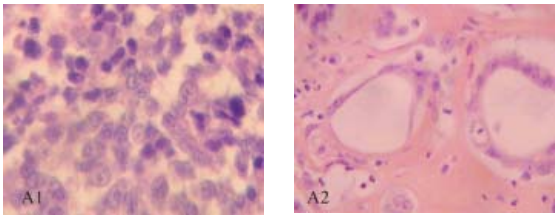

Fig. A1 Tubular adenocarcinoma, simple type: before doxorubicin chemotherapy.

Fig. A2 Tubular adenocarcinoma, simple type: after doxorubicin chemotherapy)

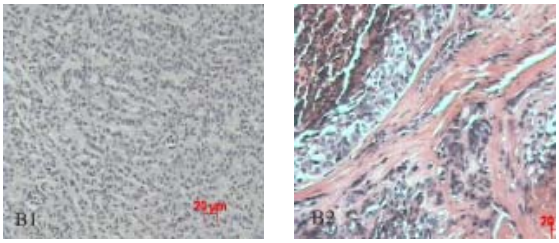

Fig. B1 Tubular adenocarcinoma, simple type: before doxorubicin chemotherapy.

Fig. B2 Tubular adenocarcinoma: after doxorubicin chemotherapy.

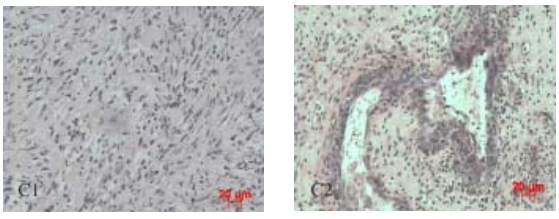

Fig. C1 Spindle cell carcinoma: before doxorubicin chemotherapy.

Fig. C2 Spindle cell carcinoma: after doxorubicin chemotherapy.

References

1. Mulligan, 1975. Am. J. Vet. Res.36: 1391-1396.
2. Hahn et al., 1994. *In Vivo*. 8: 133-143.
3. MacEven, 1990. Cancer Metastasis Rev. 9: 125-136.